

APPLICATION OF SAFETY TRIAD IN RELATION TO CHEMICAL  
HAZARDS

A Dissertation

by

TRENT FORREST PARKER

Submitted to the Graduate and Professional School of  
Texas A&M University  
in partial fulfillment of the requirements for the degree of

DOCTOR OF PHILOSOPHY

Chair of Committee,  
Committee Members,

Qingsheng Wang  
Benjamin Wilhite  
Mark Holtzapple  
Ying Li

Head of Department,

Arul Jayaraman

August 2022

Major Subject: Chemical Engineering

Copyright 2022 Trent Parker

## ABSTRACT

Within the process industries, a large number of incidents occur each year, leading to injuries, deaths, environmental damage, and economic losses. To address these incidents, various hazard analysis techniques are utilized within the process industries to determine barriers and strategies to be implemented within the facilities. However, up to this point, an overarching framework for safety system robustness evaluation has not been established. It is for this reason that the late Dr. Sam Mannan proposed the concept of a safety triad, which depicts the three layers of an effective safety system. The focus of my research is on the analysis of chemical hazards and how they fit within the concept of the safety triad. For analysis of the safety triad, appropriate methodologies for ensuring the robustness of each component have been identified and discussed in detail.

For identifying chemical reactivity hazards within facilities, 33 warehouses containing hazardous chemicals were analyzed. To do so, chemical incompatibility software was used to determine combinations of chemicals that would potentially result in heat or toxic gas generation. For these chemicals, the potential gas release offsite impacts were identified. In order to identify the safer operating regions for chemical processes, two reaction systems were investigated. These consist of the oxidation of 2-butanol to 2-butanone as well as the oxidation of cyclohexanol to cyclohexanone. Response surface methodology was used to identify the effects of each of the parameters on the heat release as well as on the product yield. Based on the results of this work, the safety triad has been determined to serve as an effective tool for identification and response to hazards within chemical facilities.

## DEDICATION

To my mother, Janet Parker and my father, Dwain Parker, who have always believed in me and supported me throughout my entire educational journey. To my brother, Garrett Parker, whose quirky sense of humor has helped motivate and inspire me throughout the course of my PhD. This is a tribute to the three of you.

## ACKNOWLEDGEMENTS

I would like to express my deepest gratitude to my advisor, Dr. Qingsheng Wang, for all his guidance, advice, and help through these years of study and work. He has served as a true mentor, giving me excellent suggestions for my research and numerous opportunities for growth and development as I have navigated my PhD journey. In spite of having to assume the role as my advisor in the middle of my PhD, he has worked tirelessly to ensure a smooth transition for me and provide me opportunities to work in many facets within the process safety domain.

I would like to thank my committee members, Dr. Benjamin Wilhite, Dr. Mark Holtzapple, and Dr. Ying Li, for their excellent advice for various aspects of my dissertation work as well as for their availabilities and commitments.

Additionally, I would like to thank Dr. S. Camille Peres for her exceptional support for me throughout my entire PhD, including during difficult times. The exposure to and knowledge of human factors and effective procedural systems I have received as a result of working with her and her lab is unparalleled, and I am honored to have had the privilege of working with her on the Advanced Procedures project.

I would like to thank Dr. Behie and all of the MKOPSC faculty and staff for the excellent opportunities and resources that I've been provided as a result of being a part of it. The MKOPSC goal of "making safety second nature" has been evident throughout all of the projects I've participated in, and I feel privileged to have been a part of it. Furthermore, I would like to thank the late Dr. M. Sam Mannan for his extensive work in developing MKOPSC as well as for initially taking me on as a student.

I extend sincere thanks to MKOPSC volunteers and visiting scholars including Mr. Goyette, Dr. Papadaki, and Dr. Paskan for their contributions to my research and professional

development. Your support and guidance in my work has been critical for my research and I greatly appreciate it.

I would like to thank all students in Dr. Wang's research group, MKOPSC, NGAP, and RIHM labs for your research guidance as well as support for me throughout my PhD. I have thoroughly enjoyed working with everyone and doing some fun activities together as well. I would also like to thank all of the friends I have made along the way, including two during my internship in Dallas, Andrew Aleman and Bryan Fajardo, who have made my PhD journey more enjoyable and provided me excellent support.

I would also like to thank my undergraduate advisor, Dr. Jacob Borden, for his excellent support and advice on joining the MKOPSC PhD program. His guidance on PhD studies was instrumental for me making the most of my PhD work.

Lastly, I would like to thank my parents, Dwain and Janet, as well as brother, Garrett, for their unwavering support for me both throughout my PhD as well as throughout my entire educational journey.

## CONTRIBUTORS AND FUNDING SOURCES

### **Contributors**

This work was supported by a dissertation committee consisting of committee chair Dr. Qingsheng Wang of the Department of Chemical Engineering and committee members Dr. Mark Holtzapple and Dr. Benjamin Wilhite of the Department of Chemical Engineering as well as Dr. Ying Li of the Department of Mechanical Engineering.

### **Funding Sources**

This work was supported in part by the Mary Kay O'Connor Process Safety Center, Multiscale Process Safety Research laboratory, and Next Generation Advanced Procedures project at Texas A&M University.

## ABBREVIATIONS

BLEVE	Boiling Liquid Expanding Vapor Explosion
CFR	Code of Federal Regulations
CRW	Chemical Reactivity Worksheet
CSB	Chemical Safety Board
DIPPR	Design Institute for Physical Properties
EPA	Environmental Protection Agency
ERT	Emergency Response Team
F&EI	Fire and Explosion Index
FMEA	Failure Modes and Effects Analysis
FTA	Fault Tree Analysis
FTIR	Fourier Transform Infrared Spectroscopy
HAZOP	Hazard and Operability Study
ICS	Incident Command System
JSA	Job Safety Analysis
LHWI	Logistic Hazard Warehouse Index
LOPA	Layer of Protection Analysis
MHI	Material Hazard Index
MKOPSC	Mary Kay O'Connor Process Safety Center
MSDS	Material Safety Data Sheet
NF	Degree of Flammability
NH	Degree of Health Hazard
NR	Degree of Reactivity

OSHA	Occupational Safety and Health Administration
P/R	Peroxide/Reactant
PAC	Protective Action Criteria
PCHP	Potential to Cause Harm to the Public
PFD	Probability of Failure on Demand
SCBA	Self-Contained Breathing Apparatus
SHF	Storage Hazard Factor
SIL	Safety Integrity Level



## PARAMETER NOMENCLATURE

$A$	Absorbance [a.u.]
$A$	Heat Transfer Area [ $\text{m}^2$ ]
$E$	Activation Energy [J/mol]
$F_i$	Penalty Factor [dimensionless]
$\gamma$	Lumped Activation Energy [dimensionless]
$\Delta H_r$	Heat of Reaction [J/mol]
$k$	Reaction Rate Constant [ $\text{s}^{-1}$ ]
$Q$	Heat Release Amount [kJ]
$qr_{rtc}$	Heat Release Rate [W]
$R$	Gas Constant [J/(mol*K)]
$T$	Temperature [K]
$T_j$	Jacket Temperature [ $^{\circ}\text{C}$ ]
$T_r$	Reactor Temperature [ $^{\circ}\text{C}$ ]
$T_w$	Wall Temperature [K]
$U$	Overall Heat Transfer Coefficient [W/( $\text{m}^2*\text{K}$ )]
$\bar{\nu}$	Wavenumber [ $\text{cm}^{-1}$ ]

# TABLE OF CONTENTS

	Page
ABSTRACT.....	ii
DEDICATION.....	iii
ACKNOWLEDGEMENTS.....	iv
CONTRIBUTORS AND FUNDING SOURCES .....	vi
ABBREVIATIONS .....	vii
PARAMETER NOMENCLATURE .....	ix
TABLE OF CONTENTS.....	x
LIST OF FIGURES .....	xii
LIST OF TABLES .....	xv
LIST OF EQUATIONS .....	xvi
CHAPTER I: INTRODUCTION.....	1
1.1 Safety triad description.....	1
1.2 Research overview .....	2
1.3 Problem statement.....	4
1.4 Objectives.....	5
CHAPTER II: SAFETY TRIAD ANALYSIS .....	7
2.1 Literature review of hazard analysis techniques .....	7
2.2 Comparison of safety triad with hazard analysis techniques .....	15
2.3 Prevention component.....	15
2.4 Mitigation component .....	18
2.5 Response component.....	19
2.6 Safety triad application for assessment of prior incidents.....	20
2.6.1 Methyl mercaptan release case study .....	23

2.7 Safety triad application to chemical industries .....	28
CHAPTER III: CHEMICAL WAREHOUSE HAZARD IDENTIFICATION.....	30
3.1 Chemical storage hazard introduction and hazard index techniques .....	30
3.2 Description of chemical storage warehouses .....	33
3.3 Description of chemical incompatibilities/modeling software.....	34
3.4 Chemical reactivity worksheet results.....	35
3.5 ALOHA modeling results and toxic gas incidents.....	38
3.6 Safety triad application to chemical storage facilities .....	45
CHAPTER IV: THERMAL HAZARD ANALYSIS OF INDUSTRIAL REACTIONS.....	46
4.1 Introduction to runaway reactions.....	46
4.2 Description of laboratory equipment.....	48
4.3 2-butanol to 2-butanone oxidation analysis .....	51
4.4 Cyclohexanol to cyclohexanone oxidation analysis.....	61
4.5 Application of safety triad to exothermic oxidation reactions .....	76
CHAPTER V: SUMMARY AND CONCLUSIONS .....	78
5.1 Safety triad application to chemical facilities .....	78
5.2 Future work .....	80
LITERATURE CITED .....	82
APPENDIX A: ALOHA WAREHOUSE DISPERSION MODELS .....	89
APPENDIX B: 2-BUTANONE HEAT RELEASE AND FTIR DATA .....	111
APPENDIX C: CYCLOHEXANONE HEAT RELEASE AND FTIR DATA.....	118

## LIST OF FIGURES

	Page
Figure 1: Safety triad .....	1
Figure 2: Research overview .....	2
Figure 3: Sample bowtie analysis diagram .....	8
Figure 4: Sample LOPA diagram .....	9
Figure 5: Sample HAZOP analysis diagram.....	10
Figure 6: Sample SIL analysis with risk matrix.....	11
Figure 7: Sample FMEA diagram.....	12
Figure 8: Sample JSA diagram .....	13
Figure 9: Sample FTA diagram .....	14
Figure 10: Hazard analysis applications .....	15
Figure 11: Procedure writer’s framework.....	17
Figure 12: Tank diking.....	19
Figure 13: Firefighting response to chemical incident .....	20
Figure 14: Arkema chemical plant fire .....	22
Figure 15: Basic organization of the ICS.....	28
Figure 16: Example data from chemical warehouses .....	33
Figure 17: Chemical reactivity worksheet for warehouse 7 .....	36
Figure 18: Chemical reactivity worksheet for warehouse 25 .....	37
Figure 19: Chemical reactivity worksheet for warehouse 33 .....	38
Figure 20: ALOHA model for carbon monoxide in warehouse 2 .....	40

Figure 21: ALOHA model for fluorine gas in warehouse 7 .....	41
Figure 22: ALOHA model for ammonia in warehouse 23 .....	42
Figure 23: Semenov diagram .....	46
Figure 24: RC1e laboratory setup (a) Photograph (b) Diagram .....	50
Figure 25: 2-butanone synthesis reaction with hydrogen peroxide side reaction.....	51
Figure 26: iControl temperature and heat release graph.....	54
Figure 27: Effects of temperature and initial 2-butanol concentration on heat release (a) Surface map (b) Contour plot.....	55
Figure 28: Effects of temperature and catalyst amount on heat release (a) Surface map (b) Contour plot .....	56
Figure 29: Effects of initial 2-butanol concentration and catalyst amount on heat (a) Surface map (b) Contour plot.....	57
Figure 30: FTIR spectra for 30 °C temperature, 0.284 mol/L 2-butanol, and 2.4 wt% catalyst ...	59
Figure 31: FTIR spectra for 45 °C temperature, 0.534 mol/L 2-butanol, and 3.6 wt% catalyst ...	60
Figure 32: Cyclohexanone synthesis reaction with hydrogen peroxide side reaction .....	62
Figure 33: iControl temperature and heat release graph for 40 °C temperature, P/R ratio of 0.5, and 4 H <sub>2</sub> O <sub>2</sub> injections.....	65
Figure 34: iControl temperature and heat release graph for 50 °C temperature, P/R ratio of 1.0, and 4 H <sub>2</sub> O <sub>2</sub> injections.....	65
Figure 35: FTIR spectra for 40 °C temperature, P/R ratio of 0.5, and 4 H <sub>2</sub> O <sub>2</sub> injections.....	67
Figure 36: FTIR spectra for 50 °C temperature, P/R ratio of 1.0, and 4 H <sub>2</sub> O <sub>2</sub> injections.....	68
Figure 37: Effects of temperature and peroxide/reactant molar ratio on heat release (a) Surface map (b) Contour plot.....	69

Figure 38: Effects of temperature and number of hydrogen peroxide injections on heat release (a) Surface map (b) Contour plot .....	70
Figure 39: Effects of peroxide/reactant molar ratio and number of hydrogen peroxide injections on heat release (a) Surface map (b) Contour plot .....	71
Figure 40: Effects of temperature and peroxide/reactant molar ratio on product yield (a) Surface map (b) Contour plot.....	73
Figure 41: Effects of temperature and number of hydrogen peroxide injections on product yield (a) Surface map (b) Contour plot .....	74
Figure 42: Effects of peroxide/reactant molar ratio and number of hydrogen peroxide injections on product yield (a) Surface map (b) Contour plot.....	75

## LIST OF TABLES

	Page
Table 1: Research objectives .....	5
Table 2: Penalty values for chemical quantities .....	32
Table 3: Toxic gas incidents .....	43
Table 4: Reaction conditions for 2-butanol oxidation experiments.....	53
Table 5: Reaction conditions for cyclohexanol oxidation experiments.....	64

## LIST OF EQUATIONS

	Page
Equation 1: Logistic Warehouse Hazard Index .....	30
Equation 2: Storage Hazard Factor .....	30
Equation 3: Potential to Cause Harm to the Public Index .....	31
Equation 4: Reaction Stability Criterion.....	47
Equation 5: Semenov Number .....	47
Equation 6: Critical Semenov Number .....	48
Equation 7: Calculation of Q .....	48
Equation 8: Calculation of $\eta_c$ .....	48



# CHAPTER I

## INTRODUCTION

### *1.1 Safety triad description*

A large number of incidents have occurred in process industries across the world throughout the years, and have resulted in injuries, deaths, economic losses, and environmental damage to surrounding communities. Notable incidents include the Williams Olefins plant explosion in 2013 in Geismar, LA that resulted in 2 deaths and 114 injuries [1] as well as the BP fire and explosion in 2005 in Texas City, TX that resulted in 5 deaths and 80 injuries [2]. In response to these incidents, the late Dr. M. Sam Mannan proposed the concept of the “safety triad,” which represents the three layers of an effective safety system. Similar to the fire triangle, which depicts the three ingredients necessary for most fires, the safety triad depicts the three layers of an effective safety system. These layers are prevention, mitigation, and response, as shown below in Figure 1.



Figure 1: Safety triad (Reprinted from [3]. O’Connor, M., Pasman, H. J., & Rogers, W. J., 2019.)

Deficiencies in any of the three layers can lead to possible incidents, with this proposed concept serving a critical role for hazard reduction in facilities. These facilities can include both onshore and offshore industrial facilities, and can include chemical, manufacturing, and aviation industries. Furthermore, this safety triad can be used to address the consequences of hazards stemming from a wide variety of initiating events, which can include climate extremes [4], fires, and loss of coolant.

### *1.2 Research overview*

The focus of my research is on analysis of hazards within chemical facilities and how they are incorporated into the concept of the safety triad in order to reduce incident likelihood within the facilities, with the components shown in Figure 2. These components consist of the safety triad itself, chemical reactivity hazards within chemical storage facilities, and thermal analysis of hazards present in chemical processes.

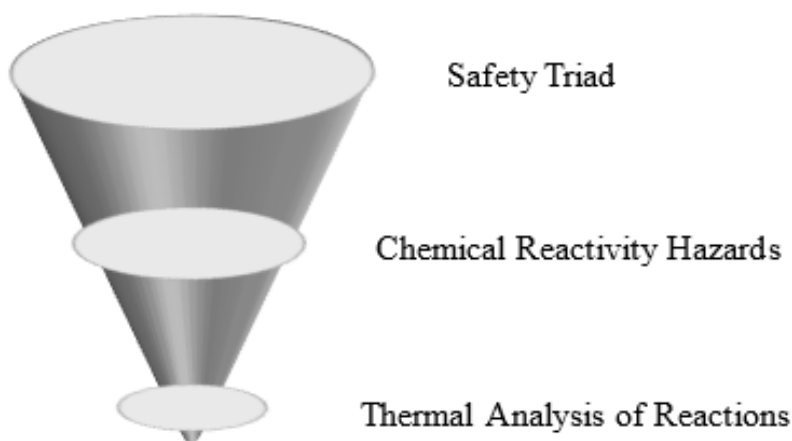


Figure 2: Research overview

In the following sections, a discussion on the motivation of my research as well as the overall problem statement and objectives will be provided. Subsequently, a literature review of hazard analysis techniques that are commonly utilized within the chemical industries is provided. Following this, each component of the safety triad is discussed in detail, and the application of the safety triad for assessment of prior incidents is discussed. This is substantiated by application of the safety triad to an incident involving methyl mercaptan release at an industrial facility. A discussion of the safety triad application to chemical industries then follows.

Following analysis and discussion of the safety triad itself, an investigation of hazards within chemical storage warehouses is presented. This includes a description of the warehouses themselves as well as a description of the chemical incompatibilities found within them. A discussion of the toxic gases that may be generated within the facilities is then provided. Furthermore, application of the safety triad to warehouses containing hazardous chemicals is then described.

Thermal hazard analyses of chemical reactions within the process industries are then discussed. This involves an introduction to runaway reactions and the associated hazards as well as the description of laboratory equipment used to identify these hazards. Furthermore, two oxidation reaction systems are investigated. These are the oxidation of 2-butanol to 2-butanone as well as the oxidation of cyclohexanol to cyclohexanone. For these, the associated heat release for various combinations of parameters is determined as well as product yields. The safety triad is then discussed in relation to exothermic oxidation reactions.

Lastly, the conclusions of this work are presented, as well as a broad discussion on application of the safety triad to chemical hazards in general. This is followed by a discussion of

future research work to be conducted for validation of the safety triad as an effective tool for addressing chemical hazards.

### *1.3 Problem statement*

Upon investigation of hazard analysis techniques, it has been found that an extensive number of these techniques have been utilized in the design and operation of chemical facilities [5-11]. However, many of these techniques involve hazard identification and analysis for very specific components and facility types, and thus do not provide a comprehensive, overarching framework to evaluate the robustness of the safety systems within the chemical facilities. Thus, there remain a number of questions related to the safety triad and its application in improving the safety of chemical facilities, as follows:

- 1) How can the safety triad be applied to the design and operation of chemical facilities, both for chemical storage facilities and those in which chemical reactions are taking place?
- 2) How should chemical storage facilities be operated such that incidents resulting from chemical incompatibilities do not occur, as well as effective methods to address the consequences in the event of an incident?
- 3) What are safer operating regions at which chemical processes can be run to ensure that thermal runaway does not occur, as well as methods to effectively address the consequences of a thermal hazard incident should it occur?

### 1.4 Objectives

The overall objective of this work is to validate the safety triad as an effective, overarching framework to evaluate the robustness of safety systems so as to minimize the number and severity of incidents in the chemical process industries. To do so, three sub-objectives have been established, as shown in Table 1 below.

<b>Objective 1: Analyze the effectiveness of the safety triad for application to past incidents and compare it with similar hazard analysis techniques</b>
<ul style="list-style-type: none"><li>• Identify similar hazard analysis techniques to safety triad and compare their applications</li><li>• Investigate elements of effective safety triad components to ensure their robustness, as follows:<ul style="list-style-type: none"><li>○ Prevention (operating procedures, safety management systems, etc.)</li><li>○ Mitigation (alert systems, backup power sources, etc.)</li><li>○ Response (evacuation, firefighting, etc.)</li></ul></li><li>• Apply safety triad to prior incidents in chemical facilities to determine its effectiveness in mitigating the occurrence and severity of incidents</li><li>• Discuss application of safety triad in the design and maintenance of chemical facilities</li></ul>

Table 1: Research objectives

<p><b>Objective 2: Determine effective methods of operating chemical storage facilities to prevent chemical incompatibility hazards</b></p>
<ul style="list-style-type: none"> <li>• Analyze chemical reactivity hazards of chemicals stored in 33 warehouses</li> <li>• Utilize dispersion modeling to determine maximum downwind distance for hazardous concentrations of toxic gases</li> <li>• Identify most effective methods for ensuring robust prevention component for chemical storage, particularly in chemical warehouses</li> <li>• Identification of effective mitigation and response measures for hazards resulting from chemical incompatibilities</li> <li>• Discuss application of safety triad in relation to chemical storage warehouses</li> </ul>
<p><b>Objective 3: Identify safer operating regions for chemical processes</b></p>
<ul style="list-style-type: none"> <li>• Analyze thermal hazards of 2-butanol oxidation to 2-butanone, consisting of: <ul style="list-style-type: none"> <li>○ Investigation of exothermic reactions occurring in industry</li> <li>○ Nine-run array of experiments with three parameters</li> <li>○ Effects of varied parameters on heat release identified using response surface methodology</li> <li>○ Identification of 2-butanone product yields for specified parameter combinations</li> </ul> </li> <li>• Analyze thermal hazards of cyclohexanol oxidation to cyclohexanone, consisting of: <ul style="list-style-type: none"> <li>○ Nine-run array of experiments with three parameters</li> <li>○ Effects of varied parameters on heat release identified using response surface methodology</li> <li>○ Effects of varied parameters on product yields identified using response surface methodology</li> </ul> </li> <li>• Discuss application of safety triad in relation to exothermic oxidation reactions</li> </ul>

Table 1: Continued

## CHAPTER II

### SAFETY TRIAD ANALYSIS\*

#### *2.1 Literature review of hazard analysis techniques*

To determine the appropriate applications of the safety triad as well as its potential for use in conjunction with other hazard analysis techniques, a literature review of these techniques was conducted, with an overview of them presented below. These techniques consist of ones that are commonly used within the process industries both in order to determine barriers and strategies that should be implemented as well as elements of effective safety systems.

#### **Bowtie analysis**

The bowtie analysis method is used to identify and analyze causal relationships in high-risk scenarios. The goal of the bowtie method to provide a visual representation of possible incidents that may occur for a given hazard and provide a representation of the control measures that can be instituted to minimize these incidents [5]. A sample bowtie diagram is provided in Figure 3.

---

\* Part of this chapter is reprinted with permission from “Application of safety triad in preparation for climate extremes affecting the process industries” by Parker, T., Shen, R., Wang, Q., 2019. Process Safety Progress, Volume 38, Pages 1-5, Copyright 2019 by John Wiley and Sons

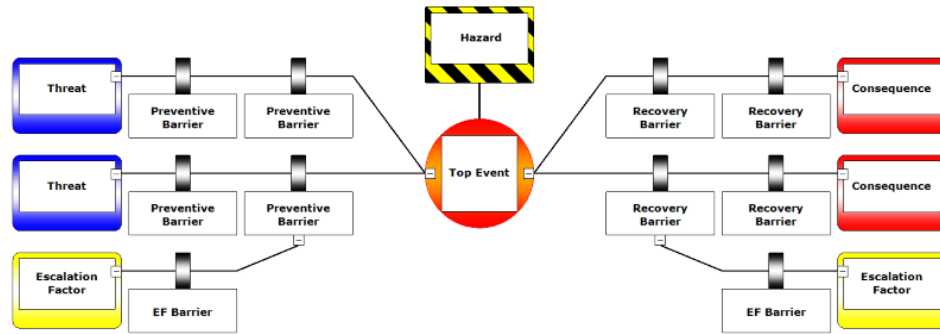


Figure 3: Sample bowtie analysis diagram (Reprinted from [5]. Parker, T., Shen, R., & Wang, Q., 2022.)

The safety triad could be utilized in conjunction with the bowtie method to identify the necessary components to construct an effective safety system. As such, bowtie diagrams could be created for each of the prevention components to identify and address specific deficiencies. For hazards related to failures of the prevention components, bowtie diagrams could be created to identify practical mitigation components. Furthermore, hazards from possible failures of the mitigation components could be utilized in additional bowtie diagrams to identify appropriate response measures. Thus, the safety triad could be applied within the bowtie analysis method to establish a more effective safety system.

### Layer of protection analysis

An alternate risk analysis method is the layer of protection analysis (LOPA) method. Under this approach, a set of undesired incidents such as fires, explosions or chemical releases are outlined and the consequences of these events are estimated. Then, independent layers of protection that can be implemented are identified. Controls and safety systems are assigned protective credits based on their ability to independently control or mitigate the specified



hazards. LOPA analysis is utilized to analyze the probability of an incident occurring both with and without a given layer of protection [6]. These independent protection layers are represented as progressively larger ovals, with a LOPA sample shown in Figure 4.



Figure 4: Sample LOPA diagram (Reprinted from [6]. Willey, R. J., 2014.)

Similar to the bowtie method, the LOPA approach could be used in conjunction with the safety triad to identify necessary system components. For example, each of the prevention components of the safety triad could be incorporated into a LOPA diagram to determine their independence as protection from a process hazard. Then, each of the mitigation components could be incorporated into an additional LOPA diagram to determine their independence. Lastly, based on the independence of the mitigation components, the response components could be incorporated into an additional LOPA. The results of the LOPA diagrams of the three components could be incorporated into one overall LOPA diagram to introduce the additional guidance that the safety triad provides.

## Hazard and operability analysis

Hazard and operability analysis (HAZOP) is a systematic method of identifying possible hazards in a work process. Similar to the Bowtie and LOPA diagrams, the HAZOP consists of determining consequences associated with deviations from normal process parameters where it may create a hazard. To do this, a guide word is first identified for possible process deviations, such as no, higher, or more. Then, deviations that correspond to the guide word are listed. Possible causes of these deviations are then listed in the HAZOP, as well as their consequences [7]. Lastly, actions to be taken to prevent or mitigate the consequences of these deviations are listed, as shown in Figure 5.

<b>Guide Word</b>	<b>Deviation</b>	<b>Causes</b>	<b>Consequences</b>	<b>Action</b>
<b>NO</b>	<b>No cooling</b>		<b>Temperature increase in reactor</b>	
<b>REVERSE</b>	<b>Reverse cooling flow</b>	<b>Failure of water source resulting in backward flow</b>		
<b>MORE</b>	<b>More cooling flow</b>			<b>Instruct operators on procedures</b>

Figure 5: Sample HAZOP analysis diagram (Reprinted from [7]. Hartwell, J., 2019.)

The HAZOP could be used in conjunction with the safety triad to comprehensively identify necessary safety system components. For this, guide words could be generated for each of the three safety triad components. Then, possible deviations associated with these guide words for each of the three components could be developed, as well as the causes, consequences, and necessary actions. This could provide a robust method of evaluating the components of the safety system.

## Safety integrity level analysis

Safety integrity level (SIL) analysis is used to determine the risk-reduction levels provided by various safety functions. For this method, the safety integrity level of each safety function is determined based on the probability of failure on demand (PFD) for that function. For example, for low demand operations, SIL 1 corresponds to a PFD of 0.1–0.01, while SIL 4 corresponds to a PFD of 0.0001–0.00001 [8]. Methods of assigning SIL values include risk matrices, as shown below in Figure 6.

<b>Frequency</b>	5	SIL3	SIL4	X	X	X
	4	SIL2	SIL3	SIL4	X	X
	3	SIL1	SIL2	SIL3	SIL4	X
	2	-	SIL1	SIL2	SIL3	SIL4
	1	-	-	SIL1	SIL2	SIL3
		1	2	3	4	5
<b>Severity of Consequence</b>						

Figure 6: Sample SIL analysis with risk matrix (Reprinted from [8]. Benmerrouche, M., & Lee, R., 2015.)

The safety triad could be used in conjunction with the SIL analysis method to identify necessary safety system components. To do so, safety system components for prevention, mitigation, and response could be organized based on their PFD and thus assigned SIL values. Then, these components could be depicted using a risk matrix to ensure that effective safety components are in place to address the hazards associated with the system.

## Failure modes and effects analysis

Failure modes and effects analysis (FMEA) is used to determine possible failures when designing a system. For this method, failure modes for a given system are identified and listed. Then, the severity of the hazards of the failure modes as well as their probabilities of occurrence are identified. Furthermore, the probability of detection for each of the failure modes is also determined, as shown in Figure 7. This allows appropriate safety measures to be implemented for each of the failure modes [9].

FAILURE MODE & EFFECTS ANALYSIS (FMEA)				Date: <u>1/1/2018</u>
Process Name: Left Front Seat Belt Install		Process Number: SBT 445		Revision: <u>1.3</u>
Failure Mode	A) Severity Rate 1-10 10=Most Severe	B) Probability of Occurrence Rate 1-10 10=Highest Probability	C) Probability of Detection Rate 1-10 10=Lowest Probability	Risk Preference Number (RPN) AxBxC
1) Select Wrong Color Seat Belt	5	4	3	60
2) Seat Belt Bolt Not Fully Tightened	9	2	8	144
3) Trim Cover Clip Misaligned	2	3	4	24

Figure 7: Sample FMEA diagram (Reprinted from [9]. Slack, N., 2015.)

The FMEA analysis method could be used in combination with the safety triad to identify and implement the components of an effective safety system. Each failure mode identified in the FMEA could be categorized into one of the three safety triad components. From this, the severity and probability of occurrence and detection for each of these failure modes could be identified. This allows the robustness of the entire safety system to be assessed, with additional components added if necessary.

## Job safety analysis

Job safety analysis (JSA) is used to identify hazards associated with each step in a task. For this analysis, each of the steps within a task are listed. Then, for each step, potential hazards are identified [10]. For each of these hazards, recommended procedures are listed to either eliminate or reduce them, as shown in Figure 8.

Basic Job Steps	Potential Hazards	Recommended Procedure
<b>1</b> / Dig hole for tree.	Strike underground utilities	Make sure underground utilities have been located and marked.
<b>2</b> / Move tree to hole location.	Lifting, back injuries	Always use a ball cart or tractor with trained operator to move tree to hole location.
<b>3</b> / Place tree in hole.	Lifting, back injuries, damage to tree	Roll tree into hole or use two people to place tree into hole, depending on tree size.

Figure 8: Sample JSA diagram (Reprinted from [10]. Kjellén Urban, & Albrechtsen, E., 2017.)

The safety triad could serve as a useful tool to complement the JSA approach. For each step within the JSA, the safety triad could be utilized to identify whether there are robust prevention, mitigation, and response components in place to address hazards. This could then guide the recommended procedures that are prepared for hazard elimination or reduction. Thus, the combination of the safety triad with JSA results in more comprehensive solution than JSA in isolation.

## Fault tree analysis

Fault tree analysis (FTA) is a top-down approach to identifying component-level failures that result in a system-level failure occurring. For this method, the primary (component-level)

failures are represented as circles in a diagram, which are connected to “and/or” gates. In the case of “or” gates, either outcome presents a primary failure in the output event which is represented by the rectangle above the gate. In the case of “and” gates, both primary failures must occur simultaneously to produce the output event. These output events are connected to additional “and/or” gates up to the location of the top output event, which is the system-level failure as shown in Figure 9 [11].

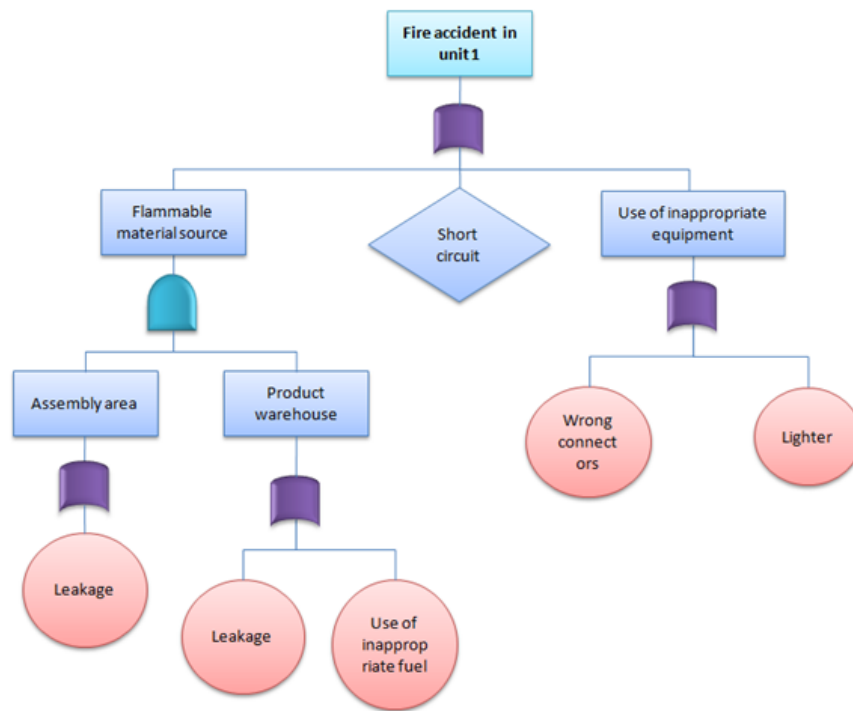


Figure 9: Sample FTA diagram (Reprinted from [11]. Pedroni, N., & Zio, E., 2012.)

The safety triad could be used in combination with the FTA method to determine the robustness of each component of the triad. For this, the initiating events can be represented as component-level failures on the FTA diagram. The prevention, mitigation, and response components can then be identified to address the progressively higher-level output events within

the diagram. Thus, using the safety triad in conjunction with the FTA ensures that each output event identified is properly addressed.

### 2.2 Comparison of safety triad with hazard analysis techniques

The hazard analysis techniques discussed in Section 2.1 are utilized for specific processes and hazards associated with them. For example, the HAZOP technique is specifically utilized for determination of possible deviations involving process parameters [7]. Moreover, the JSA technique is utilized to identify hazards within tasks that workers are performing [10]. While these techniques provide critical information in the design and operation of facilities, their scopes are limited (e.g., involving only workers or processes and limited types of facilities and equipment).

On the other hand, the safety triad provides an overarching framework for the evaluation of safety system effectiveness. As such, it can be applied to the design and operation of facilities, particularly those involving significant hazards, as shown in Figure 10. These can include chemical facilities as well as other types of facilities, such as aircraft and textile facilities.



Figure 10: Hazard analysis applications

### 2.3 Prevention component

Safeguards and barriers that result in an incident being avoided entirely comprise the prevention component of the safety triad. Examples of prevention measures are the development

of accurate, well-written operating procedures and the implementation of safety management systems [4]. In addition, this component consists of effective safety reporting and monitoring systems, hazard identification and risk assessment, and maintenance and change management systems.

Besides written guidelines and materials, this component also consists of physical components that prevent incidents from occurring, such as sufficient cooling capacity being provided to prevent thermal runaway for exothermic processes as well as diking to contain liquid to a specified area in the event of an incident resulting in overflow from tanks.

As operating procedures comprise a very significant component of the safety triad's effectiveness, significant research efforts have been conducted to identify elements and attributes of effective procedural systems. The Chemical Safety Board (CSB) has determined that the root cause of incidents to be nonexistent or poorly written operating procedures that do not comprehensively address human factors needs. As such, this illustrates pitfalls within writer's guides, which are one of the most critical elements in the development of effective operating procedures.

In response to this, a writer's guide framework was developed which is intended to guide the development of writer's guides within industries. To effectively establish this framework, 16 different writer's guides across process industries were investigated. It was found that 43 different content sections existed within them and only two sections were contained within at least 80% of the writer's guides. Furthermore, thirty categories of procedure-related regulations and standards were investigated from governmental entities, including OSHA and EPA [12].

To guide the framework, a procedure lifecycle was developed, as shown below in Figure 11. System development lifecycles across eight different industries, including software



development and architecture, were used in its development. The numbers and types of stages within these lifecycles were taken into consideration, and stages used in the final lifecycle are shown on the left in Figure 11.

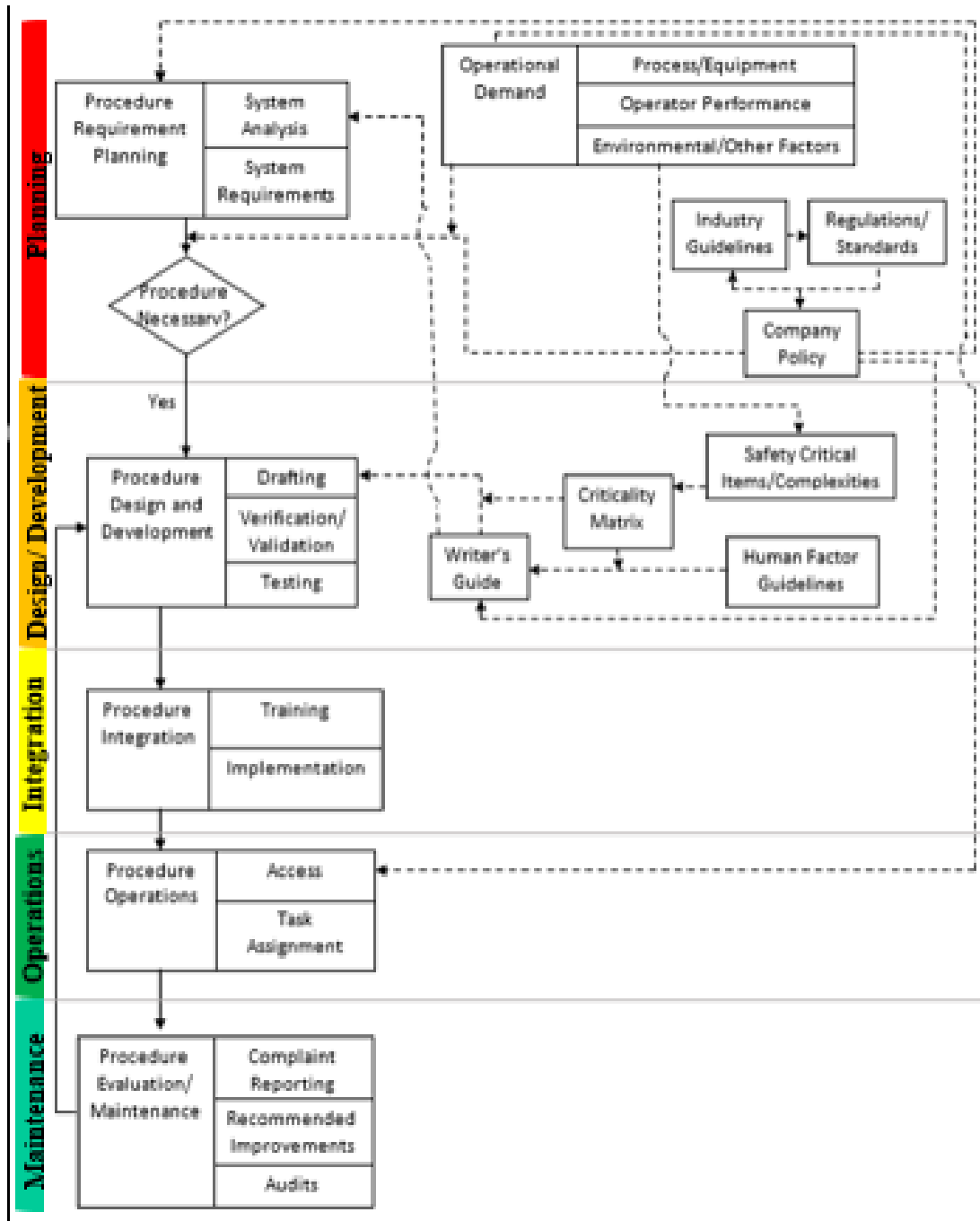


Figure 11: Procedure writer's framework (Reprinted from [12]. Parker, T., 2020.)

As the prevention component serves the most critical role in the safety triad of minimizing hazards, all prevention measures should be implemented before mitigation and response measures are considered. This is due to the fact that in cases for which multiple types of measures could be used to address the hazard, the most robust (e.g., prevention measures) should be chosen. Furthermore, by implementing prevention measures first, numbers and types of redundancies in measures can be identified.

#### *2.4 Mitigation component*

For incidents that occur in spite of the prevention measures implemented, mitigation measures should be taken to lessen the severity of the incident, either using physical barriers or alert systems to allow workers to respond appropriately. The effects to be addressed through mitigation include property damages as well as loss of life [3]. Examples of mitigation measures are sensors and alert systems, backup power sources, and the separation of hazards from people using barriers such as diking. An example of diking used for a tank is shown below in Figure 12.



Figure 12: Tank diking (Reprinted from [5]. Parker, T., Shen, R., & Wang, Q., 2022.)

Similar to the prevention component, all mitigation measures should be implemented before response measures. This is to ensure that the more robust measures are implemented in situations in which multiple measures could be used to address a hazard.

### *2.5 Response component*

When incidents occur, appropriate response measures should be taken in order to minimize the adverse impacts of the incident on the environment, property, and human life and health. Examples of response measures include evacuation, sheltering, and firefighting, as shown below in Figure 13.



Figure 13: Firefighting response to chemical incident (Reprinted from [1]. U.S. Chemical Safety and Hazard Investigation Board, 2016.)

Furthermore, following incident response, recovery involves repairs and cleanup as well as investigation and reporting of the incident to reduce the likelihood of similar incidents occurring in the future. Moreover, the incident command system (ICS) has been found to be an effective response measure for industrial facilities, which is described in detail in Section 2.6.1.

The response component should be considered the “last line of defense” when addressing hazards. That is, in situations in which prevention and mitigation measures are not sufficient to address the hazards, response measures should be taken.

### *2.6 Safety triad application for assessment of prior incidents*

The safety triad provides a useful framework for investigation and assessment of prior incidents to determine the deficiencies in the components that led to the incident. These incidents can have resulted from a wide variety of initiating events, which can include climate extremes, fires, and loss of coolant [4]. Furthermore, the incidents can occur in many types of facilities, such

as refineries, chemical storage warehouses, and offshore facilities. To investigate the effectiveness of the safety triad for assessment of prior incidents, it is herein utilized and discussed as it relates to incidents stemming from climate extremes.

A climate extreme is defined as “the occurrence of a value of a weather or climate variable above or below a threshold value near the upper or lower ends of the range of observed values of the variable [13-14].” Climate extremes have been established as the initiating events of a large number of industrial incidents over the years [15-17], and have included hurricanes [18] and extreme cold [19]. One of the most significant climate extremes in recent years was Hurricane Harvey, a Category 4 storm, which made landfall on August 25, 2017 in Rockport, Texas. Harvey resulted in a 500-year flood in the greater Houston area and 107 confirmed deaths, with an estimated \$125 billion in total damages. Harvey’s effects on the process industries included the halting of approximately one-third of U.S. chemical production as well as temporary shutdown of 20% of U.S. refineries. These unplanned shutdowns caused facilities to emit 4.6 billion pounds of airborne emissions containing harmful chemicals [20]. One of the most significant industrial incidents stemming from Hurricane Harvey was the Arkema chemical plant fires, with one of the fires shown in Figure 14. These resulted from the combustion of organic peroxides stored in refrigerated trailers [21]. Nine trailers containing the peroxides were involved, with three combusting spontaneously due to decomposition of the peroxides, and the other six intentionally ignited with controlled burns. In total, more than 350,000 pounds of organic peroxides combusted, resulted in 21 people seeking medical attention.



Figure 14: Arkema chemical plant fire (Reprinted from [22]. CBS News, 2017.)

Although the safety triad is represented as three distinct layers of an effective safety program, overlap exists between the layers, with each of the layers varying considerably based on the application. Based on the industrial incidents Dr. Mannan studied in his decades of work in the field, he observed that a deficiency in one of the layers has existed for most incidents to be initiated, with robustness of the other two layers necessary to minimize the consequences of the incident. However, for incidents in which a hazardous substance has overcome all three of the layers, catastrophic consequences have often resulted from the series of events that occurred [4].

Safety triad deficiencies for the Arkema plant chemical fires primarily involved the prevention and response layers. Prevention layer deficiencies included that all of the identified layers of protection shared the common mode of failure of flooding. This failure mode was likely to be unexpected because flooding on the scale of Harvey was very unlikely to occur during the life cycle of the plant. Response layer deficiencies included the decision to allow Highway 90 to remain open despite being located within the evacuation zone. This resulted in 21 people being exposed to the decomposition products [21].

The second incident was the propane fire at the Valero refinery in Sunray, Texas. This fire occurred on February 16, 2007 and resulted in injuries to four workers as well as a total shutdown of the facility. This incident occurred as a result of freezing temperatures, which resulted in water freezing and cracking a section of out-of-service piping, causing a release of high-pressure liquid propane which led to the fire [19]. Upon investigation, two layers of the safety triad were found to have serious deficiencies. Deficiencies within the prevention layer included that the refinery did not have an effective program to freeze-protect equipment and piping that was infrequently used or out of service. Additionally, mitigation layer deficiencies included that remotely operable shutoff valves had not been implemented, preventing shut-off of the fuel source after the fire had begun.

In the two analyses above, serious deficiencies were not present in all three layers of the safety triad, and the consequences of the incidents were not considered catastrophic. To comprehensively investigate the application of the safety triad as it relates to incidents having catastrophic consequences, a case study of the DuPont La Porte facility toxic chemical release was conducted, as presented below.

#### *2.6.1 Methyl mercaptan release case study*

To illustrate the effectiveness of the safety triad for assessment of prior incidents, a case study is herein presented involving toxic release of methyl mercaptan.

On November 14, 2014, four workers were killed from a release of approximately 24,000 pounds of highly toxic methyl mercaptan at the DuPont chemical manufacturing facility in La Porte, Texas. The initiating event of this incident was determined to be cold weather [24]. This

cold weather resulted in a domino effect, with a series of safety system deficiencies resulting in the catastrophic incident.

For the 24 hours preceding the toxic release, the average temperature had been approximately 40 °F and under 55 °F for the previous three days [25]. At temperatures below 52 °F, water and methyl mercaptan form the solid, ice-like material of methyl mercaptan clathrate hydrate [26]. Unbeknownst to the workers, the solid hydrate had formed in the methyl mercaptan feed piping leading to the reaction section, preventing its restart. During early troubleshooting stages, the operators were unaware of the cause of the feed piping blockage. Two days later, with collaboration between engineers and other experienced employees, the possibility that water had entered the piping and formed a solid hydrate was identified. The operations personnel then worked to warm the piping to allow the hydrate to be removed. To avoid over pressurization of the piping, valves along the methyl mercaptan piping as well as a waste gas vent header were opened, providing a pathway for the liquid methyl mercaptan to drain from the piping inside the manufacturing building. However, no operating procedures had been established involving opening the vent line, so the personnel were unaware of the hazards involved. Methyl mercaptan escaped from the waste gas vent header to the atmosphere and filled the manufacturing buildings with highly toxic vapors, killing the shift supervisor and three operators [24].

For methyl mercaptan, no facility within the manufacturing building was equipped to contain the leak and direct it to an incinerator for destruction. Furthermore, the two ventilation fans on the roof were not in operation during the release and lacked the capability to control the large quantity of gas at an acceptable exposure level. Alarms indicating high methyl mercaptan concentration were located only in the control room, with none to alert fieldworkers. Thus, when operators entered the manufacturing building to respond, they were unaware that respiratory



protection was needed. Furthermore, even operators who heard the alarms in the control room did not realize a release incident had occurred, as they had previously detected methyl mercaptan gas based solely on odor [24].

The emergency response team (ERT) was not immediately notified when the gas alarms were activated. Furthermore, when the ERT was called upon by the board operator to respond, they did not understand that a major toxic chemical release had occurred, and thus came with only technical rescue gear. When the ERT discovered the incident's magnitude, a 9-1-1 operator was contacted, but insufficient information was given to the operator, delaying the emergency response to the incident. With the loss of the shift supervisor, the emergency response plan prohibited assigning a different worker the role of providing hazard information. Without an accurate method to estimate the methyl mercaptan release rate, the dispersion plume size and concentration profile were significantly underestimated, with no detectors located along facility boundaries to monitor the real time concentrations of hazardous gases. For the emergency responders, self-contained breathing apparatus (SCBAs) were not immediately available as planned, resulting in air monitoring inside the building being delayed. In addition to being toxic, methyl mercaptan is a flammable gas and without air monitoring, the ERT could not determine if an explosive atmosphere existed within the building. Additionally, when performing the rescue of personnel, the ERT had no map of the building, and there were no cameras to assist in locating personnel remaining inside the building [24].

As a result of the issues that were determined to have led to this incident, the safety triad is utilized to identify effective strategies for ensuring robustness of each of the three components. This is done to ensure that similar incidents do not reoccur.

## **Prevention**

Although the potential for methyl mercaptan hydrate formation had been identified years earlier, it was likely unrecognized as a failure mode as a result of very low temperatures sustained for several days being unexpected. To address prevention layer deficiencies which led to the incident, heat tracing or some other process should be implemented to prevent the formation of hydrate. Additionally, detailed, well-written operating procedures should be developed regarding how to safely dissociate hydrate that forms to prevent methyl mercaptan release. Furthermore, the formation of hydrate should be monitored regularly, and operators should be trained on the hazards of hydrate formation and procedures for hydrate dissociation. If the operators had been trained on these topics, they would have likely recognized the presence of hydrate quickly and worked to dissociate it safely. Operators should also be trained on the toxic and flammable characteristics of methyl mercaptan if released, so as to be sensitive to abnormal operations within the reaction system.

## **Mitigation**

To mitigate the hazards, an open building structure should be considered for the processing of methyl mercaptan. If this is not viable, a facility should be equipped to contain the methyl mercaptan and route it to an incinerator. Furthermore, a ventilation system with sufficient capacity should be installed to maintain the air at an acceptable exposure level of gas regardless of the quantity released. Visual and audible alarms should be located both inside and outside buildings to alert workers to dangerously high concentrations of the gas so they know to wear appropriate respiratory protection. Furthermore, operators should be trained not to detect the presence of

methyl mercaptan based on odor, but based on the alarms that alert of dangerous concentrations of the gas.

## **Response**

In response to the incident, a comprehensive emergency response plan should be developed, with all involved personnel trained on the plan. For example, emergency vehicles should be maintained in good operating condition, maps of each building should be provided, SCBAs should be stored in quickly accessible locations, and detectors should be located along property lines to monitor real time gas concentrations. Plant emergency procedures should clearly outline the notification protocols for each type of plant emergencies, so the ERT can immediately identify the incident type and how to respond. Furthermore, in the emergency response plan, sufficient backup capabilities should be provided in the event that the designated individual is unable to respond.

To further enhance the robustness of the mitigation and response components of the safety triad in relation to this incident, the Incident Command System (ICS) is recommended for the integration of personnel, facilities, equipment, and communication systems within an organization to aid in proper incident mitigation and response. With this system, the incident commander manages all aspects of the emergency response [27]. Guided by the body of knowledge of all members as shown in Figure 15, each of whom have specialized knowledge and experience, the incident commander should identify all possible hazards of methyl mercaptan, determine any risks associated with emergency responses, and assess the incident consequences. Based on the eight-step process of the ICS, the incident commander should then develop and execute emergency

response procedures to minimize the impact of the incident on the emergency responders, operators, general public, facility, and environment.

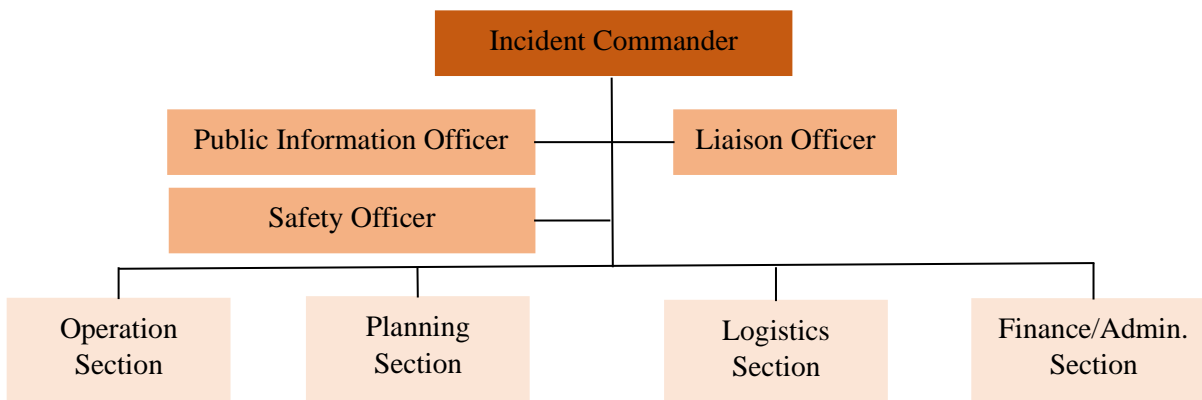


Figure 15: Basic organization of the ICS (Reprinted from [27]. Wang, Q., Ma, T., Hanson, J., & Larranaga, M., 2012.)

### *2.7 Safety triad application to chemical industries*

As was shown in Section 2.6, the safety triad can be applied after an incident has occurred in order to identify deficiencies that led to the incident as well as strategies to prevent the hazards from reoccurring. However, the safety triad also should be utilized in the design and maintenance of facilities, particularly those involving hazardous materials. This is so as to proactively design the facility in manner that prevents incidents from occurring.

Effective process safety management programs involve good design principles, engineering, and operating practices. As a result of this, OSHA Standard “29 CFR 1910.110” requires written management systems and written procedures [28]. From these, effective process safety management programs result in prevention and control of hazards, which translates to reduction in risk and thus sustained value [29]. One of the major hazards in chemical industrial

facilities is that of process scale-up [30-32], in which a reaction is conducted at the laboratory scale which is then increased to the industrial scale in order to produce some desired product. This is particularly significant in the context of the safety triad, as eliminating thermal and chemical reactivity hazards is critical to ensuring a robust prevention component for the scale-up of chemical processes.

Investigation of potential hazards associated with chemical facilities forms the basis for the following two chapters of research. This includes hazards associated with chemicals stored within warehouses as well as hazards associated with chemical reactions that are performed at industrial scales. By proactively conducting analyses of chemical hazards within facilities, the appropriate safety measures can be identified for the design and operation of the facilities. Furthermore, using the safety triad in conjunction with these identified hazards allows there to be verification that each of the components of the safety triad are sufficiently addressed. If deficiencies are found, additional testing can be conducted to further identify the appropriate strategies.

CHAPTER III  
CHEMICAL WAREHOUSE HAZARD IDENTIFICATION

*3.1 Chemical storage hazard introduction and hazard index techniques*

In chemical storage facilities, particularly chemical storage warehouses, many incidents have occurred. The hazards involved with chemical storage can depend on both the inherent characteristics of the chemicals as well as the storage conditions within the facilities. It has been shown that chemical incidents resulting from improper storage comprise nearly 25% of all chemical incidents [33-34]. Hazards inherent within chemicals include flammability, toxicity, reactivity, and interactions among chemical types.

In response to this, a number of hazard indices have been developed, such as the Dow Fire and Explosion Index (F&EI) [35] as well as the Logistic Warehouse Hazard Index (LWHI) [36]. The LWHI equation is shown below as Equation 1.

$$LHWI = \Sigma F_i * SHF$$

Equation 1: Logistic Warehouse Hazard Index

In this equation,  $F_i$  represents the penalty factors to account for material quantity, population density, and incident history. Furthermore, the SHF is the storage hazard factor and is determined by Equation 2.

$$SHF = 2^{NF} + 2^{NR} + 2^{NH}$$

Equation 2: Storage Hazard Factor

For this, NF represents the degree of flammability, which is based on the DIPPR 801 database. NR represents the degree of reactivity, which is determined using the original NFPA rating. Furthermore, NH represents the degree of the health hazard, which is modified using the corresponding PAC-3 (Protective Action Criteria) value for the material [36].

In addition to the hazard indices described above, MKOPSC developed a hazard index known as the PCHP (Potential to Cause Harm to the Public) index. This was developed so as to provide a means for assessing chemical process facilities on the basis of their potential to cause harm to the public [37]. For this, the hazard rating system is a function of the hazards associated with the chemicals within the facilities, the quantities of chemicals, and the population density within a two-mile radius from the facility. This index is shown below as Equation 3.

$$PCHP\ Index = MHI * \Pi F_i$$

Equation 3: Potential to Cause Harm to the Public Index

In this equation, MHI (material hazard index) represents the inherent chemical hazards, while  $F_i$  represents the penalty value for  $I =$  quantity, population density, and incident history. As such, a lower PCHP value represents a material with lower relative hazards when stored within a facility. This and similar hazard indices, such as the Dow Fire and Explosion Index (F&EI), have been utilized to quantify the hazards of potential fire, explosion, and reactive chemicals incidents in process units.

To implement the PCHP index as a tool for quantifying hazards within the warehouses, penalty values were determined regarding the quantities of chemicals stored, as shown below in Table 2. For this, quantity codes for each chemical type were identified based on chemical quantity ranges, as shown.

Quantity Code	Min (lbs.)	Max (lbs.)	Penalty Value
1	0	99	1.2
2	100	499	1.4
3	500	999	1.4
4	1,000	4,999	1.6
5	5,000	9,999	1.6
6	10,000	24,999	1.8
7	25,000	49,999	1.8
8	50,000	74,999	1.8
9	75,000	99,999	1.8
10	100,000	499,999	2
11	500,000	999,999	2
12	1,000,000	9,999,999	2
13	10,000,000		2

Table 2: Penalty values for chemical quantities (Reprinted from [37]. Mary Kay O'Connor Process Safety Center, 2016)

As shown, the quantity penalty values range from 1.2 – 2 and are solely based on the quantities of each type of chemical stored within the warehouses. However, the aforementioned hazard indices do not take into account hazards associated with specific combinations of chemicals stored together. As such, the quantities of toxic gases that may be released upon reaction of the chemicals with each other has not been investigated. Thus, this is herein investigated so as to identify hazards within warehouses directly related to their mixing and reactivity. This includes both unintentional chemical mixing, in which multiple chemicals are



inadvertently combined as a result of an incident, as well as intentional chemical mixing, in which the combination of chemicals results in a security threat.

### 3.2 Description of chemical storage warehouses

For the identification of chemical hazards, a total of 33 chemical warehouses were analyzed. The Houston Chronicle has published a series of articles that are aimed at identifying incident root causes that result in severe incidents. As part of this, more than 18000 records from 2581 facilities located in the Houston, TX vicinity were collected [37]. This data was compiled in accordance with the EPA Tier II format and shared with MKOPSC. An example of the raw data involving the warehouses is shown below in Figure 16.

	A	C	D	E	F	G	H	K	M	U	X
1	ID	FacilityName	FCity	FStreetAd	FZip	Latitude	Longitude	EnteredChemName	CAScorrect	MaxAmount	Code
2	46965	A	Pasadena	12900 Bay I		29.639444	95.062776	Cumene Hydroperoxide	80-15-9	10	Quantity
3	49108		Pasadena	12900 Bay I		29.639444	95.062776	Perkadox 40	94-36-0	6	
4	49111		Pasadena	12900 Bay I		29.639444	95.062776	Perkadox CH-50	94-36-0	6	
5	49112		Pasadena	12900 Bay I		29.639444	95.062776	Perkadox L	94-36-0	6	
6	49113		Pasadena	12900 Bay I		29.639444	95.062776	Perkadox L W75	94-36-0	6	
7	49114		Pasadena	12900 Bay I		29.639444	95.062776	Pro Cata	94-36-0	6	
8	8572		B	La Porte	1901 Aven	77571	29.6544	95.0369	N-PROPYL CHLOROFORMAL	109-61-5	
9	7564	La Porte		1901 Aven	77571	29.6544	95.0369	Isopropyl Chloroformate	108-23-6	9	
10	17879	HOCKLEY		14802 Park	77047	29.58167	95.27777	ALLUMINUM BICARBONATE	20850-72-8	8	

Figure 16: Example data from chemical warehouses (Reprinted from [36]. Zhang, Z., 2019.)

For this work, 33 warehouses were chosen from these, which contained more than 400 records. Within these warehouses, a total of 170 different chemical types were stored, with maximum quantities of the chemicals ranging from 500 lbs. to 100000 lbs. (corresponding to quantity codes ranging from 1-10). Of these chemicals, a large number possessed the potential to result in toxic gas and heat generation if combined [38-41].

### *3.3 Description of chemical incompatibilities/modeling software*

In response to this, CRW (Chemical Reactivity Worksheet) software was utilized to identify the compatibilities of the stored chemicals with each other as well as the associated toxic gases and heat generated. The CRW provides a database of more than 5000 chemicals and can be used to identify chemical reactivity, compatibility of absorbents, and the suitability of various materials of construction in relation to chemical processes.

Based on the incompatibilities identified, Aerial Locations of Hazardous Atmospheres (ALOHA) software was utilized to model potential gas release offsite impacts. ALOHA is an atmospheric dispersion model that allows the downwind dispersion distance of a chemical cloud to be estimated based on the toxicological and physical characteristics of the released chemical, atmospheric conditions, and specific circumstances of the release.

For this modeling, the maximum possible storage quantities within the warehouses for each of the chemicals were utilized (e.g., for a warehouse in which a maximum of 10,000 lbs. of a particular chemical would be stored within it at any point in time, this was the quantity input to the model). From this, the maximum downwind distances for the corresponding PAC values of each chemical were determined.

PAC (Protective Action Criteria) values provide the necessary information to evaluate chemical releases in order to take appropriate preventative actions. In the event of an emergency, these values may be utilized in order to establish the severity of an event and thus determine the appropriate actions to be taken. PAC values are divided into three levels, 1 to 3, with increasing values corresponding to increasingly severe events resulting from higher levels of exposure to the chemicals [42]. The three PAC levels are defined as follows:

PAC-1 : Mild, transient health effects.

PAC-2 : Irreversible or other serious health effects that could impair the ability to take protective action.

PAC-3 : Life-threatening health effects.

In addition to chemical hazard identification and chemical release modeling, prior incidents involving the chemicals stored in the warehouses were identified. To do so, the FACTS hazardous materials knowledge database was utilized. This database contains information on more than 25,700 industrial incidents and near-misses involving hazardous materials [40]. These incidents include BLEVEs, major spills, explosions, and derailments. These incidents were identified in order to further illustrate the hazards associated with the chemicals stored within the warehouses.

### *3.4 Chemical reactivity worksheet results*

For the hazards within the chemical warehouses, it was determined that 13 of the 33 warehouses contained chemical incompatibilities which would lead to toxic gases or heat if the chemicals were to be combined. The number of chemical incompatibilities within these warehouses ranged from one (e.g., one combination of two chemicals that if combined would present a hazard) to 143.

Examples of the chemical reactivity worksheets for three of the warehouses are shown below in Figures 17 to 19. For these worksheets, red boxes with “N” indicate that the two chemicals are not compatible with each other. The yellow boxes with “C” indicate that caution should be taken if the chemicals are combined. The green boxes with “Y” indicate that the

chemicals are compatible with each other and thus do not present reactivity hazards. Lastly, the orange boxes with “SR” indicate that the chemical is self-reacting and thus precautions must be taken in the storage of the chemical.

	2,2'-DICHLORODIETHYL ETHER	ACETIC ACID, SOLUTION, MORE THAN 80% ACID	AMMONIUM BIFLUORIDE, SOLUTION	AMMONIUM CHLORIDE	AMMONIUM PERSULFATE	BENZYL CHLORIDE	CALCIUM CHLORIDE	CITRIC ACID	ETHOXYLATED NONYLPHENOL	FUMARIC ACID	MALEIC ANHYDRIDE
2,2'-DICHLORODIETHYL ETHER	X										
ACETIC ACID, SOLUTION, MORE THAN 80% ACID	C	X									
AMMONIUM BIFLUORIDE, SOLUTION	N	N	X								
AMMONIUM CHLORIDE	N	C	C	X							
AMMONIUM PERSULFATE	N	N	N	N	X						
BENZYL CHLORIDE	Y	C	N	N	N	X					
CALCIUM CHLORIDE	N	C	C	Y	N	N	X				
CITRIC ACID	Y	N	N	C	N	Y	C	X			
ETHOXYLATED NONYLPHENOL	Y	N	N	N	N	Y	N	N	X		
FUMARIC ACID	C	Y	N	C	N	Y	C	N	N	X	
MALEIC ANHYDRIDE	C	N	N	C	N	Y	C	C	C	C	X

Figure 17: Chemical reactivity worksheet for warehouse 7

As can be seen from the CRW for Warehouse 7, 11 different chemicals were stored within it. From these, 29 combinations of chemicals are not compatible with each other as they could produce heat and/or toxic gases when combined. Furthermore, 17 combinations require caution in the event that they are combined and 8 are fully compatible with each other.

	ACETONE	BENZYLDMETHYLAMINE	CYCLOHEXANONE	ETHYLENEDIAMINE	FORMALDEHYDE	LEAD	METHANOL	NAPHTHALENE	O-XYLENE	PERCHLOROETHYLENE	PHENOL, LIQUID	PYRIDINE	SODIUM	VANADIUM PENTOXIDE
ACETONE	X													
BENZYLDMETHYLAMINE	Y	X												
CYCLOHEXANONE	Y	Y	X											
ETHYLENEDIAMINE	Y	Y	Y	X										
FORMALDEHYDE	C	N	C	N	SR									
LEAD	C	C	C	C	N	X								
METHANOL	C	Y	C	Y	C	Y	X							
NAPHTHALENE	Y	Y	Y	Y	Y	Y	Y	X						
O-XYLENE	Y	Y	Y	Y	Y	Y	Y	Y	X					
PERCHLOROETHYLENE	Y	N	Y	N	C	N	Y	Y	Y	X				
PHENOL, LIQUID	Y	C	Y	C	N	Y	Y	Y	Y	Y	X			
PYRIDINE	Y	Y	Y	Y	N	C	Y	Y	Y	N	C	X		
SODIUM	N	N	N	N	N	C	N	Y	Y	N	N	N	X	
VANADIUM PENTOXIDE	N	N	N	N	N	N	N	N	N	N	N	N	N	X

Figure 18: Chemical reactivity worksheet for warehouse 25

As can be seen from the CRW for Warehouse 25, 14 different chemicals were stored within it. From these, 24 combinations of chemicals are not compatible with each other as they could produce heat and/or toxic gases when combined. Additionally, 15 combinations require caution in the event that they are combined and 45 are fully compatible with each other. Furthermore, one chemical (formaldehyde) can self-react, indicating that precautions must be taken in its storage.

	2,2'- DICHLORODIETHYL ETHER	AMMONIUM PERSULFATE	BENZYL CHLORIDE	ETHANOLAMINE	ETHOXYLATED NONYLPHENOL	ETHYLENE GLYCOL MONOBUTYL ETHER	FUMARIC ACID	MALEIC ANHYDRIDE
2,2'-DICHLORODIETHYL ETHER	X							
AMMONIUM PERSULFATE	N	X						
BENZYL CHLORIDE	Y	N	X					
ETHANOLAMINE	N	N	N	X				
ETHOXYLATED NONYLPHENOL	Y	N	Y	Y	X			
ETHYLENE GLYCOL MONOBUTYL ETHER	Y	N	Y	Y	Y	X		
FUMARIC ACID	C	N	Y	N	N	N	X	
MALEIC ANHYDRIDE	C	N	Y	N	C	C	C	X

Figure 19: Chemical reactivity worksheet for warehouse 33

As can be seen from the CRW for Warehouse 33, 8 different chemicals were stored within it. From these, 13 combinations of chemicals are not compatible with each other as they could produce heat and/or toxic gases when combined. Furthermore, 5 combinations require caution in the event that they are combined and 5 are fully compatible with each other.

From the chemical reactivity worksheets produced for each of the facilities, it was found that 13 of the 33 warehouses contained chemicals that are incompatible if combined, leading to the generation of heat or toxic gas. Furthermore, 10 of these 13 warehouses contained chemicals that require caution in the event that they are combined. Moreover, 5 of the warehouses contained chemicals that are self-reactive, which must be carefully accounted for in their storage.

### 3.5 ALOHA modeling results and toxic gas incidents

After the chemical incompatibilities were determined within the warehouses, ALOHA modeling was conducted to determine the potential offsite impacts of the gas releases. To

conduct the ALOHA simulations, a number of assumptions were made in the model. These assumptions included that each of the facilities was located in Houston, TX (all were, in fact, located in the Greater Houston area), with average wind speed of 8 mph, air temperature of 67 °F, and partly cloudy weather.

To determine the quantities of gases for the ALOHA models, the maximum possible storage quantities for each of the chemicals within the warehouses were utilized, as described in Section 3.2. Then, the limiting reactant (on a molar basis) for each of the chemical combinations was determined and the gas quantities were determined with the assumption that the limiting reactant was consumed entirely and the reaction proceeded to completion.

To account for the toxic gas generation within all 13 warehouses with chemical incompatibilities, a total of 64 ALOHA models were generated involving the toxic gases identified. The PAC values (described in Section 3.2) for these gases varied significantly, with hydrogen gas having a PAC-3 value of 400000 ppm and phosgene having a PAC-3 value of 0.75 ppm. Examples of the ALOHA models for toxic gases generated within three of the warehouses are shown below in Figures 20 to 22.

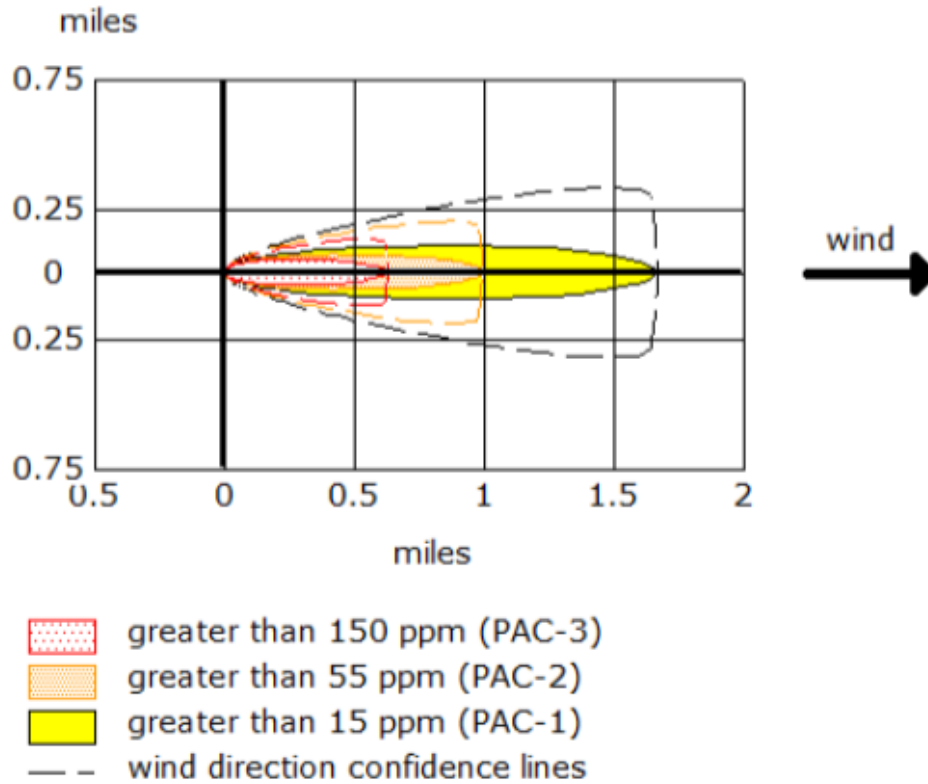


Figure 20: ALOHA model for carbon monoxide in warehouse 2

As can be seen from Figure 20, carbon monoxide has a PAC-1 value of 15 ppm, PAC-2 of 55 ppm, and PAC-3 of 150 ppm. In this warehouse, a maximum of 1300 lbs. of carbon monoxide could be released if the limiting reactant was consumed entirely to form it. Thus, in this case the PAC-1 would be attained a maximum of 1.7 miles from the source, the PAC-2 attained 0.95 miles from it, and the PAC-3 attained 0.65 miles from it.



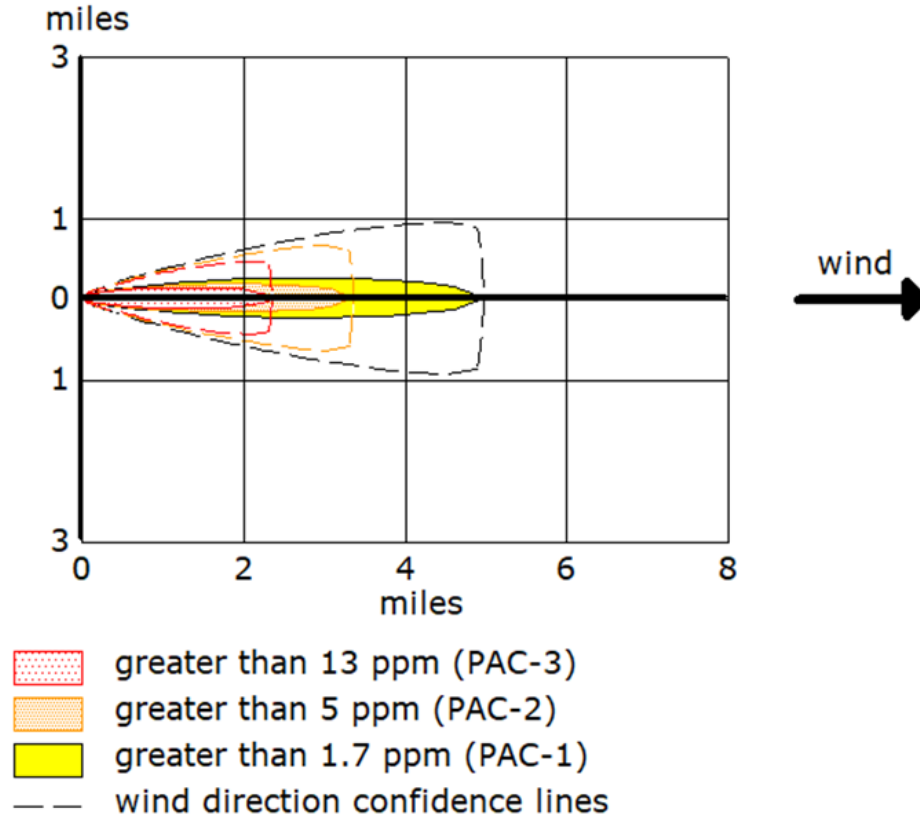


Figure 21: ALOHA model for fluorine gas in warehouse 7

As can be seen from Figure 21, fluorine gas has a PAC-1 value of 1.7 ppm, PAC-2 of 5 ppm, and PAC-3 of 13 ppm. In this warehouse, a maximum of 2080 lbs. of fluorine gas could be released if the limiting reactant was consumed entirely to form it. Thus, in this case the PAC-1 would be attained a maximum of 5.0 miles from the source, the PAC-2 attained 3.4 miles from it, and the PAC-3 attained 2.4 miles from it.

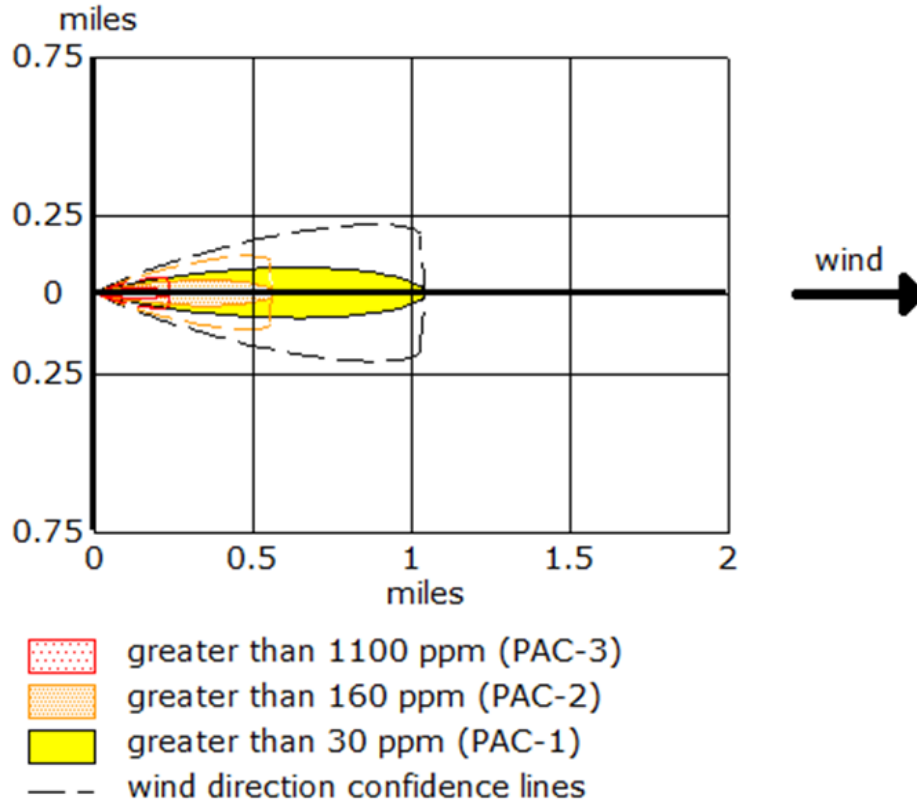


Figure 22: ALOHA model for ammonia in warehouse 23

As can be seen from Figure 22, ammonia has a PAC-1 value of 30 ppm, PAC-2 of 160 ppm, and PAC-3 of 1100 ppm. In this warehouse, a maximum of 1760 lbs. of ammonia could be released if the limiting reactant was consumed entirely to form it. Thus, in this case the PAC-1 would be attained a maximum of 1.0 miles from the source, the PAC-2 attained 991 yards from it, and the PAC-3 attained 418 yards from it.

As shown from the results of the ALOHA models, it is seen that the predicted downwind dispersion distances for each PAC value can vary significantly for each of the toxic gases. This is due to both the types and quantities of chemicals stored within the warehouses, with each producing a significant effect for this result. The 64 ALOHA models for the generated products within the 13 warehouses are provided in Appendix A.

In order to determine the real-world consequences associated with the toxic gases generated, investigation reports were examined regarding incidents involving 25 of the toxic gases. These reports were published by U.S. federal agencies involved with safety and health, including CSB [43] and OSHA [44], and a summary of these reports is shown below in Table 3.

<b>Chemical Name</b>	<b>Date/Company/Description</b>	<b>Injuries</b>	<b>Deaths</b>
Alcohol (Isopropyl)	December 31, 2018 - Bayer Healthcare Llc Isopropyl Alcohol Asphyxia	4	0
Ammonia	March 1, 2011 - Millard Ammonia Release Incident	150	0
Benzene	January 2, 2004 - Chevron Texaco Gasoline Leak Containing Benzene	1	0
Carbon Dioxide	August 3, 2007 - Primavera Ristorante Storage Room Carbon Dioxide Release	0	1
Carbon Monoxide	February 3, 2019 - Nr Construction, Inc. Home Carbon Monoxide Poisoning	0	4
Chlorine Dioxide	September 3, 2007 - Pacific Coast Producers, Inc. Exposure Incident	39	0
Chlorine Gas	May 30, 2017 - Holmes Foods Chlorine Gas Release	0	1
Ethanol	October 10, 2016 - Southwest Iowa Renewable Energy Ethanol Release and Fire	0	1
Formaldehyde	May 21, 2004 - Mc Gill Corporation Chemical Baking Oven Explosion	1	0
Hexane	March 28, 2018 - Firestone Polymers, Llc Hexane Release and Flash Fire	2	0
Hydrochloric Acid	March 10, 2019 - Basin Concrete, Inc. Hydrochloric Acid Release	0	1
Hydrofluoric Acid	January 23, 2019 - Monroe Energy, Llc Hydrofluoric Acid Release	5	0

Table 3: Toxic gas incidents

<b>Chemical Name</b>	<b>Date/Company/Description</b>	<b>Injuries</b>	<b>Deaths</b>
Hydrogen Cyanide	April 17, 2013 - Death of Doctor from Cyanide Poisoning	0	1
Hydrogen Fluoride	March 7, 2006 - JV Industrial Companies Hydrogen Fluoride Release	8	0
Hydrogen Gas	January 8, 2007 - Muskingum River Power Plant Hydrogen Explosion	0	1
Hydrogen Sulfide	December 11, 2002 - Environmental Enterprises Hydrogen Sulfide Release	1	0
Methane	November 28, 2017 - Rockwell Mining Llc Methane Asphyxia	0	1
Nitric Acid	November 2, 2017 - Diamond Innovations, Inc. Nitric Acid Vapor Cloud	1	0
Nitric Oxide	August 28, 2016 - Airgas Nitrogen Oxide Decomposition and Explosion Incident	0	1
Nitrogen Gas	July 3, 2017 - Industrial Gas Distributors Gas Room Nitrogen Release	0	1
Oxygen Gas	September 21, 2014 - United States Steel Corporation Oxygen Release and Fire	2	1
Phosgene	July 7, 2011 - DuPont Corporation's Belle, West Virginia Exposure Incident	0	1
Sodium Hydroxide	April 14, 2018 - Hain Pure Protein Corporation Sodium Hydroxide Release	1	0
Sulfur Dioxide	October 8, 2017 - Rio Tinto Kennecott Copper Company Sulfur Dioxide Release	0	1
Sulfuric Acid	September 15, 2002 – Farragut, TN Derailment / Acid Spill	17	0

Table 3: Continued

As can be seen by the table, a large number of injuries and deaths have occurred as a result of hazards associated with toxic gas generation. These include an incident involving ammonia release, which resulted in 150 injuries, as well as an incident involving carbon

monoxide poisoning, which resulted in 4 deaths. From this data, it is evident that toxic gases generated by chemicals reacting with each other pose significant threats to human health and safety, particularly within chemical storage warehouses.

### *3.6 Safety triad application to chemical storage facilities*

From these results, it was determined that the use of the CRW and ALOHA software to identify hazards provides useful information for identifying potential hazards within chemical storage facilities. Additionally, many chemical warehouses have the potential for generation of toxic gases based on the chemicals stored within them. Furthermore, the dispersion distances of toxic gases can be very significant, particularly when large quantities of chemicals are stored.

The results from this modeling highlights the need for each of the components of the safety triad to be robust for facilities with stored chemicals that can react with each other. Examples of measures for the prevention component include clear labeling of the chemicals with the associated material safety data sheet (MSDS) information easily accessible by all workers. Furthermore, chemicals that can react with each other should be located a sufficient distance from each other such that they cannot be inadvertently combined.

Example mitigation measures for chemical storage facilities include barriers to separate the chemicals from workers in the event that the chemicals are combined as well as alert systems to notify workers in the event of hazardous chemical reactions occurring. Additionally, example response measures include providing well-defined evacuation routes for workers with corresponding training as well as ensuring that fires associated with the chemicals can be extinguished quickly.

## CHAPTER IV

### THERMAL HAZARD ANALYSIS OF INDUSTRIAL REACTIONS\*

#### 4.1 Introduction to runaway reactions

Industrial processes must be controlled carefully to ensure that thermal runaway as a result of process scale-up does not occur. Thermal runaway occurs when the heat generated by an exothermic reaction exceeds the ability of the cooling system to remove the heat, and is based on the Semenov theory, shown in Figure 23.

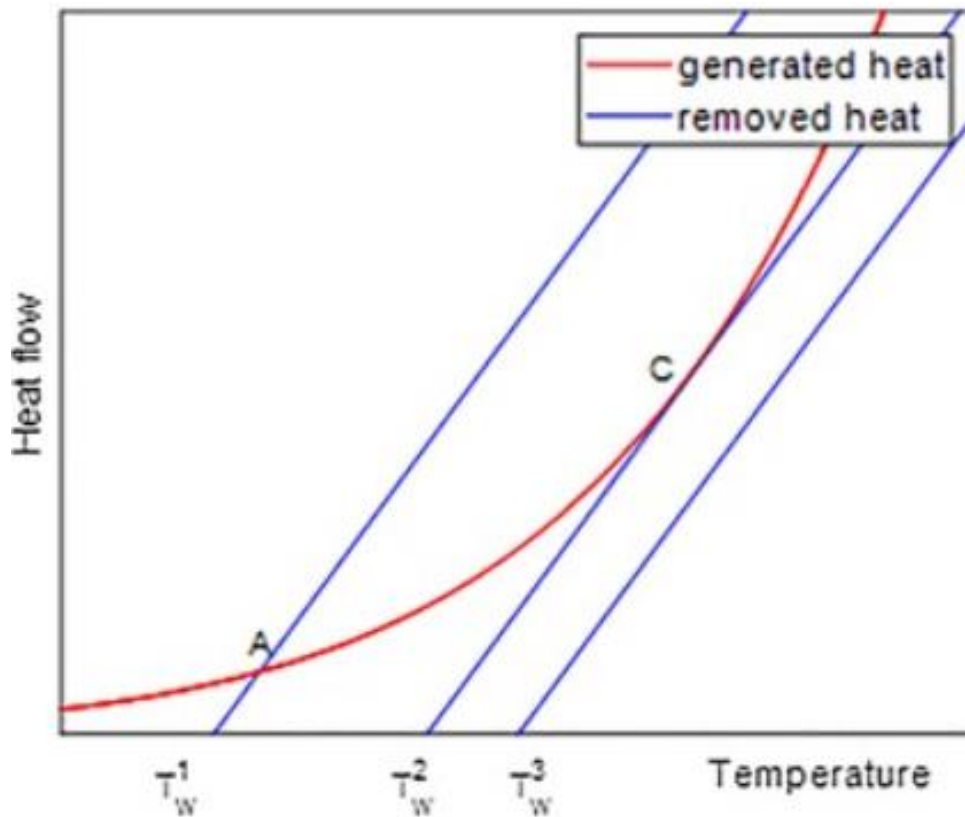


Figure 23: Semenov diagram (Reprinted from [45]. Shouman, A. R., 2006.)

\* Part of this chapter is reprinted with permission from “Application of response surface methodology for hazard analysis of 2-butanol oxidation to 2-butanone using RC1 calorimetry” by Parker, T., Mao, Y., Wang, Q., 2022. Journal of Loss Prevention in the Process Industries, Volume 75, Pages 1-10, Copyright 2022 by Elsevier

The criterion for reaction stability based on the Semenov theory is shown below in Equation 4.

$$(T - T_w) \leq \frac{RT_w^2}{E}$$

Equation 4: Reaction Stability Criterion

For this,  $T_w$  is the wall temperature,  $R$  is the gas constant, and  $E$  is the activation energy. Furthermore, the Semenov number is the ratio of dimensionless reaction heat parameter and the heat transfer, shown below in Equation 5 [45]:

$$\psi = \frac{(-\Delta H_r)kc^n}{UA} \frac{E}{RT^2}$$

Equation 5: Semenov Number

For this,  $\Delta H_r$  is the heat of reaction,  $k$  is the reaction rate constant,  $C$  is the concentration,  $U$  is the overall heat transfer coefficient,  $A$  is the heat transfer area,  $E$  is the activation energy, and  $R$  is the gas constant. Solving from this criterion, a critical point for  $\psi$  occurs at the value of  $e^{-1}$  (0.368). That is, for  $\psi \geq e^{-1}$ , the system is at an unsteady state and thermal runaway can occur. Likewise, for  $\psi \leq e^{-1}$ , the system is at a steady state.

In addition to this, the Van Welsenaere and Froment criterion provides a model for determination of when thermal runaway will occur for a batch reactor with overall first-order kinetics [46]. For this, the critical Semenov number is defined as shown in Equation 6 below.

$$\Psi_c(t) = \left(1 + \frac{1}{Q} + \frac{1}{Q^2}\right)(\eta_c - \eta_a) \left(\exp\left(-\frac{\eta_c}{1 + \frac{\eta_c}{\gamma}}\right)\right)$$

Equation 6: Critical Semenov Number

For this, Q and  $\eta_c$  are defined as shown in Equation 7 Equation 8 below.

$$Q = \frac{\sqrt{1 + 4\left(\frac{B(t)}{\eta_c - \eta_a} - 1\right)}}{2}$$

Equation 7: Calculation of Q

$$\eta_c = \frac{\gamma}{2} \left[ (\gamma - 2) - \sqrt{\gamma(\gamma - 4) - 4\eta_a} \right]$$

Equation 8: Calculation of  $\eta_c$

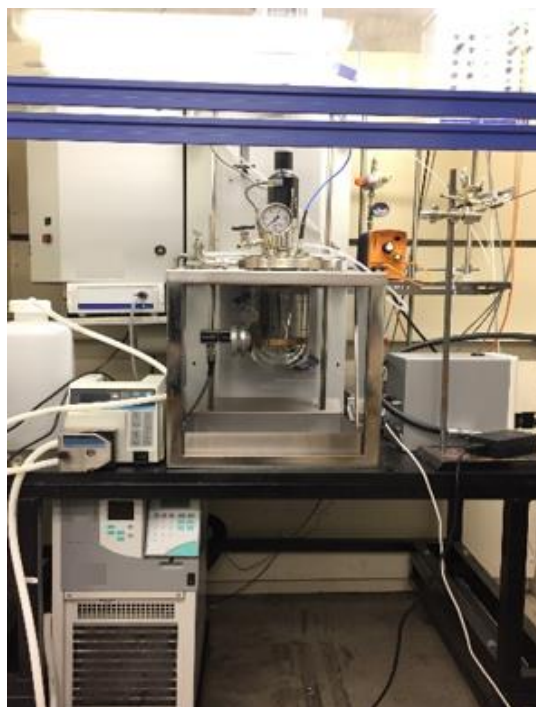
For this criterion, in situations in which the Semenov number exceeds the value of the critical Semenov number, system cooling alone is insufficient to prevent thermal runaway. Thus, this criterion provides useful insight into the potential for thermal runaway within a reaction system [46].

#### 4.2 Description of laboratory equipment

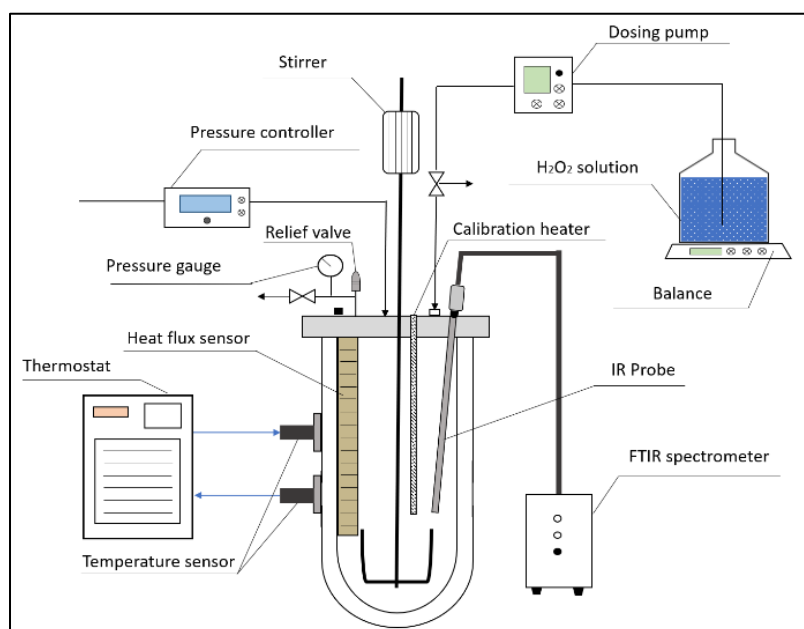
For the identification of safer operations of chemical processes, the Mettler Toledo RC1e calorimeter is utilized. The Mettler Toledo RC1e calorimeter setup is shown in Figure 24. Image (a) shows a photograph of the RC1e setup while image (b) shows a diagram of the major components of the calorimeter. The calorimeter consists of a 1 L glass reactor which is resistant



to a pressure of up to 10 barg. As can be seen in image (b), the temperature sensor allows the temperature of the vessel contents to be maintained at a specified value as a result of a silicone oil heating/cooling jacket. The reactor contains heat flux sensors within it for heat flow measurement. Additionally, the reactor contains a pressure gauge (analog AISI316, digital HC-22) and rupture disk (set to 10 barg) in order to perform reactions at controlled pressures. Batch or semi batch dosing can be attained with a ProMinent solenoid metering pump, which contains an interlock that halts the dosing if the temperature or pressure exceeds 150 °C or 6 barg, respectively. To measure the product composition, a ReactIR 15 spectrometer that is composed of a mercury cadmium detector and diamond-composite *in situ* FTIR (Fourier-transform infrared spectroscopy) sensor probe can be used. In order to maintain the vessel contents as well-mixed, a stirring rod is used within the vessel which rotates at a specified speed and is positioned in such a manner as to not contact the probes and sensors within the vessel. The temperature within the vessel is maintained in real-time using a high performance RTCal box which is connected to a Julabo temperature-controlled chiller. The iControl software is connected to the RC1e which allows data analysis in real-time.



a



b

Figure 24: RC1e laboratory setup (a) Photograph (b) Diagram (Reprinted from [46]. Liu, G., & Wilhite, B. A., 2019)

### 4.3 2-butanol to 2-butanone oxidation analysis

2-butanone is an organic solvent of relatively low toxicity which is found in many applications. These include being used in industrial and commercial products as a solvent for paints, adhesives, and cleaning agents [47]. Furthermore, it can be used as a dewaxing agent and in the manufacture of smokeless powder and colorless synthetic resins. One method of generation of 2-butanone involves the oxidation of 2-butanol using hydrogen peroxide in the presence of a catalyst. This catalyst can consist of a number of compounds, with titanium silicalite-1 ( $\text{TiO}_2/\text{SiO}_2$ ) being a commonly used catalyst [48]. The complete reaction is shown in Figure 25, including the decomposition of hydrogen peroxide.

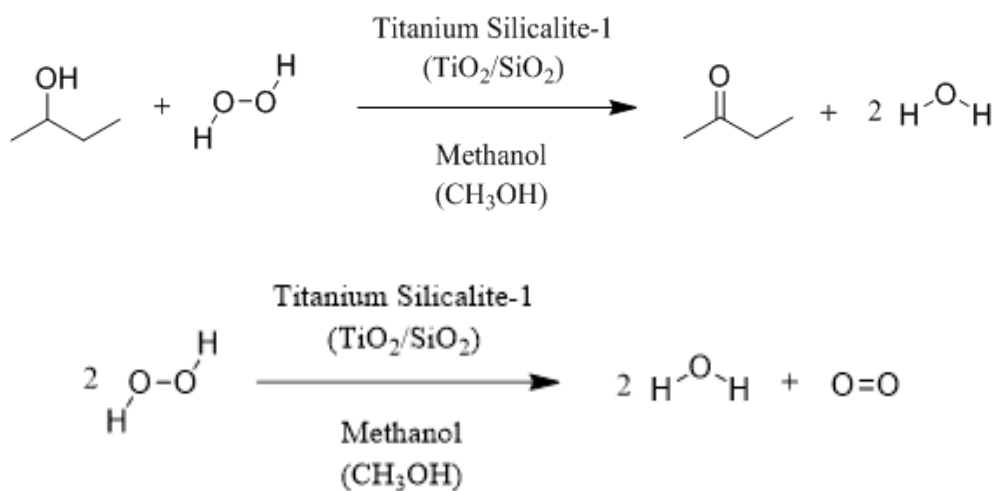


Figure 25: 2-butanone synthesis reaction with hydrogen peroxide side reaction

Hydrogen peroxide as the oxidant provides the benefit of being a relatively “green” oxidant, as it produces only the side product of water rather than other harmful products [49]. Furthermore, it is an effective oxidant for a variety of organic oxidation reactions [50-52]. One of the drawbacks of using hydrogen peroxide, however, is that its decomposition is highly

exothermic, with the heat released from self-decomposition being 98.2 kJ/mol [49]. As such, its use in industrial processes must be controlled carefully to ensure that thermal runaway as a result of process scale-up does not occur [53-62].

In past works, the interaction effects of multiple parameters on the heat release for the synthesis of 2-butanone from 2-butanol have not been investigated. In response to this, the effects of catalyst amount, reactant (2-butanol) amount, and reaction temperature on the heat release amounts during the synthesis of 2-butanone from 2-butanol are investigated herein.

For the experiments, titanium silicalite-1, 2-butanol, and methanol were added to the vessel initially. Titanium silicalite-1 was chosen as the catalyst because it is a commonly utilized catalyst in oxidation reactions [48]. Furthermore, methanol was chosen as the solvent because its oxidation rate is significantly lower than those of secondary alcohols [48]. The amounts of titanium silicalite-1 and 2-butanol were varied for the different experiments to determine their effects on the heat release amounts. Sufficient methanol was added to the vessel for each experiment so that the total contents had a volume of 0.4 L. This was to ensure that there was sufficient volume of contents to ensure that the reaction mixture would be well-mixed throughout the experiments. These reactants were then heated to the desired reaction temperature, with the pressure held constant as atmospheric pressure and the stirrer speed set to 150 rpm in order to provide sufficient mixing. Once the temperature was sufficiently stabilized at the proper value, room temperature hydrogen peroxide was added to the mixture over the course of a 10-minute period. For this, 20.4 mL of hydrogen peroxide was added in total, with 5.1 mL added in 2.5-minute increments.

For this work, the influences of reaction temperature, 2-butanol concentration, and catalyst amount on the heats of reaction were investigated. The conditions for each of the experiments are shown below in Table 4.

<b>Experiment</b>	<b>Temperature (°C)</b>	<b>2-Butanol Volume (mL)</b>	<b>Catalyst Concentration (wt%)</b>
1	30	19.89	2.4
2	45	19.89	3.6
3	60	19.89	4.8
4	30	37.39	2.4
5	45	37.39	3.6
6	60	37.39	4.8
7	30	54.95	2.4
8	45	54.95	3.6
9	60	54.95	4.8

Table 4: Reaction conditions for 2-butanol oxidation experiments

To reduce the number of experiments to 9 while effectively capturing the system characteristics, response surface methodology was utilized to model curvature of the data and identify factors that contribute most to the response [63-75]. For this, Minitab software was used, and the method of least squares was used to generate surface maps and contour plots illustrating the contributions of each variable, including the initial 2-butanol concentration, catalyst amount, and reaction temperature, to the overall heat release amounts [76].

For each of the 9 experiments conducted, a graph showing the heat release rates and vessel temperature in real-time were generated using the iControl software. An example of one

of these graphs for the experiment conducted with a 2-butanol concentration of 0.534 mol/L, catalyst concentration of 2.4 wt %, and temperature of 28 °C is shown in Figure 26.

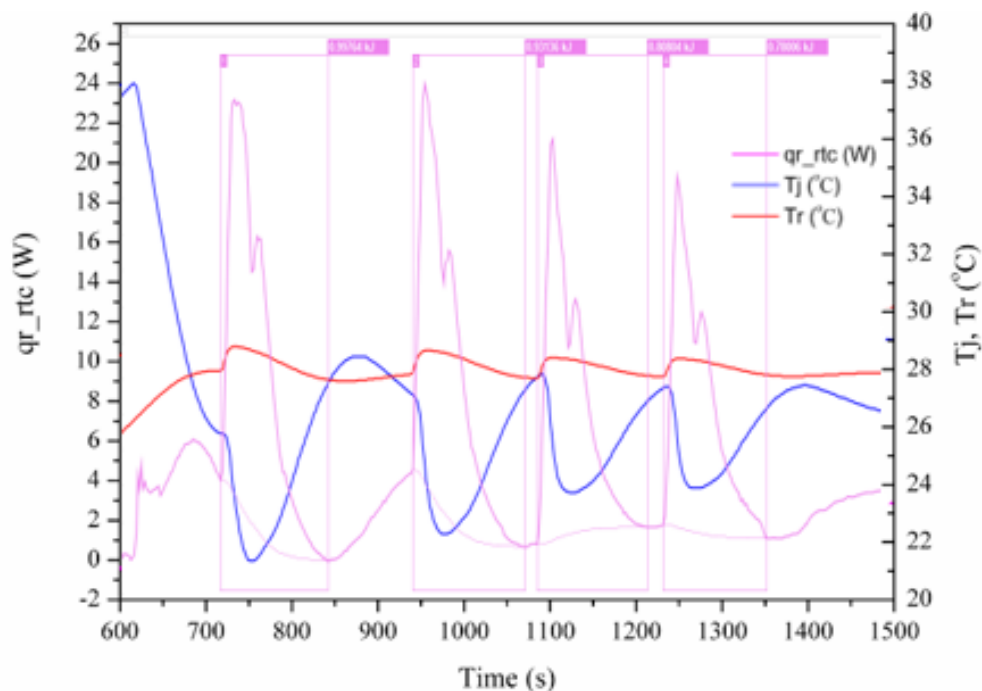


Figure 26: iControl temperature and heat release graph

Integration and summation of the 4 heat release peaks for each of the experiments provided the total heat release amount (kJ) for each of the experiments. The integrals for each peak were obtained over the interval from the time the hydrogen peroxide was added until the change in heat release rate ( $dq/dt$ ) was 0 W, as shown in Figure 26. This was normalized to the scale-independent parameter of kJ/kg reaction mass and served as the response variable for each of the surface maps and contour plots.

Figure 27 shows the surface map and contour plot for the effects of vessel temperature and initial 2-butanol concentration on the heat release amounts. For these, the catalyst concentrations at each data point correspond to the reaction conditions in Table 4.

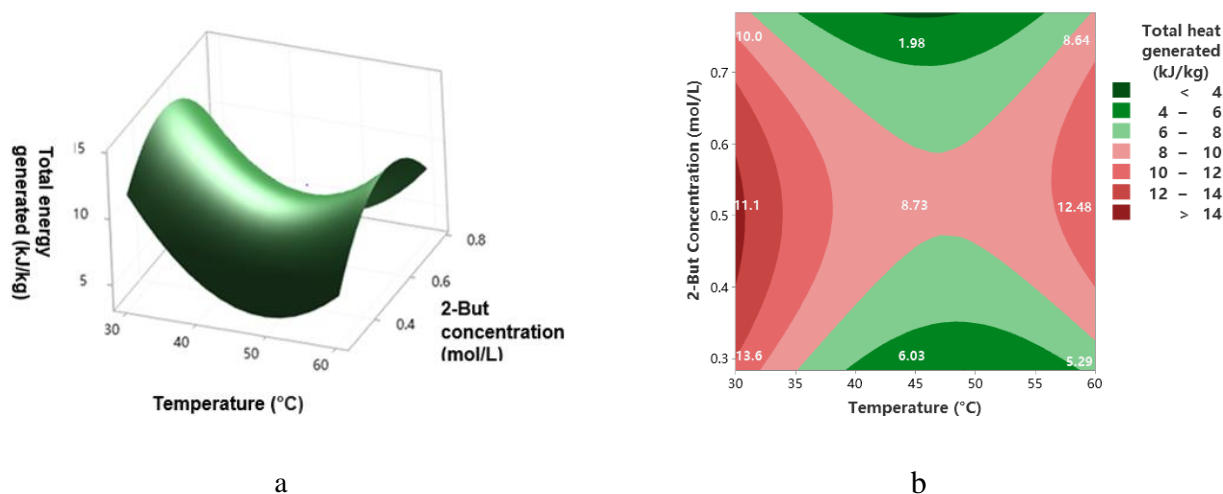


Figure 27: Effects of temperature and initial 2-butanol concentration on heat release

(a) Surface map (b) Contour plot

As can be seen from the contour plot in Figure 27 (a), the highest amount of heat release (kJ/kg reaction mass) occurred at a temperature of 30 °C with a 2-butanol concentration of approximately 0.5 mol/L. Furthermore, the lowest total heat release amount occurred at 2-butanol concentrations of approximately 0.3 and 0.78 mol/L at a temperature of 45 °C. Possible explanations for the lowest heat release occurring at moderate temperatures include that the side reaction of hydrogen peroxide decomposition may be prominent at the lower temperature due to the slower primary reaction of 2-butanol to 2-butanone. Thus, a higher heat release at low temperatures occurs. Furthermore, the primary reaction of butanol to butanone occurs faster at higher temperatures, leading to higher heat release at high temperatures. The p-value is a statistical measure that describes the probability of obtaining results at least as extreme as the observed results of a statistical hypothesis test. For this, a lower p-value corresponds to a pattern observed being more statistically significant. Furthermore, the  $R^2$  value is a statistical measure of

fit, with values close to 100% representing that variation of a dependent variable is nearly entirely explained by the independent variable(s). The p-value for this regression model is 0.099. Furthermore, the regression model has an  $R^2$  of 89.93%, indicating that the data fits relatively closely with the regressed model. The quality of the fit for this model indicates that the effects of reaction temperature in combination with the initial concentration of 2-butanol play a very significant role in the heat generation from the reaction.

Figure 28 shows the surface map and contour plot for the effects of vessel temperature and catalyst concentration on the total heat release amounts.

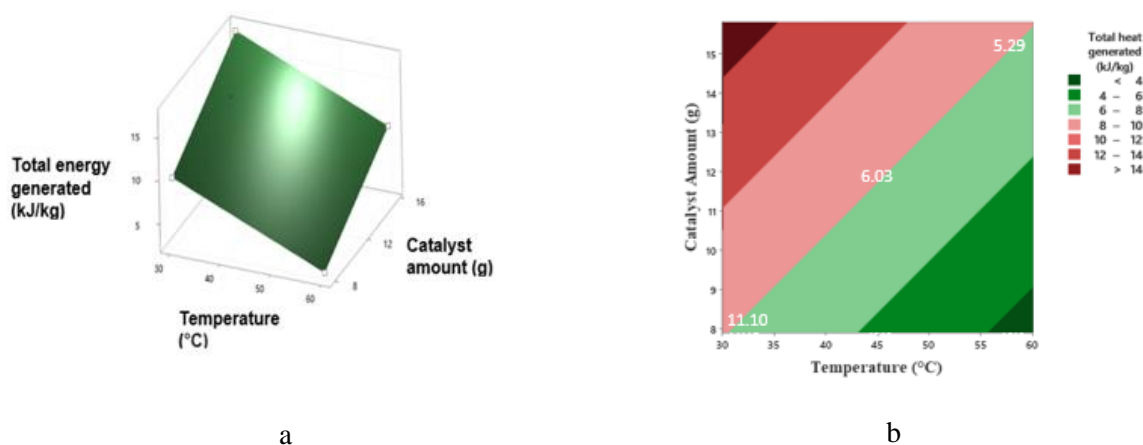


Figure 28: Effects of temperature and catalyst amount on heat release

(a) Surface map (b) Contour plot

The contour plot in Figure 28 (a) indicates that lower temperatures of approximately 30 °C and high catalyst amounts of approximately 15 g (4.8 wt %) resulted in higher total heat release amounts (kJ/kg reaction mass), while higher temperatures of approximately 60 °C and low catalyst amounts of approximately 8 g (2.4 wt %) resulted in lower heat release amounts.

The p-value for this regression model is 0.115. Furthermore, this regression model has a  $R^2$  of



51.31%. This indicates that these data do not fit closely with the regressed model. The quality of the fit for this model indicates that the effects of reaction temperature in combination with the catalyst amount play a less significant role in the heat generation from the reaction.

Figure 29 shows the surface map and contour plot for the effects of catalyst amount and initial 2-butanol concentration on the total heat release amounts.

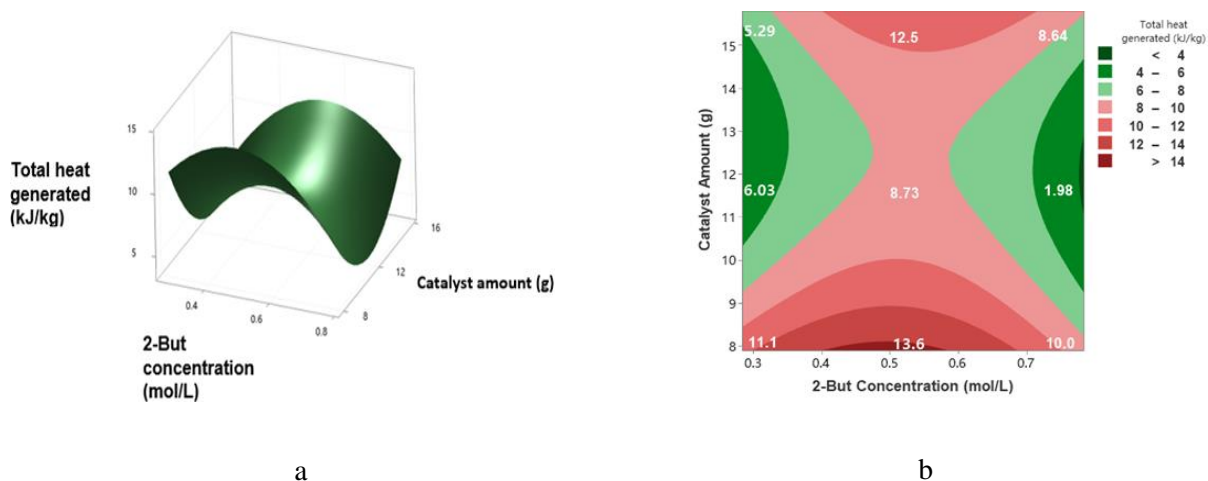


Figure 29: Effects of initial 2-butanol concentration and catalyst amount on heat

(a) Surface map (b) Contour plot

The contour plot in Figure 29 (a) indicates that a 2-butanol concentration of approximately 0.5 mol/L combined with either a low amount of catalyst of approximately 8 g (2.4 wt %) or high amount of approximately 15 g (4.8 wt %) resulted in higher total heat release amounts (kJ/kg reaction mass), while low 2-butanol concentrations of approximately 0.3 mol/L or high concentrations of approximately 0.78 mol/L combined with moderate catalyst amounts of approximately 12 g resulted in the lowest total heat release amount. The p-value for this regression model is 0.098. Furthermore, this regression model has a  $R^2$  of 90.03%, indicating

that the data fits relatively closely with the regressed model. The quality of the fit for this model indicates that the effects of the initial concentration of 2-butanol in combination with the catalyst amount play a very significant role in the heat generation from the reaction. Potential reasons that moderate temperatures and catalyst amounts result in the lowest heat release amounts include that for lower temperatures, more of the hydrogen peroxide will decompose and thus more heat is released. Furthermore, for higher temperatures, a higher 2-butanone conversion is achieved, resulting in an increase in the quantity of heat released. For higher catalyst amounts, the 2-butanone synthesis reaction proceeds more quickly and thus the heat release cannot be moderated readily. Moreover, for lower catalyst amounts, more of the hydrogen peroxide will decompose.

To determine 2-butanone yields associated with the oxidation of 2-butanol to 2-butanone, FTIR spectroscopy was utilized for two combinations of parameters. To do so, pure 2-butanone was added to 300 mL of methanol in 1-gram increments in order to identify the location and intensity of the peaks associated with the carbonyl (C=O) group, as this group is unique to the 2-butanone for the compounds involved in these experiments. From this, it was determined that the location of the peaks corresponding to the carbonyl group occurred at a wavenumber of approximately  $1715\text{ cm}^{-1}$ . Furthermore, the change in the height of the reaction spectra corresponding to each addition of the 2-butanone was determined, and the FTIR calibration curve was generated from these data, which is shown in Appendix B.

To determine the reaction yields for 2-butanol oxidation to 2-butanone, two of the reaction systems previously investigated were carried out using FTIR spectroscopy. These were the reaction system at a temperature of  $30\text{ }^{\circ}\text{C}$  with a 2-butanol concentration of  $0.284\text{ mol/L}$  and catalyst concentration of  $2.4\text{ wt}\%$  as well as the reaction system at a temperature of  $45\text{ }^{\circ}\text{C}$  with a

2-butanol concentration of 0.534 mol/L and catalyst concentration of 3.6 wt%. The FTIR spectra are shown below in Figures 30 and 31.

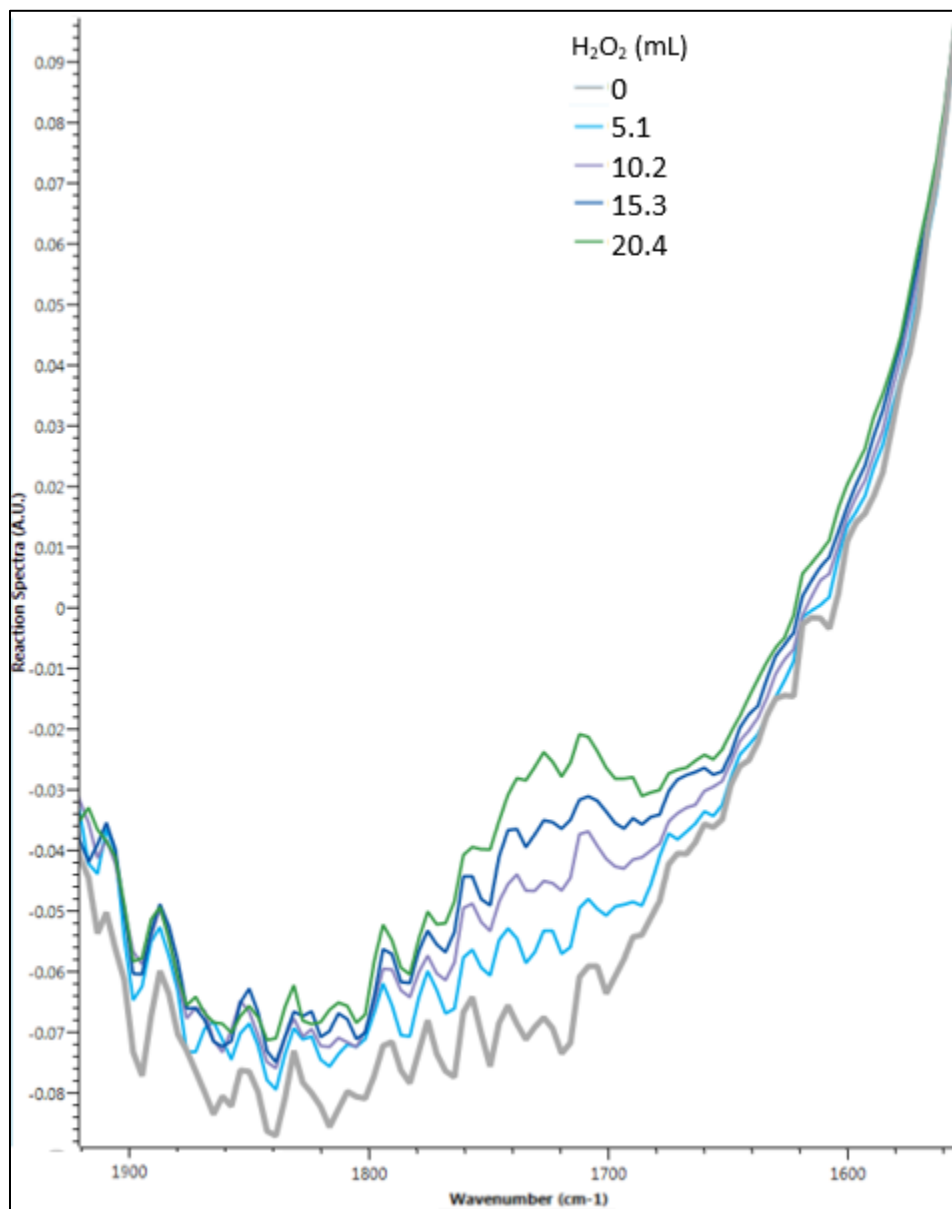


Figure 30: FTIR spectra for 30 °C temperature, 0.284 mol/L 2-butanol, and 2.4 wt% catalyst

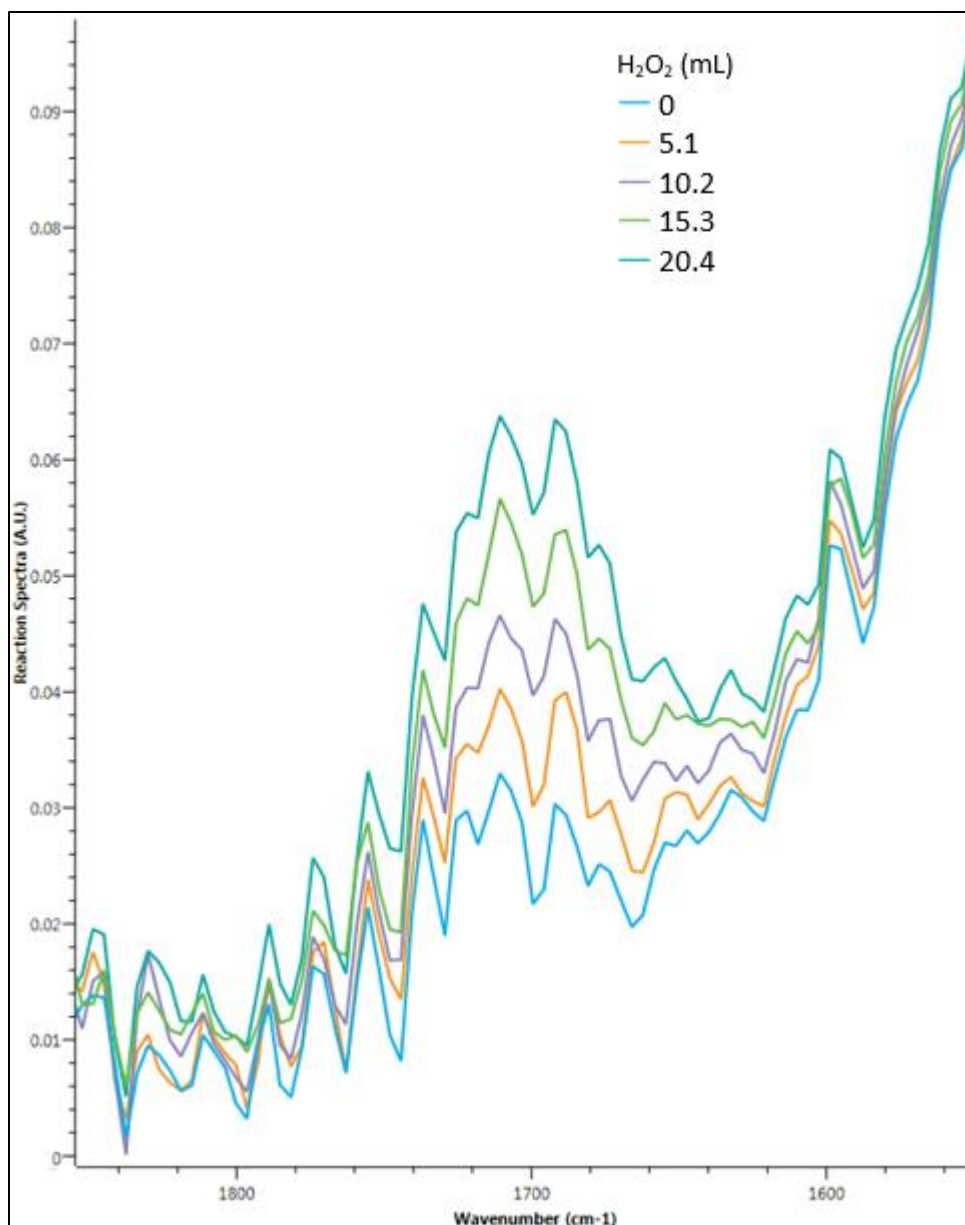


Figure 31: FTIR spectra for 45 °C temperature, 0.534 mol/L 2-butanol, and 3.6 wt% catalyst

For the two reaction systems discussed, the hydrogen peroxide was the limiting reactant in the reaction, with a total of 0.210 moles of it added in total. Thus, for the reaction system of Figure 30, a total of 0.107 moles of 2-butanone were generated, corresponding to a product yield

of 51% based on the limiting reactant ( $\text{H}_2\text{O}_2$ ). Furthermore, for the reaction system of Figure 31, a total of 0.087 moles of 2-butanone were generated, corresponding to a product yield of 41%.

In the reaction system of Figure 30, a total heat of 11.10 kJ/kg was released, as described previously. Furthermore, in the reaction system of Figure 31, a total heat of 8.73 kJ/kg was released. This illustrates that greater product yields are often accompanied by greater amounts of heat released and thus this must be accounted for in the scaling up of the systems for industrial use.

For the experiments in this section, it was determined that the amount of 2-butanol used as a reactant played the most significant role in the heat release amount and thus must be carefully accounted for when determining the cooling requirements for the reaction vessel. Response surface methodology was found to be an effective method for identifying optimum ranges of parameters under which 2-butanone synthesis from 2-butanol takes place to minimize cooling requirements for the reaction.

#### *4.4 Cyclohexanol to cyclohexanone oxidation analysis*

Cyclohexanone is an organic compound of moderate toxicity that consists of a six-carbon cyclic molecule with a ketone functional group. It is slightly soluble in water and miscible with common organic solvents, including methanol [77]. It is used in a number of industrial applications, particularly in the production of precursors to nylon 6 and nylon 6,6. This includes conversion to adipic acid, one of two precursors for nylon 6,6, as well as conversion to cyclohexanone oxime, which is a precursor for nylon 6 [78].

One of the methods of cyclohexanone production involves the oxidation of cyclohexanol to cyclohexanone [79], as shown in Figure 32 below. Similar to the oxidation of 2-butanol to 2-

butanone, hydrogen peroxide serves as an effective oxidant, with the distinct advantage of being a “green” oxidant as a result of generating water as the side product [49]. However, for cyclohexanol oxidation, tungsten-based catalysts have been utilized in recent years in combination with hydrogen peroxide as a result of their effectiveness in catalyzing the reaction [80-81]. Thus, in this work, sodium tungstate dihydrate is utilized as the catalyst within the reaction system. The oxidation reaction of cyclohexanol to form cyclohexanone and the side decomposition reaction of hydrogen peroxide are shown below in Figure 32.

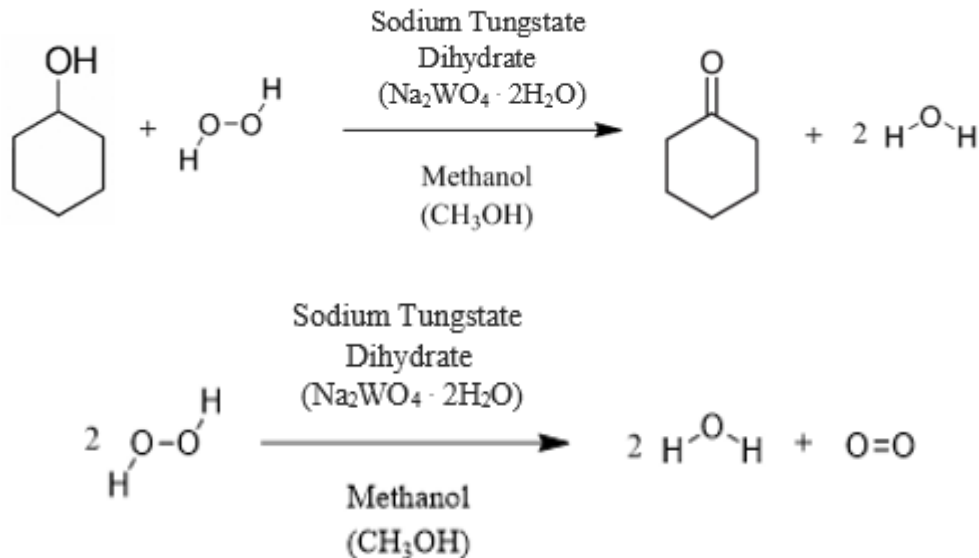


Figure 32: Cyclohexanone synthesis reaction with hydrogen peroxide side reaction

For these experiments, methanol and sodium tungstate dihydrate catalyst were added to the vessel initially. Sodium tungstate dihydrate was chosen as the catalyst for this reaction system because tungsten-based catalysts have been shown to be effective for a number of oxidation reactions [82-83], and sodium tungstate dihydrate has been previously utilized in

oxidation of cyclic alcohols [80-81]. Furthermore, methanol was chosen as the solvent because of its low oxidation rate [20].

The peroxide to reactant ratio as well as the number of injections of hydrogen peroxide were varied for the different experiments to determine their effects on the heat release amounts as well as the product yields. For each experiment, 300 mL of methanol was utilized so that there was sufficient volume of contents to ensure that the reaction mixture would be well-mixed throughout the experiments. Furthermore, 5 g of sodium tungstate dihydrate was added to the vessel for each experiment. These reactants were then heated to the desired reaction temperature, with the pressure held constant at atmospheric pressure. The stirrer speed was chosen as 200 rpm, as speeds of 150 to 250 rpm were tested for this reaction system and it was determined that 200 rpm provided sufficient mixing.

As cyclohexanol is solid at room temperature (with a melting point of 25.93 °C [84]), it was heated to a temperature of 30 °C. The vessel contents were then heated to a temperature of 30 °C and 10.3 g of cyclohexanol was added to the vessel for each experiment. The vessel contents were then further heated to the target value, and once the temperature was sufficiently stabilized, room temperature hydrogen peroxide was added to the mixture.

For this, the peroxide-to-reactant molar ratio was varied from 0.5 and 1.5 (corresponding to additions of 5 g, 10 g, and 15 g of 35 wt % hydrogen peroxide). Furthermore, in order to simulate the semi-batch process, the hydrogen peroxide was added in 4, 7, or 10 injections for each experiment. These parameters were chosen to be varied in order to identify their effects on the overall heat release as well as the yield of cyclohexanone. Furthermore, the temperature was varied, with the effects of temperatures of 40, 50, and 60 °C investigated as they related to the

overall heat release and cyclohexanone yield. The conditions for each of the experiments are shown below in Table 5.

<b>Experiment</b>	<b>Temperature (°C)</b>	<b>Peroxide/Reactant Molar Ratio</b>	<b>Number of Peroxide Injections</b>
1	40	0.5	4
2	50	1	4
3	60	1.5	4
4	40	1	7
5	50	1.5	7
6	60	0.5	7
7	40	1.5	10
8	50	0.5	10
9	60	1	10

Table 5: Reaction conditions for cyclohexanol oxidation experiments

Similar to the experiments involving 2-butanol oxidation, response surface methodology was utilized to model curvature of the data and identify factors that contribute most to the response. In this case, the effects of the reaction temperature, peroxide/reactant molar ratio, and number of peroxide injections were investigated in relation to both the total heat release as well as the cyclohexanone yield.

For each of the 9 experiments conducted, a graph depicting the heat release rates and vessel/jacket temperatures in real-time were generated using the iControl software. Two examples of these graphs are shown below in Figures 33 and 34.



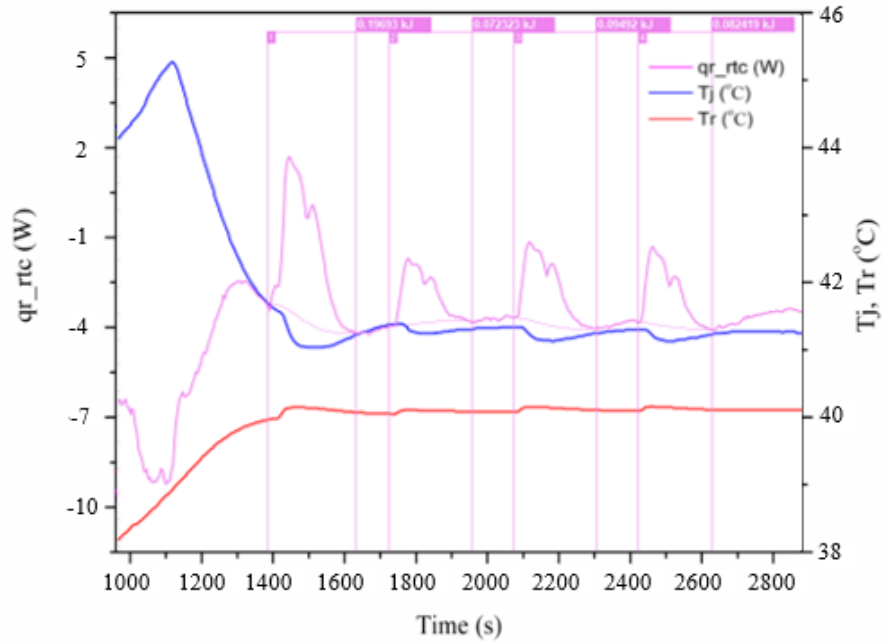


Figure 33: iControl temperature and heat release graph for 40 °C temperature, P/R ratio of 0.5, and 4 H<sub>2</sub>O<sub>2</sub> injections

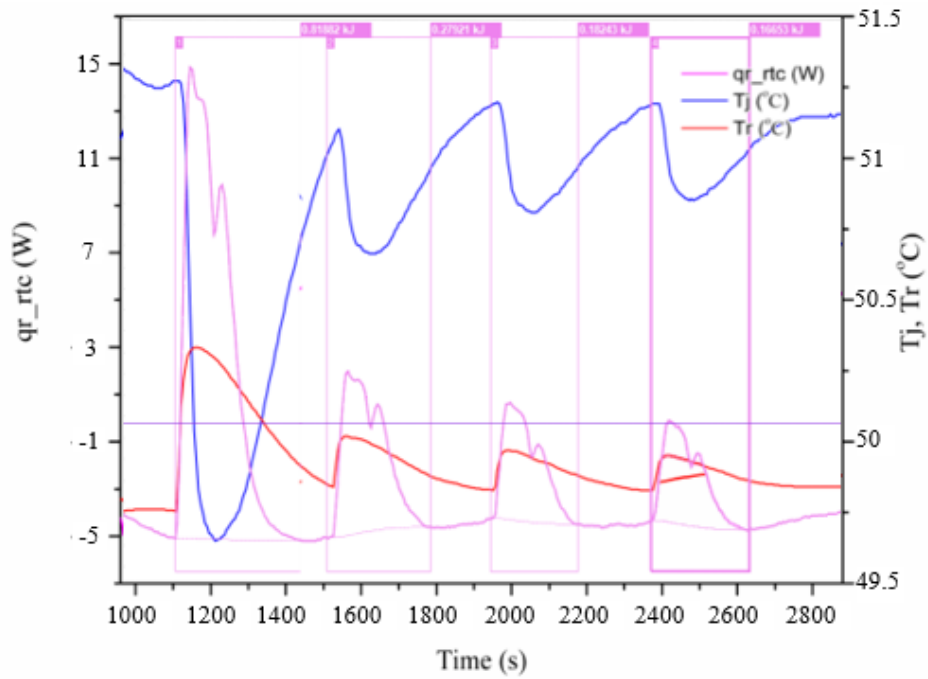


Figure 34: iControl temperature and heat release graph for 50 °C temperature, P/R ratio of 1.0, and 4 H<sub>2</sub>O<sub>2</sub> injections

Similar to the 2-butanol oxidation experiments, integration and summation of the heat release peaks for each of the experiments provided the total heat release amount (kJ) for each of the experiments. This was normalized to the scale-independent parameter of kJ/kg reaction mass and served as one of the response variables for the surface maps and contour plots. In addition to the heat release amount, the yield of cyclohexanone resulting from the oxidation reaction served as the other response variable.

In order to determine the cyclohexanone yields, an FTIR calibration curve for cyclohexanone was generated. To do so, a total of 20 g of pure cyclohexanone was added to 300 mL of methanol in 2 g increments. It was found that the carbonyl group of the cyclohexanone occurred at a wavenumber of approximately  $1705\text{ cm}^{-1}$ . Furthermore, the change in the height of the reaction spectra corresponding to each addition of the cyclohexanone was determined, and the FTIR calibration curve was generated from these data, which is shown in Appendix C.

The FTIR data for two of the experiments are shown in Figures 35 and 36 below. Figure 35 involves the FTIR spectra for the incremental injections of the reaction system at a temperature of  $40\text{ }^{\circ}\text{C}$ , P/R ratio of 0.5, and 4  $\text{H}_2\text{O}_2$  injections. Figure 36 involves the FTIR spectra for the incremental injections of the reaction system at a temperature of  $50\text{ }^{\circ}\text{C}$ , P/R ratio of 1, and 4  $\text{H}_2\text{O}_2$  injections.

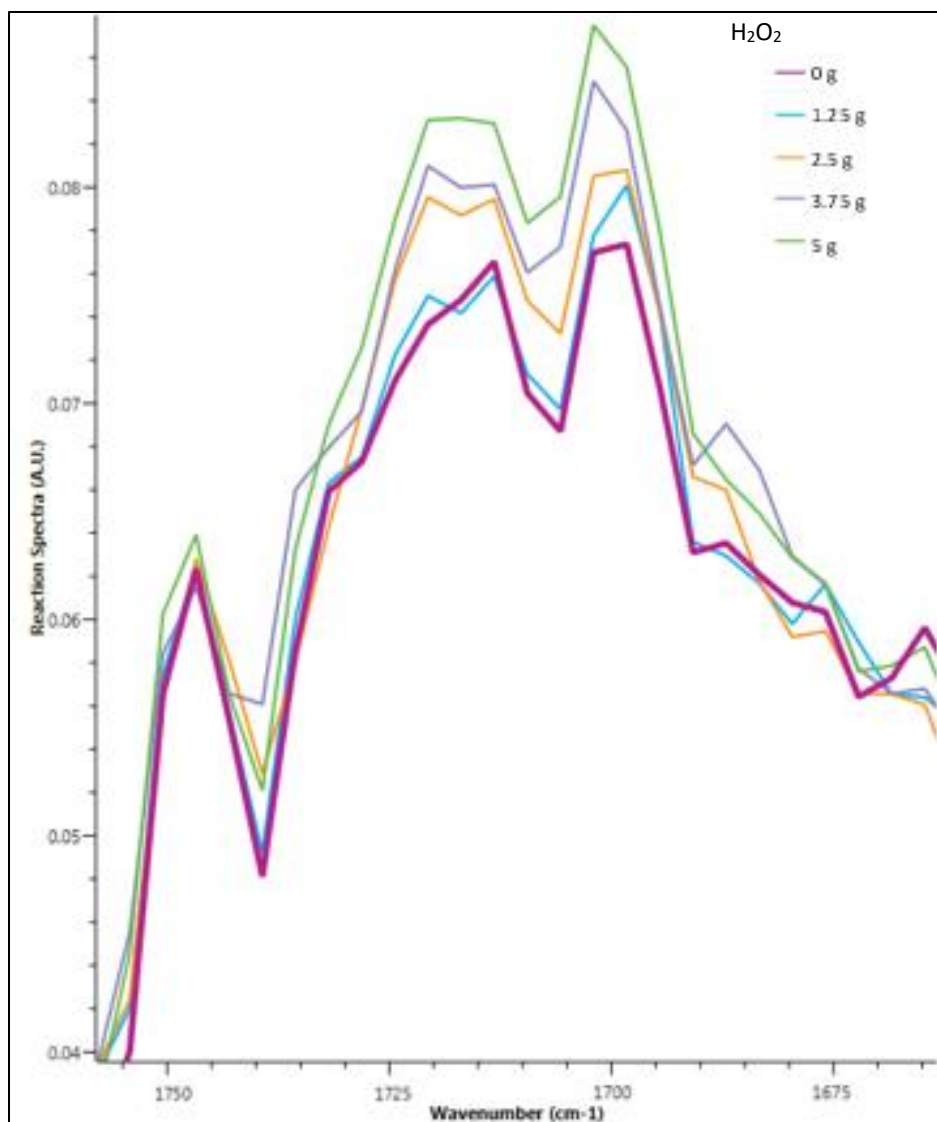


Figure 35: FTIR spectra for 40 °C temperature, P/R ratio of 0.5, and 4 H<sub>2</sub>O<sub>2</sub> injections

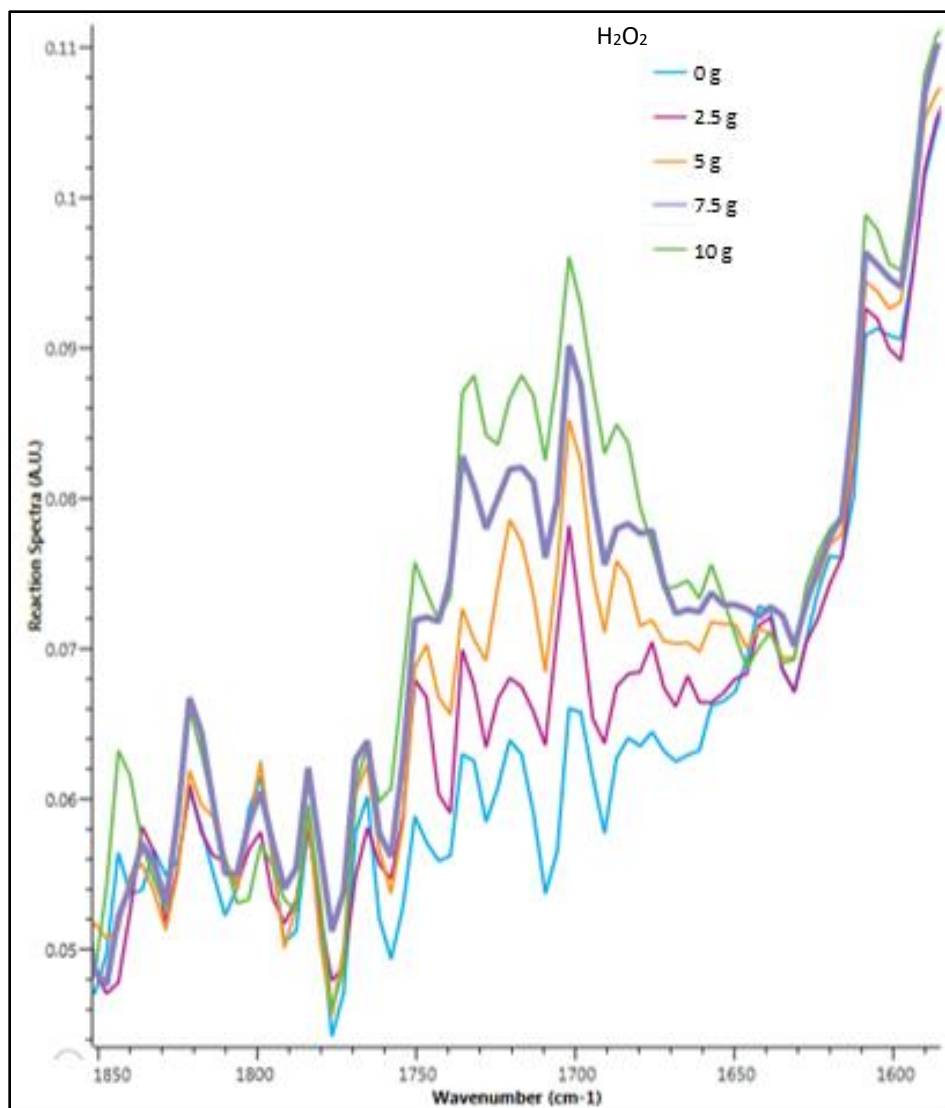


Figure 36: FTIR spectra for 50 °C temperature, P/R ratio of 1.0, and 4 H<sub>2</sub>O<sub>2</sub> injections

Figure 37 shows the surface map and contour plot for the effects of vessel temperature and peroxide-to-reactant molar ratio on the heat release amounts. For these, the number of hydrogen peroxide injections at each data point correspond to the reaction conditions in Table 5.

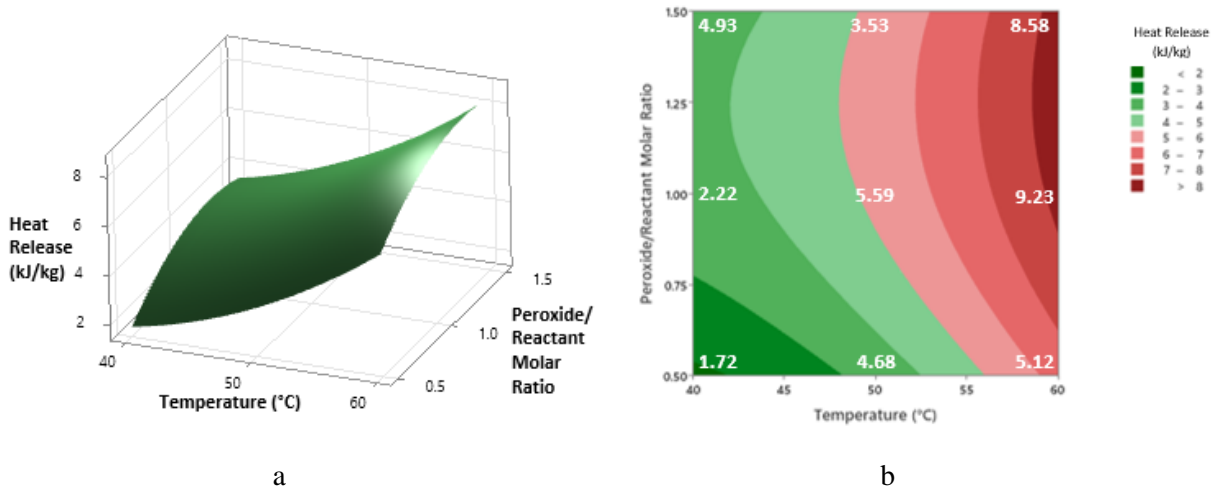


Figure 37: Effects of temperature and peroxide/reactant molar ratio on heat release

(a) Surface map (b) Contour plot

As can be seen from the contour plot in Figure 37, the highest amount of heat release (kJ/kg reaction mass) occurred at a temperature of 60 °C with a peroxide-to-reactant ratio of 1.0. Furthermore, the lowest total heat release amount occurred at a temperature of 40 °C with a peroxide-to-reactant ratio of 1.0. Explanations for the highest amount of heat release occurring at 60 °C with a 1.0 peroxide-to-reactant ratio include that these conditions are most favorable for the oxidation of cyclohexanol to cyclohexanone, as evidenced by the product yields discussed previously. Similarly, the occurrence of the lowest heat release at 40 °C with a 1.0 peroxide-to-reactant ratio is due to the lower product yields associated with those parameters. The p-value for this regression model is 0.036. Furthermore, the regression model has an  $R^2$  of 78.64%, indicating that the test result is statistically significant and that the data fits relatively closely with the regressed model. The quality of the fit for this model indicates that the effects of reaction temperature in combination with the peroxide-to-reactant ratio play a very significant role in the heat generation from the reaction.

Figure 38 shows the surface map and contour plot for the effects of vessel temperature and number of hydrogen peroxide injections on the total heat release amounts.

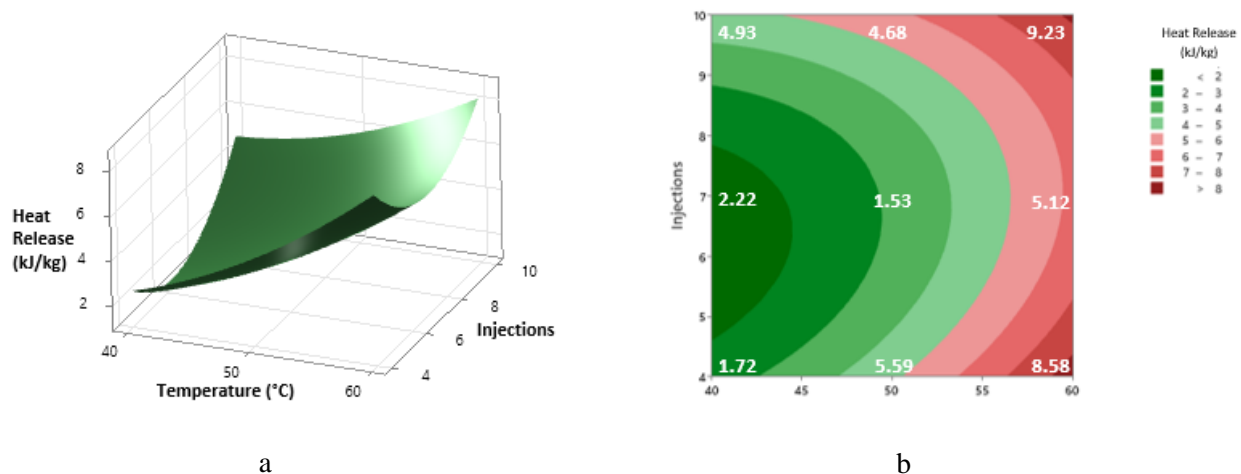


Figure 38: Effects of temperature and number of hydrogen peroxide injections on heat release

(a) Surface map (b) Contour plot

As can be seen from the contour plot in Figure 38, the highest amounts of heat release occurred at a temperature of 60 °C with numbers of peroxide injections of 4 and 10. Furthermore, the lowest total heat release amount occurred at a temperature of 40 °C with 7 peroxide injections. Explanations for the highest amount of heat release occurring at 60 °C with peroxide injections of 4 and 10 include that these conditions are highly favorable for the oxidation of cyclohexanol to cyclohexanone, as evidenced by the product yields discussed previously. Similarly, the occurrence of the lowest heat release at 40 °C with 7 peroxide injections is due to the lower product yields associated with those parameters. The p-value for this regression model is 0.051. Furthermore, the regression model has an  $R^2$  of 89.54%, indicating that the test result for this is moderately statistically significant and that the data fits closely with the regressed model. The quality of the fit for this model indicates that the effects of

reaction temperature in combination with the number of hydrogen peroxide injections play a highly significant role in the heat generation from the reaction.

Figure 39 shows the surface map and contour plot for the effects of the peroxide/reactant ratio and number of hydrogen peroxide injections on the total heat release amounts.

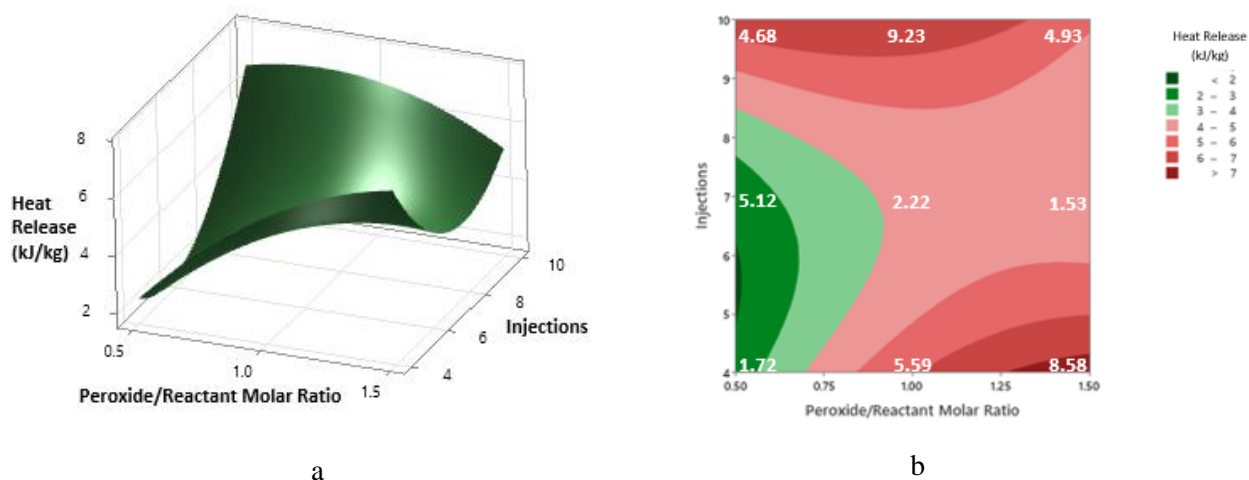


Figure 39: Effects of peroxide/reactant molar ratio and number of hydrogen peroxide injections on heat release (a) Surface map (b) Contour plot

As can be seen from the contour plot in Figure 39, the highest amount of heat release occurred at a peroxide/reactant ratio of 1.5 with 4 peroxide injections as well as at a peroxide/reactant ratio of 1.0 with 10 peroxide injections. Moreover, the lowest total heat release amount occurred at a peroxide/reactant ratio of 0.5 and 4 peroxide injections. The occurrence of the highest heat release at the aforementioned peroxide/reactant ratio and number of injections is a result of the higher cyclohexanone yields at those conditions, while the combination of parameters resulting in the lowest heat release is due to the lower cyclohexanone yield. The p-value for this regression model is 0.134. Furthermore, the regression model has an  $R^2$  of 55.09%,

indicating that the data does not fit particularly closely with the regressed model. The quality of the fit for this model indicates that the effects of the peroxide/reactant ratio in combination with the number of hydrogen peroxide injections do not play a significant role in the heat generation from the reaction.

In addition to the heat release amounts, the fractional product yields of cyclohexanone were investigated as a response variable to the combinations of parameters consisting of reaction temperature, peroxide/reactant ratio, and number of peroxide injections. The product yields were determined based on the limiting reactant in the oxidation reaction. As the cyclohexanol reacts with hydrogen peroxide in a 1:1 molar ratio to form the cyclohexanone, the peroxide/reactant molar ratio affects the limiting reactant for each experiment. For a peroxide/reactant ratio of 0.5, the hydrogen peroxide was the limiting reactant, while for a peroxide/reactant ratio of 1.0, both reactants were present in equal molar quantities. Furthermore, for a peroxide/reactant ratio of 1.5, the cyclohexanol was the limiting reactant. Thus, the fractional yield was determined using the number of moles of cyclohexanone produced per the amount of limiting reactant consumed.

Figure 40 shows the surface map and contour plot for the effects of vessel temperature and peroxide-to-reactant molar ratio on the cyclohexanone yields. For these, the number of hydrogen peroxide injections at each data point correspond to each of the reaction conditions described in Table 5.



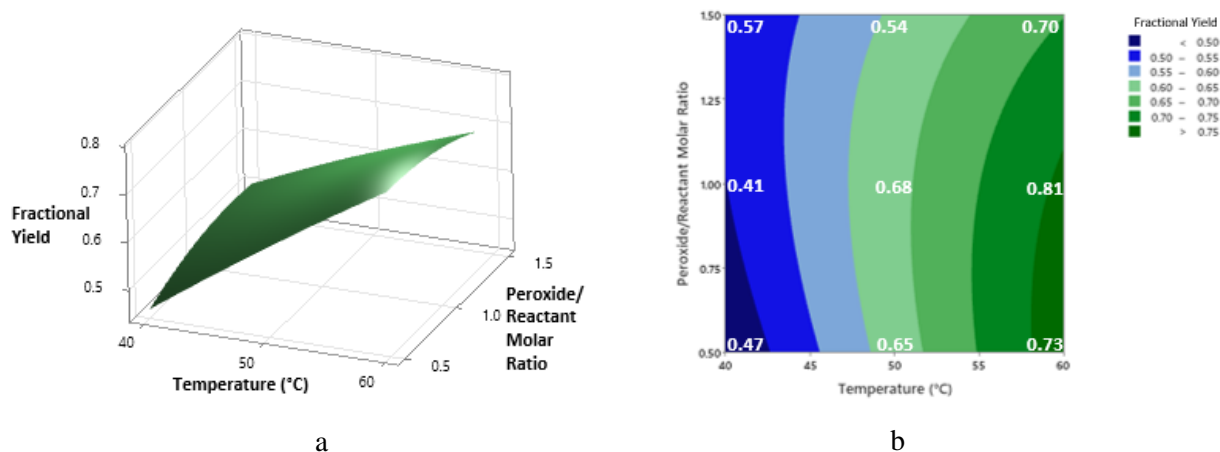


Figure 40: Effects of temperature and peroxide/reactant molar ratio on product yield

(a) Surface map (b) Contour plot

As can be seen from the contour plot in Figure 40, the greatest product yield occurred at a temperature of 60 °C with a peroxide-to-reactant ratio of 1.0. Furthermore, the product yield occurred at a temperature of 40 °C with a peroxide-to-reactant ratio of 1.0. Explanations for the greatest product yield at 60 °C with a peroxide-to-reactant ratio of 1.0 include that the cyclohexanol to cyclohexanone reaction is favored at these conditions more than the hydrogen peroxide decomposition reaction. Conversely, at lower temperatures, the hydrogen peroxide decomposition reaction is more favored. The p-value for this regression model is 0.002. Furthermore, the regression model has an  $R^2$  of 82.97%, indicating that the test result is very statistically significant and that the data fits relatively closely with the regressed model. The quality of the fit for this model indicates that the effects of reaction temperature in combination with the peroxide-to-reactant ratio play a very significant role in the cyclohexanone yield from the reaction.

Figure 41 shows the surface map and contour plot for the effects of vessel temperature and number of hydrogen peroxide injections on the cyclohexanone yield.

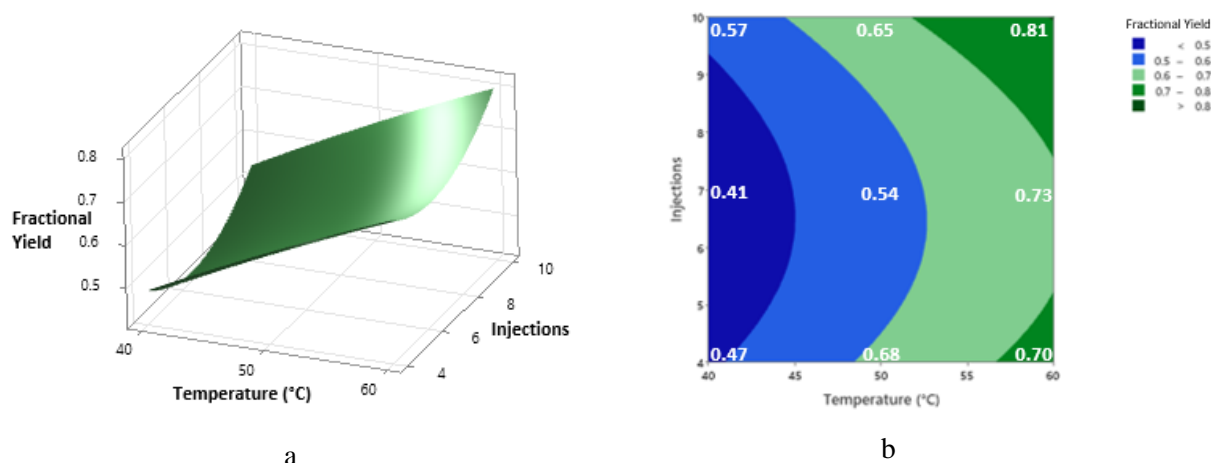


Figure 41: Effects of temperature and number of hydrogen peroxide injections on product yield

(a) Surface map (b) Contour plot

As can be seen from the contour plot in Figure 41, the greatest cyclohexanone yield occurred at a temperature of 60 °C with 10 peroxide injections. Furthermore, the lowest cyclohexanone yield occurred at a temperature of 40 °C with 7 peroxide injections. Explanations for the greatest product yield at 60 °C with more hydrogen peroxide injections include that the cyclohexanol to cyclohexanone reaction is favored at greater temperatures as well as with larger numbers of hydrogen peroxide injections, as less unreacted hydrogen peroxide remains in the vessel at any given time to decompose. Conversely, at lower temperatures and with fewer peroxide injections, the hydrogen peroxide decomposition reaction is more favored. The p-value for this regression model is 0.001. Furthermore, the regression model has an  $R^2$  of 92.71%, indicating that the test result for this is very statistically significant and that the data fits closely with the regressed model. The quality of the fit for this model indicates that the effects of reaction temperature in combination with the number of hydrogen peroxide injections play a highly significant role in the cyclohexanone yield for the reaction.

Figure 42 shows the surface map and contour plot for the effects of the peroxide/reactant ratio and number of hydrogen peroxide injections on the cyclohexanone yield.

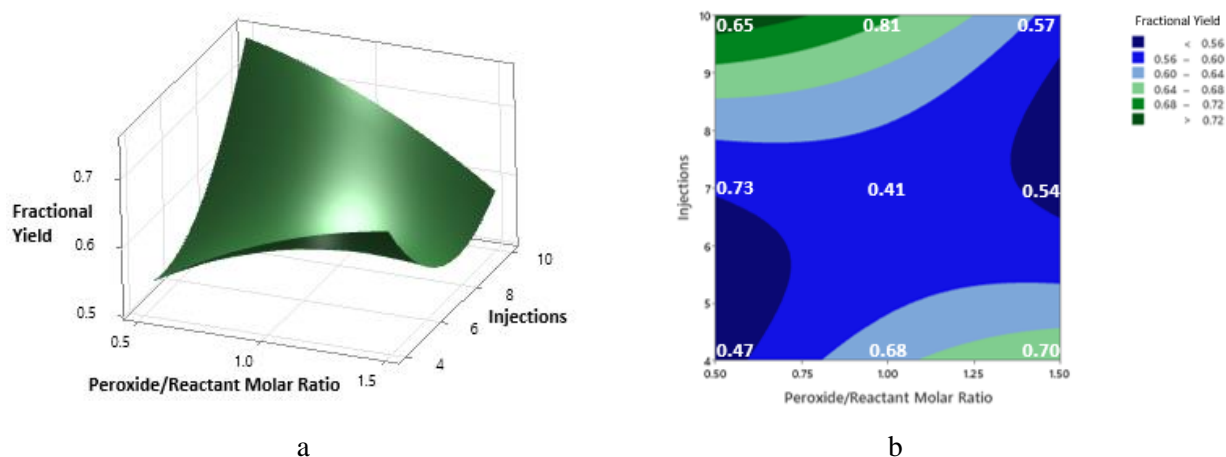


Figure 42: Effects of peroxide/reactant molar ratio and number of hydrogen peroxide injections on product yield (a) Surface map (b) Contour plot

As can be seen from the contour plot in Figure 42, the greatest cyclohexanone yield occurred at a peroxide/reactant ratio of 1.0 with 10 peroxide injections. Moreover, the lowest cyclohexanone yield occurred at a peroxide/reactant ratio of 0.5 and 4 peroxide injections. Explanations for these results include that temperature plays the greatest role in the cyclohexanone yield and thus the peroxide/reactant molar ratio and number of peroxide injections do not significantly affect the cyclohexanone yield. The p-value for this regression model is 0.112. Furthermore, the regression model has an  $R^2$  of 32.60%, indicating that the data does not fit closely with the regressed model. The quality of the fit for this model indicates that the effects of the peroxide/reactant ratio in combination with the number of hydrogen peroxide injections do not play a significant role in the cyclohexanone yield for this reaction.

For the experiments in this section, it was determined that the reaction temperature played the most significant role in both the heat release amount and cyclohexanone yield for each set of experiments. Furthermore, it was found that greater amounts of heat released typically corresponded to greater cyclohexanone yields. Thus, a trade-off exists between maximizing product yield and minimizing cooling requirements for the reactions, which must be carefully considered for industrial applications. Response surface methodology was found to be an effective method for identifying combinations of parameters for which cyclohexanol oxidation to cyclohexanone results in the lowest amount of heat released as well as the greatest product yield.

#### *4.5 Application of safety triad to exothermic oxidation reactions*

As has been demonstrated both with the oxidation of 2-butanol to 2-butanone and cyclohexanol to cyclohexanone, oxidation reactions tend to be exothermic, generating significant amounts of heat as they are carried out. Thus, industrially relevant reactions must be thoroughly analyzed to ensure that sufficient cooling capacity is able to be provided to prevent the possibility of thermal runaway.

The primary component of the safety triad related to the avoidance of thermal runaway in exothermic oxidation reactions is the prevention component, as sufficient cooling capacity plays a significant role in this. However, the mitigation component also plays a role in addressing thermal runaway, as effective strategies for minimizing the effects of the thermal runaway must be implemented.

A strategy for mitigating the effects of thermal runaway that has occurred in a reactor is through thermal quenching of the reaction mixture. For this, a quenching reagent is added to the

reaction mixture as part of an emergency protocol [85-86]. However, one of the drawbacks of this method is that it results in a loss of the entire batch of reactants because of being contaminated with the quenching reagent. Thus, prevention of thermal runaway from occurring in the first place should be ensured to prevent hazards to human health and safety as well as waste of the reaction mixture.

## CHAPTER V

### SUMMARY AND CONCLUSIONS

#### *5.1 Safety triad application to chemical facilities*

In this research, the safety triad has been validated as an effective tool for evaluating the robustness of safety systems within industrial facilities, particularly those involving hazardous chemicals. To do so, each of the components of the safety triad has been analyzed in detail. This involves analysis of effective measures for each component, with an example prevention measure being the development of effective, well-written operating procedures.

A review of hazard analysis techniques commonly utilized within the chemical process industries illustrated that the techniques often provide critical information for hazard reduction in the design and operation of facilities. However, their scopes are often limited to specific processes or workers within the facilities. On the other hand, the safety triad provides an overarching framework to evaluate the effectiveness of safety systems.

Application of the safety triad as a tool to assess prior incidents demonstrated that it serves a very useful role in identifying causes that led to the incidents, particularly those within industrial facilities. Analysis of incidents that led to non-catastrophic consequences revealed that significant deficiencies tended to be present in one or two of the safety triad components. However, incidents that did lead to catastrophic consequences tended to have significant deficiencies in all three of the components. This further illustrated the need for all components of the safety triad to be sufficiently robust.

Following this, the safety triad was investigated as a tool to be utilized in the design and maintenance of chemical facilities. To do so, chemical hazards within storage facilities were

analyzed. This involved investigation of 33 warehouses containing hazardous chemicals and identifying potential chemical incompatibilities if the chemicals were combined with each other. Furthermore, the maximum downwind dispersion distances to result in hazardous concentrations were identified for each of the toxic gases determined to be potentially generated. From this, it was determined that significant hazards are present within chemical storage warehouses and that each component of the safety triad must be thoroughly accounted for to prevent incidents.

Lastly, thermal hazards associated with exothermic oxidation reactions were investigated. This included calorimetric analysis of the heat release of the 2-butanol to 2-butanone and cyclohexanol to cyclohexanone oxidation reactions. Furthermore, FTIR analysis was utilized to identify the product yields associated with these oxidation reactions. It was determined that a trade-off tended to exist between the heat released and the product yield, meaning that greater product yields tended to result in greater amounts of heat release. Moreover, it was determined that response surface methodology is a very effective method for identifying operating regions that result in the lowest heat release amounts as well as the greatest product yields. This provided critical information for determination of the amount of cooling necessary to prevent thermal runaway for the reactions.

Based on the aforementioned research, the safety triad has been thoroughly investigated as an overarching tool to evaluate the robustness of safety systems, specifically for industries involving chemical hazards. Because of its effectiveness both with regard to being a useful tool for investigation of prior incidents as well as for guiding the design and operation of facilities, it serves as a promising framework to become an industry standard for facility safety evaluation. As such, it may serve to evaluate safety systems in additional industries besides those involving chemical hazards.

## *5.2 Future work*

In addition to the safety triad being evaluated and validated as an effective tool for use within the chemical process industries, future work involves it being validated for use in additional industries that contain significant hazards. These include a variety of types of facilities, such as offshore and manufacturing facilities.

For offshore petroleum facilities, associated hazards include fires, explosions, falling objects, structural failure, and extreme weather conditions. For these types of facilities, the safety triad should be utilized as a framework to analyze past incidents involving them. One of these incidents is the Macondo blowout and explosion, which resulted in the deaths of 11 workers and 4 million barrels of oil being released into the Gulf of Mexico [87]. Furthermore, the safety triad should be used proactively in the design and operation of these types of facilities, with distinct consideration for the hazards associated with offshore facilities as compared to onshore ones. These include the fact that oceanographic conditions can have severe impacts on the safety of offshore facilities, and thus robust prevention and mitigation measures must be taken to account for this. Furthermore, timely emergency response is much more difficult to attain for offshore as opposed to onshore facilities, and thus this must be comprehensively accounted for in the response component.

For manufacturing facilities, associated hazards include electrical hazards, fire hazards, machine hazards, and moving vehicles. Incidents involving manufacturing facilities include the Imperial Sugar Company dust explosion and fire, in which combustible sugar dust resulted in a large fire. This caused 14 deaths and 38 injuries, including 14 with serious and life-threatening burns [88]. Thus, the safety triad should be used to assess these incidents to identify deficiencies as well as used in the design and operation of new facilities. Thorough consideration should be



given to hazards that are prevalent specifically within manufacturing facilities, such as hazards due to lack of appropriate machine guarding as well as equipment malfunctions.

By validating the safety triad as a safety system evaluation tool for differing industries, its broad applicability can be fully determined. Thus, it serves as a promising tool for enhancement of safety and reduction of hazards across many types of industries.

## LITERATURE CITED

- [1] U.S. Chemical Safety and Hazard Investigation Board. (2016). Williams Olefins Plant Explosion and Fire. Retrieved September 06, 2020, from <https://www.csb.gov/williams-olefins-plant-explosion-and-fire/>
- [2] U.S. Chemical Safety and Hazard Investigation Board. (2007). BP America Refinery Explosion. Retrieved from <https://www.csb.gov/bp-america-refinery-explosion/>
- [3] O'Connor, M., Pasman, H. J., & Rogers, W. J. (2019). Sam Mannan's safety triad, a framework for risk assessment. *Process Safety and Environmental Protection*, 129, 202–209. doi: 10.1016/j.psep.2019.07.004
- [4] Parker, T., Shen, R., O'Connor, M., & Wang, Q. (2019). Application of safety triad in preparation for climate extremes affecting the process industries. *Process Safety Progress*, 38(3), e12091. <https://doi.org/10.1002/prs.12091>
- [5] Parker, T., Shen, R., & Wang, Q. (2022). Application of Safety Triad in Process Safety. In A. R. K. Gollakota, S. Gautam, & C. M. Shu (Eds.), *Bow Ties in Process Safety and Environmental Management: Current Trends and Future Perspectives* (1st ed.). essay, CRC Press.
- [6] Willey, R. J. (2014). Layer of protection analysis. *Procedia Engineering*, 84, 12–22. doi:10.1016/j.proeng.2014.10.405
- [7] Hartwell, J. (2019). HAZOP - Hazard and Operability Study. Retrieved September 30, 2020, from <https://www.iqasystem.com/news/hazop/>
- [8] Benmerrouche, M., & Lee, R. (2015). Safety Integrity Level and Redundancy Requirements for the Top-Off Safety System. doi:10.2172/1493227
- [9] Slack, N. (2015). Failure Mode and Effect Analysis. *Wiley Encyclopedia of Management*, 1–2. doi:10.1002/9781118785317.weom100151. Wiley Publishing. Hoboken, New Jersey.
- [10] Kjellén Urban, & Albrechtsen, E. (2017). In *Prevention of accidents and unwanted occurrences: Theory, methods, and tools in safety management* (pp. 363–370). essay, CRC Press, Taylor & Francis Group. Oxfordshire, England.
- [11] Pedroni, N., & Zio, E. (2012). Uncertainty analysis in fault tree models with dependent basic events. *Risk Analysis*, 33(6), 1146–1173. doi:10.1111/j.1539-6924.2012.01903.x
- [12] Parker, T. (2020). Development of a Comprehensive Procedure Writers' Guide Framework. Poster presented at AIChE Spring Meeting and Global Congress on Process Safety

- [13] IPCC. (2012). Managing the Risks of Extreme Events and Disasters to Advance Climate Change Adaptation. Retrieved from <https://www.ipcc.ch/report/managing-the-risks-of-extreme-events-and-disasters-to-advance-climate-change-adaptation/>
- [14] Extreme Weather and Climate Change. (2019). Retrieved from <https://www.c2es.org/content/extreme-weather-and-climate-change/>
- [15] Smith, A. B. (2019). 2018's Billion Dollar Disasters in Context. Retrieved from <https://www.climate.gov/news-features/blogs/beyond-data/2018s-billion-dollar-disasters-context>
- [16] Smith, P., Kincannon, H., Lehnert, R., Wang, Q., & Larrañaga, M. D. (2013). Human error analysis of the Macondo well blowout. *Process Safety Progress*, 32(2), 217-221. doi:10.1002/prs.11604
- [17] Mannan, M., & Wang, Q. (2011). Stretch in Technology and Keeping the Focus on Process Safety for Exploration and Production in the 21st Century. In *Hazards XXII* (Ser. 156, pp. 99-103). IChemE.
- [18] Liserio, F. F., Jr., & Mahan, P. W. (2019). Manage the Risks of Severe Wind and Flood Events. Retrieved from <https://www.aiche.org/resources/publications/cep/2019/april/manage-risks-severe-wind-and-flood-events#fig6>
- [19] U.S. Chemical Safety and Hazard Investigation Board. (2008). Valero Refinery Propane Fire. Retrieved from <https://www.csb.gov/valero-refinery-propane-fire/>
- [20] Cassidy, L. (2018). Lessons Learned from Hurricane Harvey. Retrieved from <https://www.aocs.org/stay-informed/inform-magazine/featured-articles/lessons-learned-from-hurricane-harvey-march-2018>
- [21] U.S. Chemical Safety and Hazard Investigation Board. (2018). Arkema Inc. Chemical Plant Fire. Retrieved from <https://www.csb.gov/arkema-inc-chemical-plant-fire-/>
- [22] CBS News. (2017). Arkema Chemical Plant Fire [Digital image]. Retrieved from <https://www.cbsnews.com/news/flames-erupt-at-arkema-chemical-plant-flooded-by-harvey-in-crosby-texas/>
- [23] U.S. Chemical Safety and Hazard Investigation Board. (2015). DuPont La Porte, Texas Chemical Facility Toxic Chemical Release: Interim Recommendations. Retrieved from [https://www.csb.gov/assets/1/20/dupont\\_la\\_porte\\_interim\\_recommendations\\_2015-09-30\\_final1.pdf?15526](https://www.csb.gov/assets/1/20/dupont_la_porte_interim_recommendations_2015-09-30_final1.pdf?15526)
- [24] U.S. Chemical Safety and Hazard Investigation Board. (2019). Toxic Chemical Release at the DuPont La Porte Chemical Facility. Retrieved from <https://www.csb.gov/dupont-la-porte-facility-toxic-chemical-release-/>

- [25] US Department of Commerce, & NOAA. (2019). Houston IAH Climate Data. Retrieved from [https://www.weather.gov/hgx/climate\\_iah](https://www.weather.gov/hgx/climate_iah)
- [26] Mohammadi, A. H., & Richon, D. (2011). Equilibrium Data of Sulfur Dioxide and Methyl Mercaptan Clathrate Hydrates. *Journal of Chemical & Engineering Data*, 56(4), 1666-1668. doi:10.1021/je9009893
- [27] Wang, Q., Ma, T., Hanson, J., & Larranaga, M. (2012). Application of Incident Command System in Emergency Response. Retrieved from <https://aiche.onlinelibrary.wiley.com/doi/epdf/10.1002/prs.11538>
- [28] Occupational Safety and Health Administration. *1910.110 - Storage and Handling of Liquefied Petroleum Gases*; United States Department of Labor, 2013.
- [29] Process Safety Management: What is it and why do we need it? <https://www.dekra.us/en/process-safety-management-what-is-it/> (accessed 14 May 2021).
- [30] CSB, 2009. T2 Laboratories Inc. Reactive Chemical Explosion. <https://www.csb.gov/t2-laboratories-inc-reactive-chemical-explosion/> (accessed 14 May 2021).
- [31] CSB, 2018. Arkema Inc. Chemical Plant Fire. <https://www.csb.gov/arkema-inc-chemical-plant-fire-/> (accessed 14 May 2021).
- [32] CSB, 2006. MFG Chemical Inc. Toxic Gas Release. <https://www.csb.gov/mfg-chemical-inc-toxic-gas-release/> (accessed 14 May 2021).
- [33] Hazard Investigation: Improving Reactive Hazard Management (2001). U.S. Chemical Safety and Hazard Investigation Board.
- [34] Recommendations for Addressing Recurring Chemical Incidents in the U.S. (2005). United States Department of Energy.
- [35] DOW fire & explosion index: Hazard classification guide., 7th ed. ed., American Institute of Chemical Engineers, 1994.
- [36] Zhang, Z. Develop a hazard index using machine learning approach for the hazard identification of chemical logistic warehouses, Texas A&M University, College Station, TX, 2019.
- [37] Ranking of Chemical Facilities Based on the Potential to Cause Harm to the Public (2016). Mary Kay O'Connor Process Safety Center.
- [38] FLACS Software. (2020). Retrieved December 08, 2020, from <https://www.gexcon.com/products-services/flacs-software/>

- [39] Process Hazard Analysis Software - PHAST. (n.d.). Retrieved December 08, 2020, from <https://www.dnvgl.com/software/services/phast/index.html>
- [40] Chemical and Industrial Accident Database. (n.d.). Retrieved December 08, 2020, from <http://www.factsonline.nl/>
- [41] Fatality and Catastrophe Investigation Summaries. (n.d.). Retrieved December 08, 2020, from <https://www.osha.gov/pls/imis/accidentsearch.html>
- [42] Protective Action Criteria for Chemicals - Including AEGLs, ERPGs, & TEELs. (2012). *Emergency Management Issues Special Interest Group*.
- [43] *Completed investigations*. CSB. (n.d.). Retrieved April 10, 2022, from <https://www.csb.gov/investigations/completed-investigations/>
- [44] *Accident Search*. Accident Search Results Page | Occupational Safety and Health Administration. (n.d.). Retrieved April 10, 2022, from [https://www.osha.gov/pls/imis/accidentsearch.search?acc\\_keyword=](https://www.osha.gov/pls/imis/accidentsearch.search?acc_keyword=)
- [45] Shouman, A. R. (2006). A review of one aspect of the thermal-explosion theory. *Journal of Engineering Mathematics*, 56(2), 179–184. <https://doi.org/10.1007/s10665-006-9083-9>
- [46] Liu, G., & Wilhite, B. A. (2019). Model-based design for inhibition of thermal runaway in free-radical polymerization. *Industrial & Engineering Chemistry Research*, 58(37), 17244–17254. <https://doi.org/10.1021/acs.iecr.9b02007>
- [47] 2-Butanone [http://www.chemicalbook.com/ChemicalProductProperty\\_EN\\_CB4854386.htm](http://www.chemicalbook.com/ChemicalProductProperty_EN_CB4854386.htm) (accessed 14 May 2021).
- [48] Maspero, F., & Romano, U. (1994). Oxidation of Alcohols with H<sub>2</sub>O<sub>2</sub> Catalyzed by Titanium Silicalite-1. *J. Catal.* 146 (2), 476–482.
- [49] Pędziwiatr, P., Mikołajczyk, F., Zawadzki, D., Mikołajczyk, K., & Bedka, A. (2018). Decomposition of Hydrogen Peroxide - Kinetics and Review of Chosen Catalysts. *Acta Innov.*, No. 26, 45–52.
- [50] Colladon, M., Scarso, A., & Strukul, G. (2008). Mild Catalytic Oxidation of Secondary and Tertiary Amines to Nitrones and N-Oxides with H<sub>2</sub>O<sub>2</sub> Mediated by Pt(Ii) Catalysts. *Green Chem.*, 10 (7), 793.
- [51] Nyamunda, B. C., Chigondo, F., Moyo, M., Guyo, U., Shumba, M., & Nharingo, T. (2013). Hydrogen Peroxide as an Oxidant for Organic Reactions. *Journal of Atoms and Molecules*, 3 (1), 23–44.

- [52] Sun, Y., Ni, L., Papadaki, M., Zhu, W., Jiang, J., Mashuga, C., Wilhite, B., & Mannan, M. S. (2019). Process Hazard Evaluation for Catalytic Oxidation of 2-Octanol with Hydrogen Peroxide Using Calorimetry Techniques. *Chem. Eng. J.*, 378 (122018), 122018.
- [53] Wang, Q. Theoretical and Experimental Evaluation of Chemical Reactivity, Texas A&M University, College Station, TX, 2011.
- [54] Pineda-Solano, A., Saenz, L. R., Carreto, V., Papadaki, M., & Mannan, M. S. (2012). Toward an Inherently Safer Design and Operation of Batch and Semi-Batch Processes: The N-Oxidation of Alkylpyridines. *Journal of Loss Prevention in the Process Industries*, 25 (5), 797–802.
- [55] Wang, J., Mannan, M. S., & Wilhite, B. A. Integrated Thermodynamic and Kinetic Model of Homogeneous Catalytic N -Oxidation Processes. (2019). *AIChE Journal*, 66 (4).
- [56] Papadaki, M. & Gao, J. Kinetic Models of Complex Reaction Systems. (2005). *Computers & Chemical Engineering*, 29 (11-12), 2449–2460.
- [57] Wang, Q., Rogers, W. J., & Mannan, M. S. (2009). Thermal Risk Assessment and Rankings for Reaction Hazards in Process Safety. *J. Therm. Anal. Calorim.*, 98 (1), 225–233.
- [58] Shilcrat, S. (2011). Process Safety Evaluation of a Tungsten-Catalyzed Hydrogen Peroxide Epoxidation Resulting in a Runaway Laboratory Reaction. *Organic Process Research & Development*, 15 (6), 1464–1469.
- [59] Wang, W., Su, W., Jiao, Z., & Wang, Q. (2020). Thermal Hazard Analysis of Inorganic Peroxide Initiators with Varying Water Concentrations. *J. Therm. Anal. Calorim.*, <https://doi.org/10.1007/s10973-020-10090-6>.
- [60] Wang, B., Yi, H., Xu, K., & Wang, Q. (2017). Prediction of the Self-Accelerating Decomposition Temperature of Organic Peroxides Using QSPR Models. *J. Therm. Anal. Calorim.*, 128 (1), 399–406.
- [61] Jiao, Z., Escobar-Hernandez, H. U., Parker, T., & Wang, Q. (2019). Review of Recent Developments of Quantitative Structure-Property Relationship Models on Fire and Explosion-Related Properties. *Process Saf. Environ. Prot.*, 129, 280–290.
- [62] Pan, Y., Qi, R., He, P., Shen, R., Jiang, J., Ni, L., Jiang, J., & Wang, Q. (2020). Thermal Hazard Assessment and Ranking for Organic Peroxides Using Quantitative Structure–Property Relationship Approaches. *J. Therm. Anal. Calorim.*, 140 (5), 2575–2583.
- [63] Wang, J., Huang, Y., Wilhite, B. A., Papadaki, M., & Mannan, M. S. (2019). Toward the Identification of Intensified Reaction Conditions Using Response Surface Methodology: A Case Study on 3-Methylpyridine N-Oxide Synthesis. *Ind. Eng. Chem. Res.*, 58 (15), 6093–6104.

- [64] Montgomery, D. C. (2012). *Design and Analysis of Experiments*, 8th ed.; John Wiley & Sons: Nashville, TN.
- [65] Danmaliki, G. I., Saleh, T. A., & Shamsuddeen, A. A. (2017). Response Surface Methodology Optimization of Adsorptive Desulfurization on Nickel/Activated Carbon. *Chem. Eng. J.*, 313, 993.
- [66] Xu, W., Ge, X. D., Yan, X. H., & Shao, R. (2015). Optimization of Methyl Ricinoleate Synthesis with Ionic Liquids as Catalysts Using the Response Surface Methodology. *Chem. Eng. J.*, 275, 63.
- [67] Zheng, Y., Tang, Q., Wang, T., & Wang, J. (2015). Molecular Size Distribution in Synthesis of Polyoxymethylene Dimethyl Ethers and Process Optimization Using Response Surface Methodology. *Chem. Eng. J.*, 278, 183.
- [68] Zheng, Y., Liu, Y., & Wang, A. (2011). Fast Removal of Ammonium Ion Using a Hydrogel Optimized with Response Surface Methodology. *Chem. Eng. J.*, 171, 1201.
- [69] Cheng, R., Li, G., Cheng, C., Liu, P., Shi, L., Ma, Z., & Zheng, X. (2014). Removal of Bacteriophage F2 in Water by Nanoscale Zero-Valent Iron and Parameters Optimization Using Response Surface Methodology. *Chem. Eng. J.*, 252, 150.
- [70] Liu, Q., Li, R., & Fang, T. (2015). Investigating and Modeling Pet Methanolysis under Supercritical Conditions by Response Surface Methodology Approach. *Chem. Eng. J.*, 270, 535.
- [71] Zhang, Y. & Pan, B. (2014). Modeling Batch and Column Phosphate Removal by Hydrated Ferric Oxide-Based Nanocomposite Using Response Surface Methodology and Artificial Neural Network. *Chem. Eng. J.*, 249, 111.
- [72] Ahmad, A., Oh, P. C., & Shukor, S. A. (2011). Synthesis of 2-Oxo-4- Phenylbutanoic Acid: Parameter Optimization Using Response Surface Methodology. *Chem. Eng. J.*, 171, 640.
- [73] Kacker, R. N., Lagergren, E. S., & Filliben, J. J. (1991). Taguchi's orthogonal arrays are classical designs of experiments. *Journal of Research of the National Institute of Standards and Technology*, 96(5), 577. <https://doi.org/10.6028/jres.096.034>
- [74] Bezerra, M. A., Santelli, R. E., Oliveira, E. P., Villar, L. S., & Escaleira, L. A. (2008). Response Surface Methodology (Rsm) as a Tool for Optimization in Analytical Chemistry. *Talanta*, 76, 965.
- [75] Wilcock, E. & Rogers, R. L. (1997). A Review of the Phi Factor during Runaway Conditions. *J. Loss Prev. Process Ind.*, 10 (5–6), 289–302.

- [76] Parker, T., Mao, Y., & Wang, Q. (2022). Application of response surface methodology for hazard analysis of 2-butanol oxidation to 2-butanone using RC1 calorimetry. *Journal of Loss Prevention in the Process Industries*, 75, 104703. <https://doi.org/10.1016/j.jlp.2021.104703>
- [77] Cyclohexanone. (2007). *Hawley's Condensed Chemical Dictionary*. <https://doi.org/10.1002/9780470114735.hawley04564>
- [78] Musser, M. T. (2011). Cyclohexanol and cyclohexanone. *Ullmann's Encyclopedia of Industrial Chemistry*. [https://doi.org/10.1002/14356007.a08\\_217.pub2](https://doi.org/10.1002/14356007.a08_217.pub2)
- [79] Chen, L., Zhou, T., Chen, L., Ye, Y., Qi, Z., Freund, H., & Sundmacher, K. (2011). Selective oxidation of cyclohexanol to cyclohexanone in the ionic liquid 1-octyl-3-methylimidazolium chloride. *Chemical Communications*, 47(33), 9354. <https://doi.org/10.1039/c1cc12989a>
- [80] Wei, J. (2002). Organic solvent- and phase transfer catalyst-free oxidation of cyclohexanol to cyclohexanone with dilute H<sub>2</sub>O<sub>2</sub>. *Chinese Science Bulletin*, 47(24), 2060. <https://doi.org/10.1360/02fb9446>
- [81] Zhao, Y.-H., Huang, G.-Q., & Cao, C.-Y. (2017). Catalytic oxidation of cyclohexanol to cyclohexanone with H<sub>2</sub>O<sub>2</sub> using Na<sub>2</sub>WO<sub>4</sub> as a catalytic system. *Reaction Kinetics, Mechanisms and Catalysis*, 122(1), 305–314. <https://doi.org/10.1007/s11144-017-1226-7>
- [82] Dai, W.-L., Ding, J., Zhu, Q., Gao, R., & Yang, X. (2016). Tungsten containing materials as heterogeneous catalysts for green catalytic oxidation process. *Catalysis*, 1–27. <https://doi.org/10.1039/9781782626855-00001>
- [83] Zhu, Z., & Bian, W. (2008). Characterization of tungsten-based catalyst used for selective oxidation of cyclopentene to glutaraldehyde. *Chinese Journal of Chemical Engineering*, 16(6), 895–900. [https://doi.org/10.1016/s1004-9541\(09\)60013-6](https://doi.org/10.1016/s1004-9541(09)60013-6)
- [84] Cyclohexanol. (2007). *Hawley's Condensed Chemical Dictionary*. <https://doi.org/10.1002/9780470114735.hawley04562>
- [85] Etchells J. (2001). Prevention and control of Exothermic Runaway: An HSE update. *Loss Prevention Bulletin*. 157(1):4-8
- [86] Fauske, H. (1984). Scale-up for safety relief of runaway reactions. *Plant/Operations Progress*. 3(1):7-11. doi:10.1002/prsb.720030105
- [87] Macondo Well Deepwater Horizon Blowout. (2011). *National Academy of Engineering*. <https://doi.org/10.17226/13273>
- [88] Vorderbrueggen, J. B. (2011). Imperial Sugar Refinery combustible dust explosion investigation. *Process Safety Progress*, 30(1), 66–81. <https://doi.org/10.1002/prs.10445>

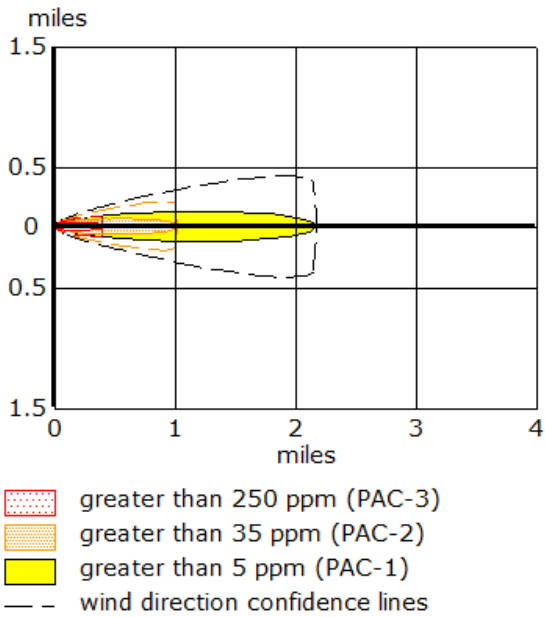


APPENDIX A

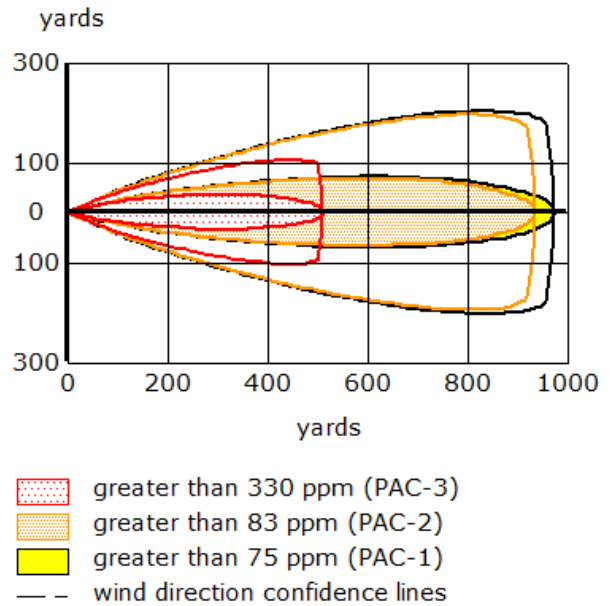
ALOHA WAREHOUSE DISPERSION MODELS

Warehouse 2

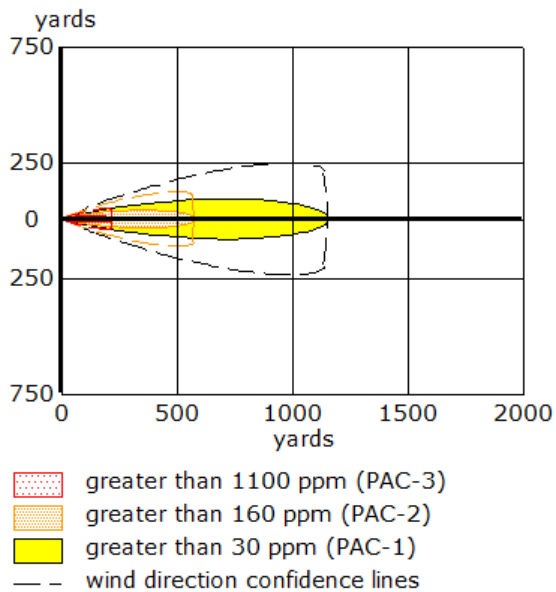
1. Acetic Acid (1132 lb.)



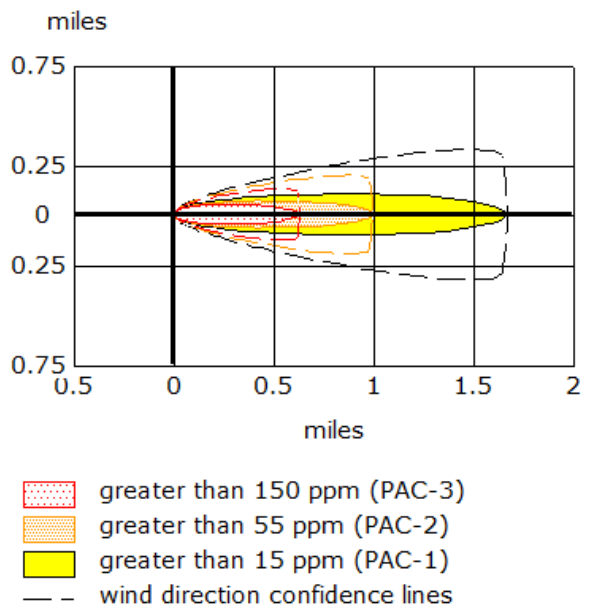
3. Ammonia (497 lb.)



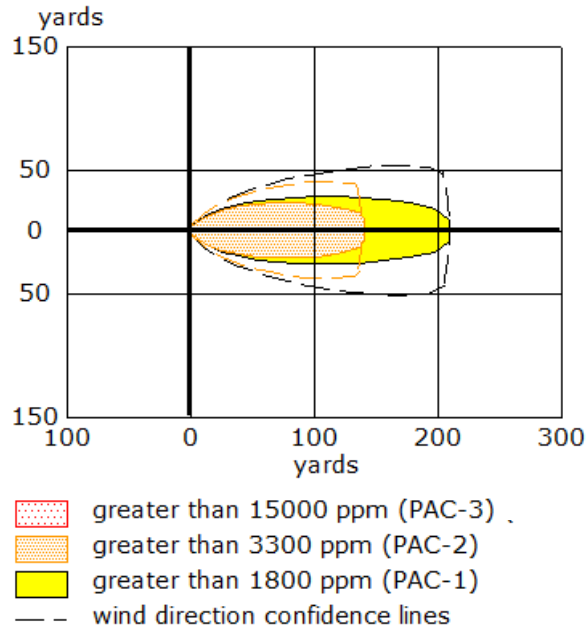
2. Ethanol (869 lb.)



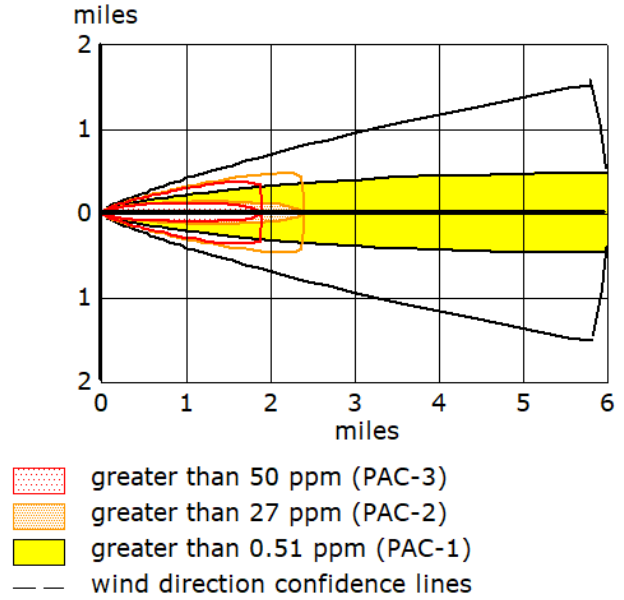
4. Carbon Monoxide (1300 lb.)



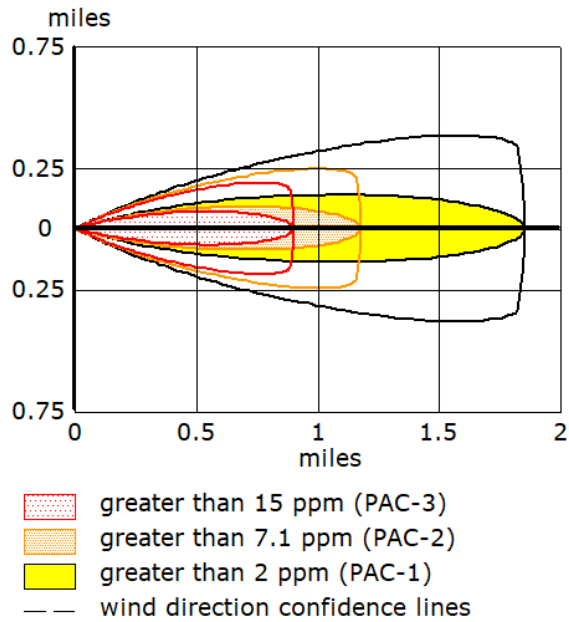
5. Carbonyl Sulfide (1725 lb.)



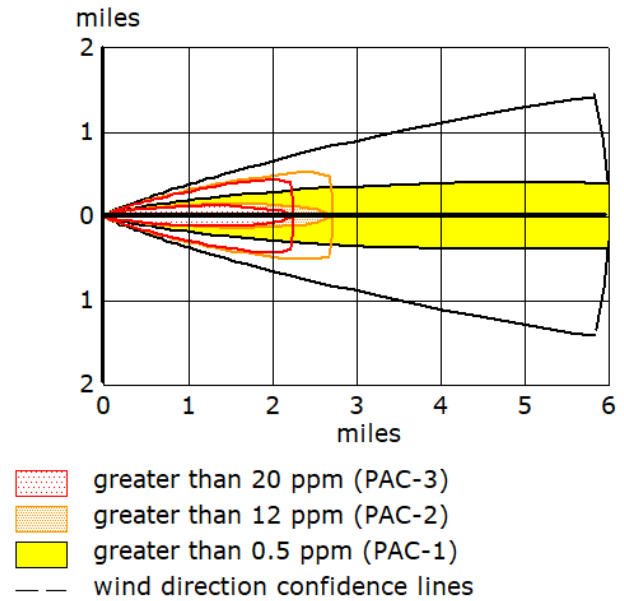
7. Hydrogen Sulfate (4178 lb.)



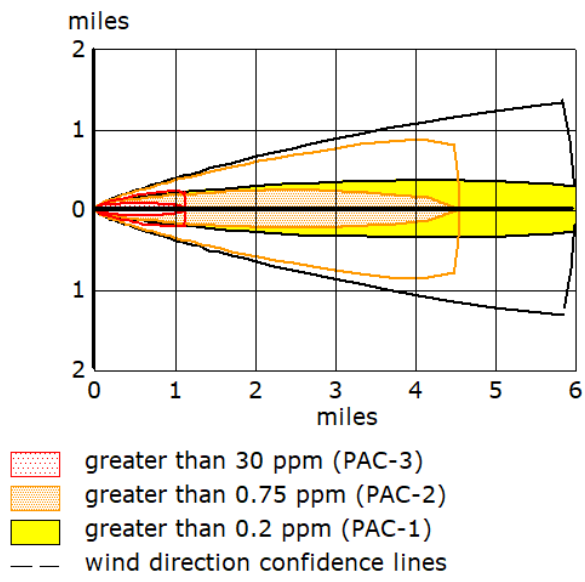
6. Hydrogen Cyanide (923 lb.)



8. Nitrous Oxide (2176 lb.)

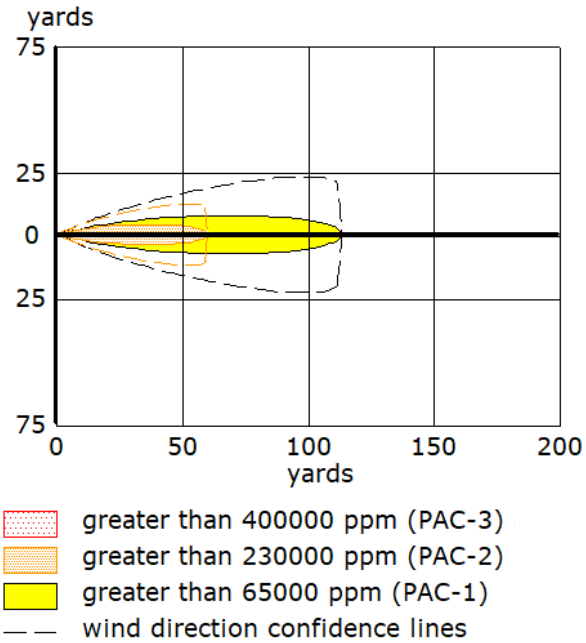


9. Sulfur Dioxide (1373 lb.)

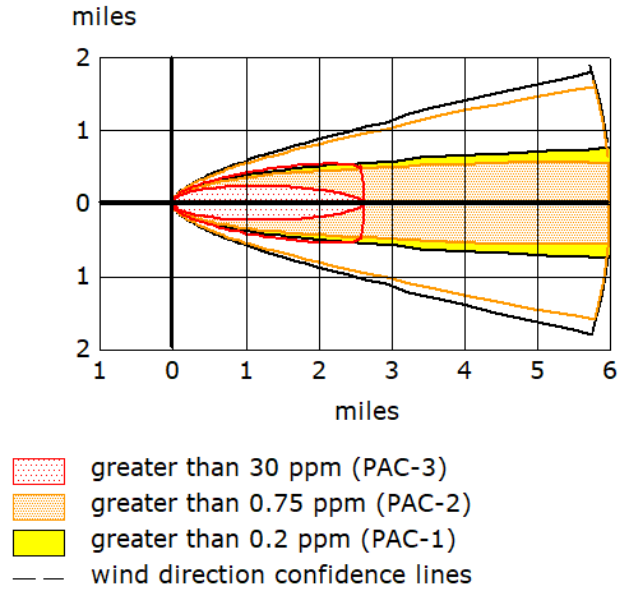


Warehouse 3

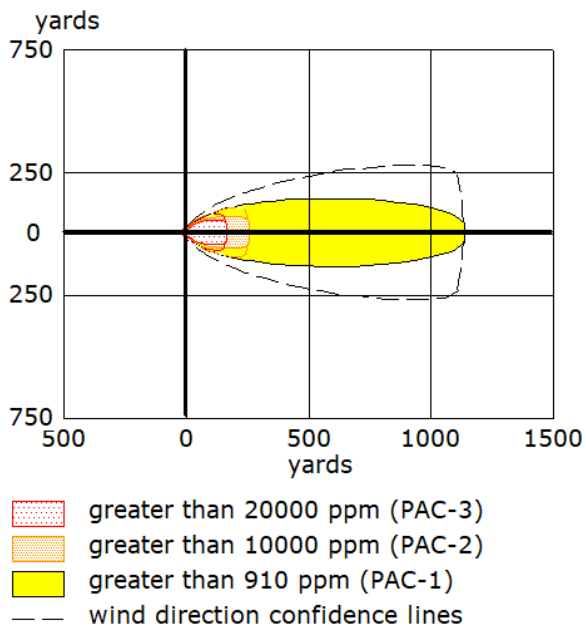
1. Hydrogen Gas (965 lb.)



3. Sulfur Dioxide (16335 lb.)

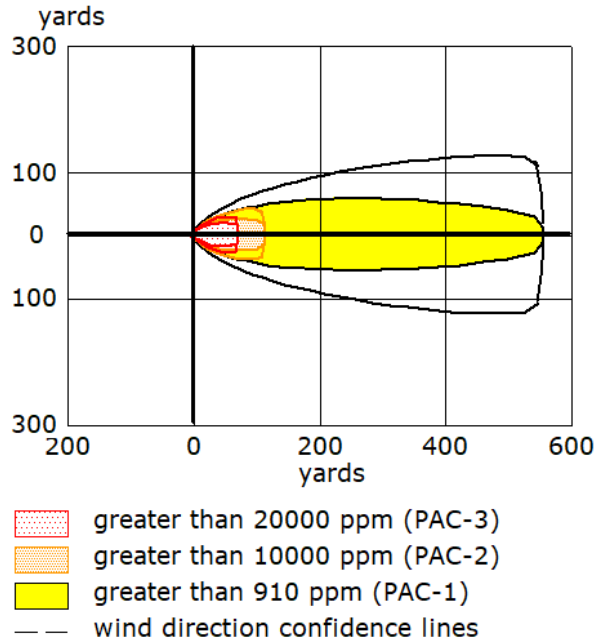


2. Nitrogen Dioxide (11213 lb.)

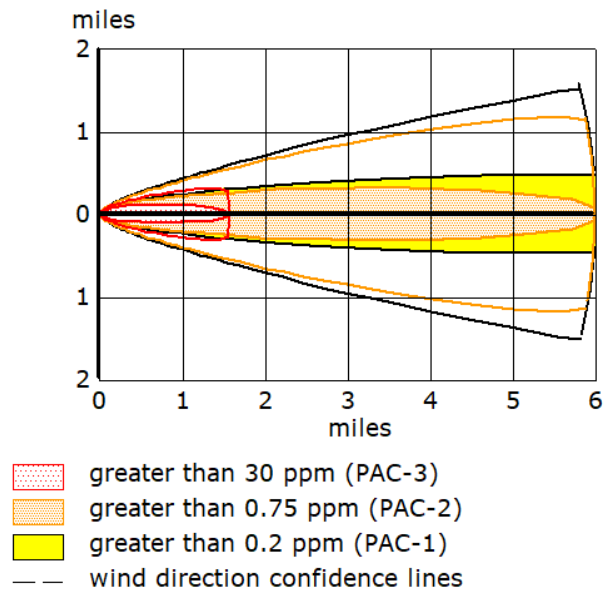


## Warehouse 5

### 1. Nitrogen Dioxide (2243 lb.)

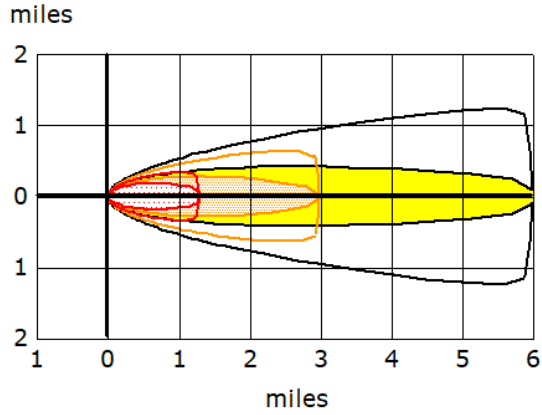


### 2. Sulfur Dioxide (3267 lb.)



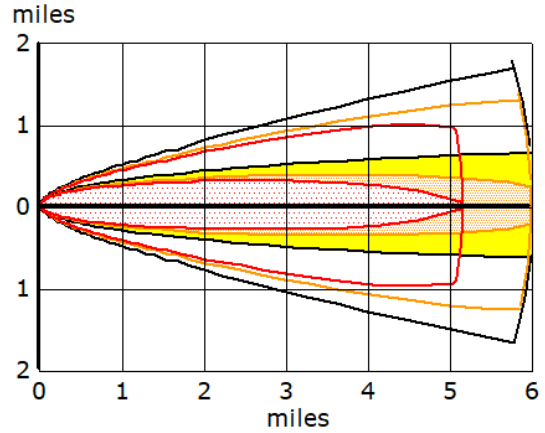
Warehouse 7

1. Acetic Acid (26360 lb.)



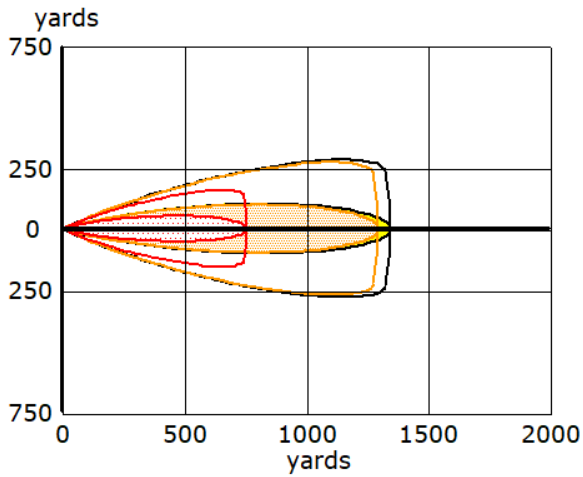
- greater than 250 ppm (PAC-3)
- greater than 35 ppm (PAC-2)
- greater than 5 ppm (PAC-1)
- wind direction confidence lines

3. Chlorine (3889 lb.)



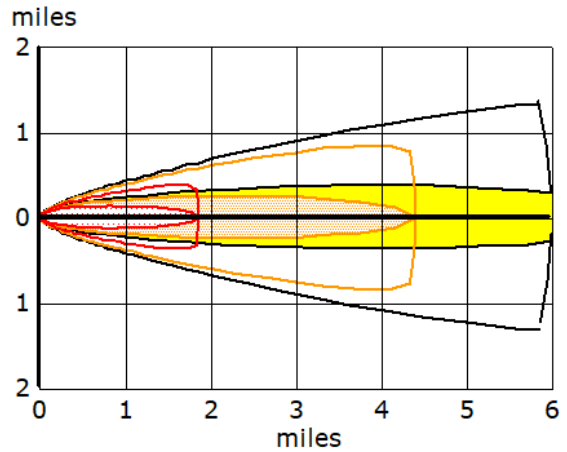
- greater than 2.4 ppm (PAC-3)
- greater than 1.1 ppm (PAC-2)
- greater than 0.15 ppm (PAC-1)
- wind direction confidence lines

2. Carbon Monoxide (3078 lb.)



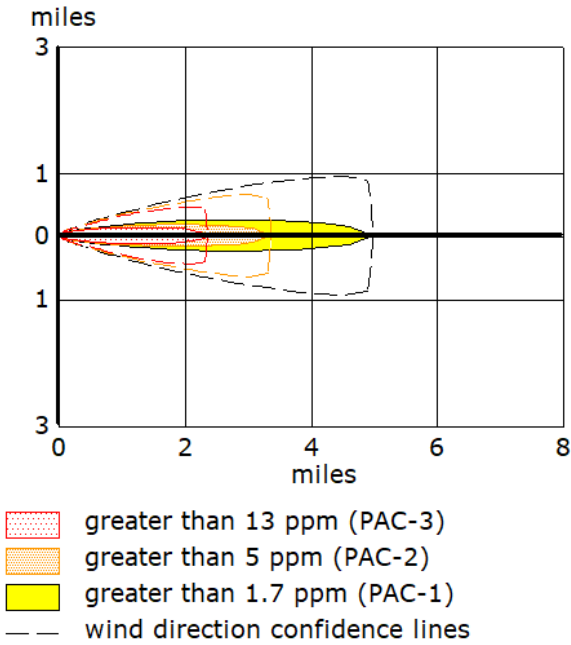
- greater than 330 ppm (PAC-3)
- greater than 83 ppm (PAC-2)
- greater than 75 ppm (PAC-1)
- wind direction confidence lines

4. Chlorine Dioxide (7395 lb.)

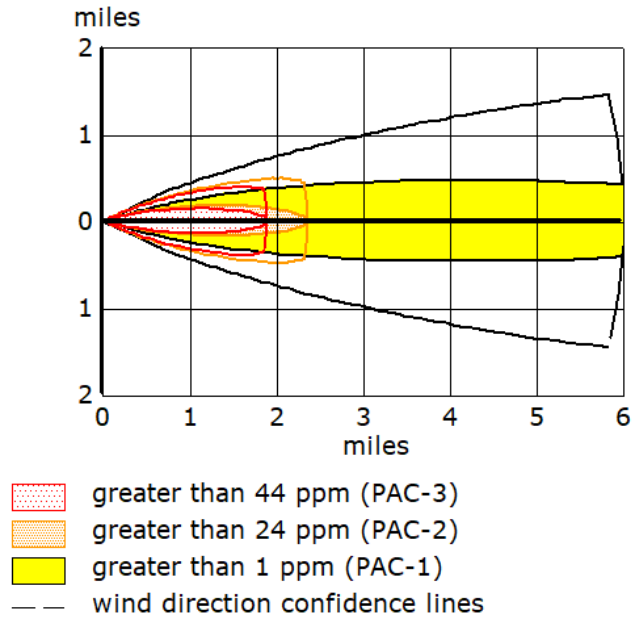


- greater than 20 ppm (PAC-3)
- greater than 2 ppm (PAC-2)
- greater than 0.5 ppm (PAC-1)
- wind direction confidence lines

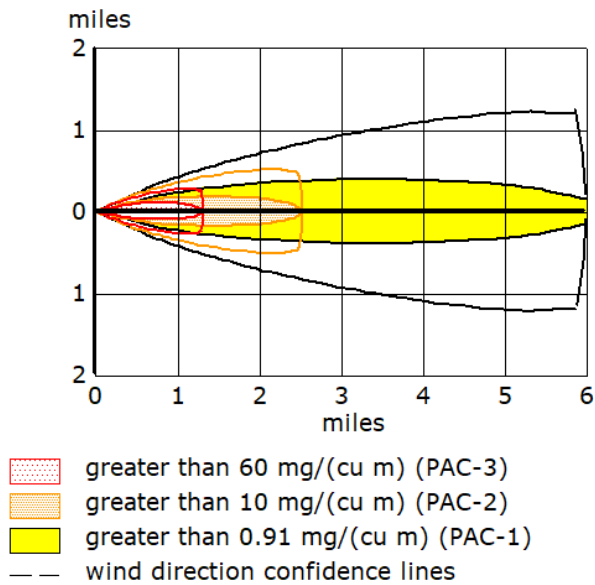
5. Fluorine Gas (2082 lb.)



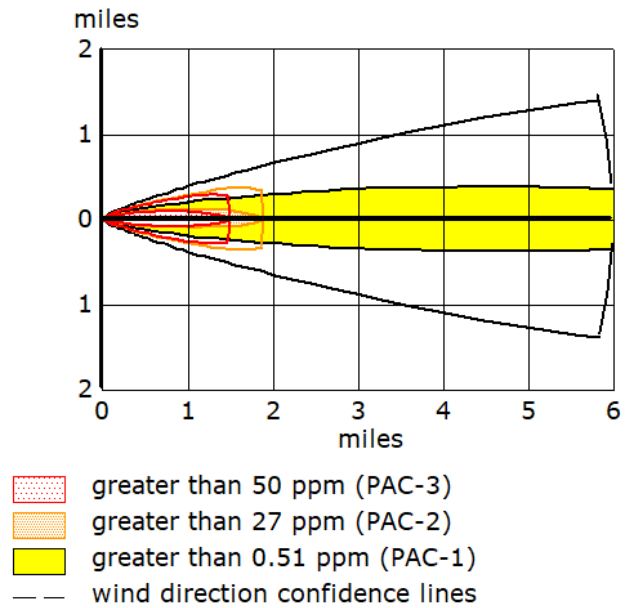
7. Hydrogen Chloride (16009 lb.)



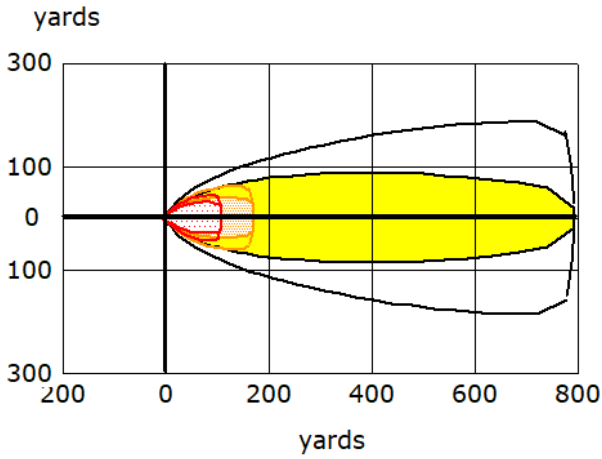
6. Fluorochloromethane (9476 lb.)







8. Hydrogen Fluoride (2191 lb.)

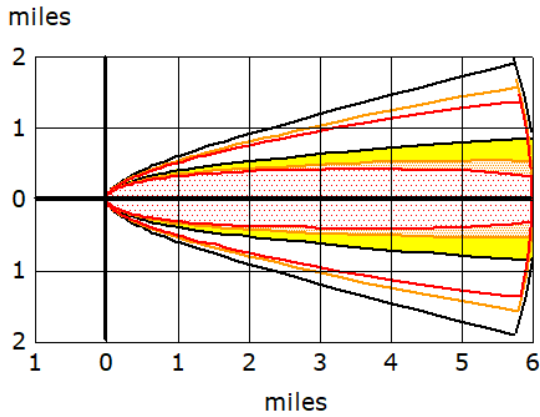





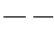
9. Nitrogen Dioxide (4820 lb.)



-  greater than 20000 ppm (PAC-3)
-  greater than 10000 ppm (PAC-2)
-  greater than 910 ppm (PAC-1)
-  wind direction confidence lines

10. Phosgene (10835 lb.)

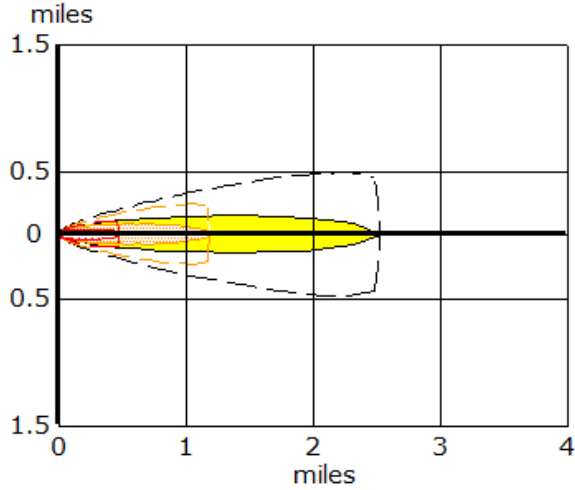


-  greater than 0.75 ppm (PAC-3)
-  greater than 0.3 ppm (PAC-2)
-  greater than 0.027 ppm (PAC-1)
-  wind direction confidence lines



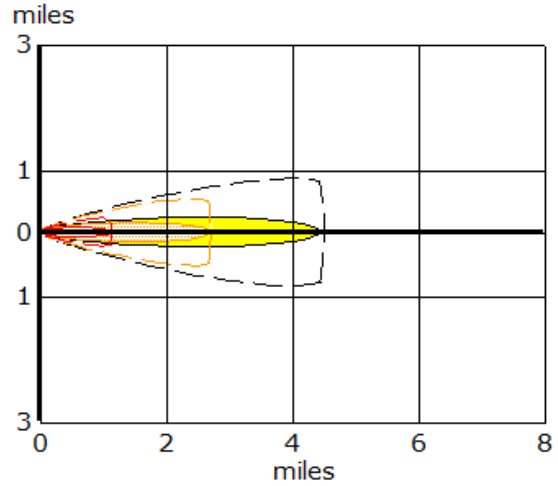
Warehouse 9

1. Acetic Acid (1717 lb.)



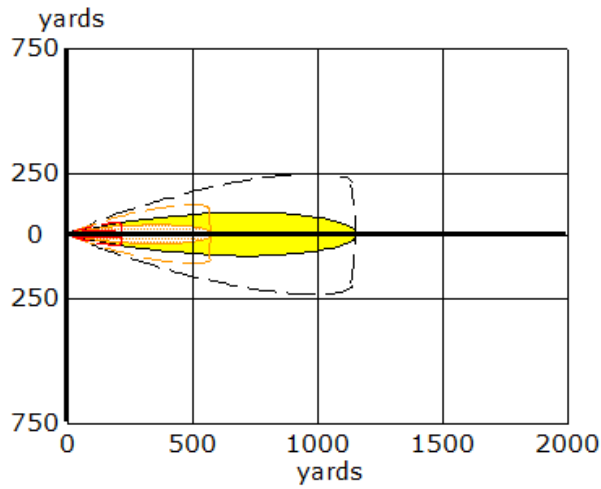
greater than 250 ppm (PAC-3)  
 greater than 35 ppm (PAC-2)  
 greater than 5 ppm (PAC-1)  
 wind direction confidence lines

3. Chlorine (1014 lb.)



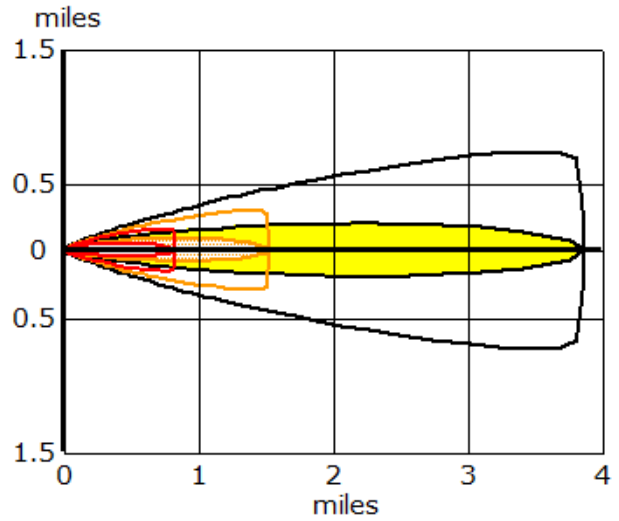
greater than 20 ppm (PAC-3)  
 greater than 2 ppm (PAC-2)  
 greater than 0.5 ppm (PAC-1)  
 wind direction confidence lines

2. Ammonia (494 lb.)



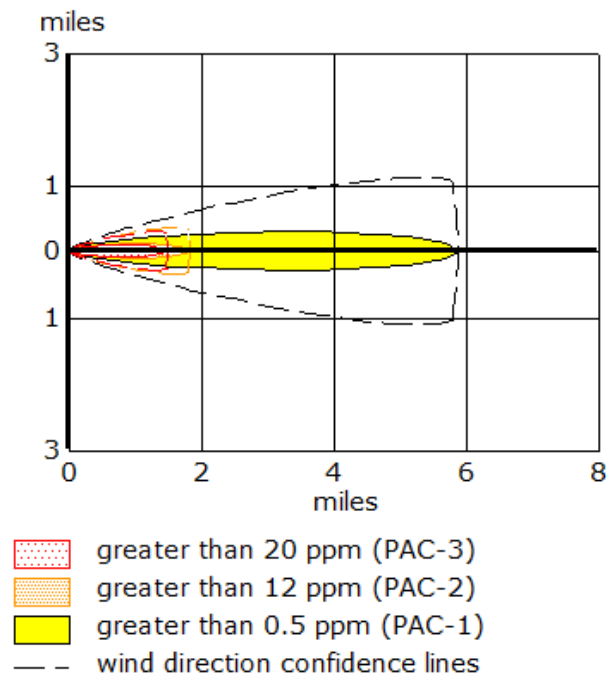
greater than 1100 ppm (PAC-3)  
 greater than 160 ppm (PAC-2)  
 greater than 30 ppm (PAC-1)  
 wind direction confidence lines

4. Hydrogen Chloride (1043 lb.)



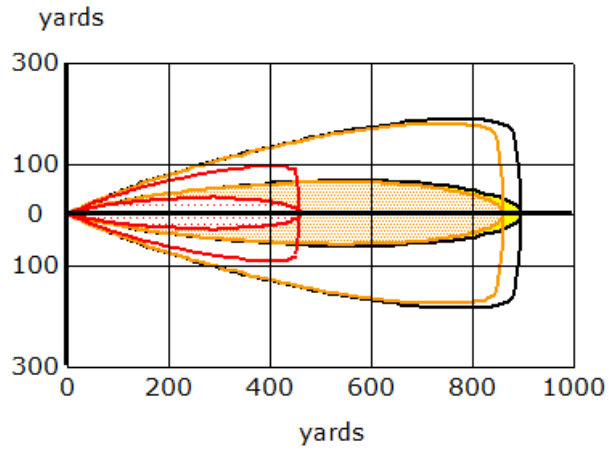
greater than 100 ppm (PAC-3)  
 greater than 22 ppm (PAC-2)  
 greater than 1.8 ppm (PAC-1)  
 wind direction confidence lines





5. Nitrogen Dioxide (1257 lb.)



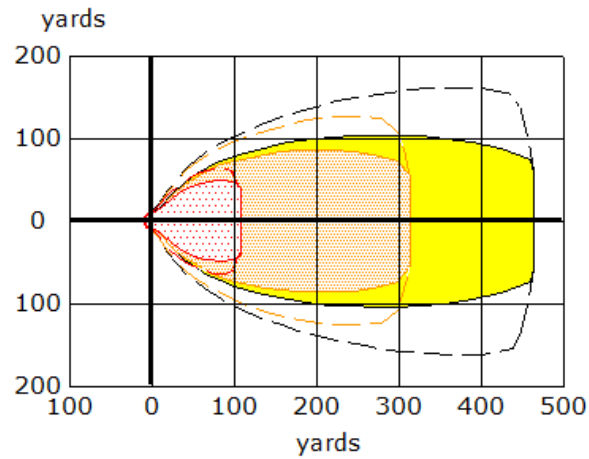
# Warehouse 14





## 1. Carbon Monoxide (1063 lb.)



-  greater than 330 ppm (PAC-3)
-  greater than 83 ppm (PAC-2)
-  greater than 75 ppm (PAC-1)
-  wind direction confidence lines

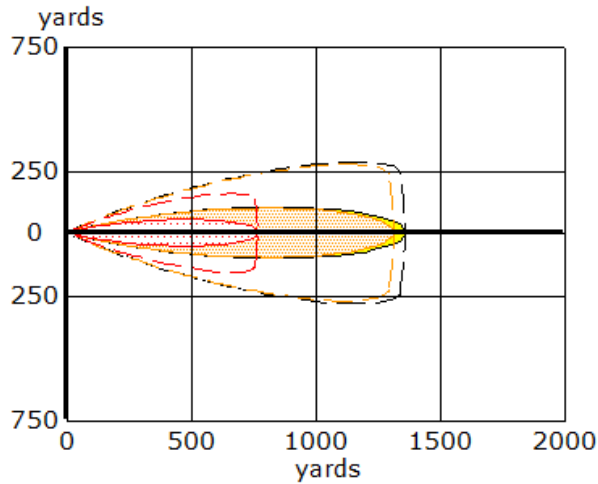
## 2. Chlorodifluoromethane (7079 lb.)



-  greater than 14000 ppm (PAC-3)
-  greater than 2400 ppm (PAC-2)
-  greater than 1250 ppm (PAC-1)
-  wind direction confidence lines

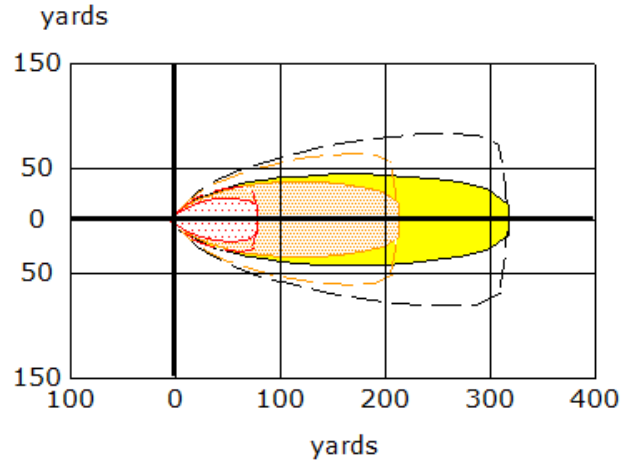
Warehouse 16

1. Carbon Monoxide (3179 lb.)



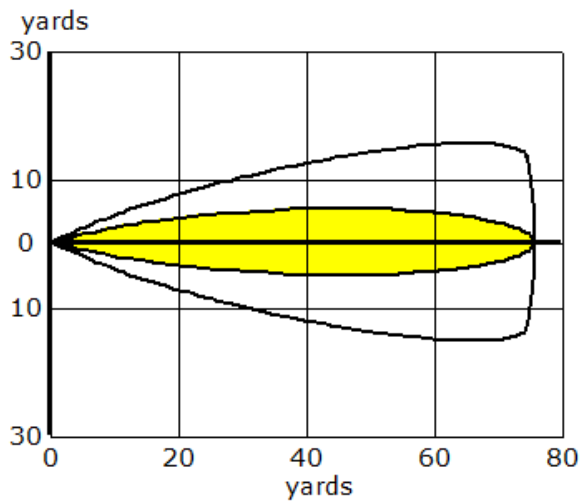
- greater than 330 ppm (PAC-3)
- greater than 83 ppm (PAC-2)
- greater than 75 ppm (PAC-1)
- wind direction confidence lines

3. Ethanol (1984 lb.)



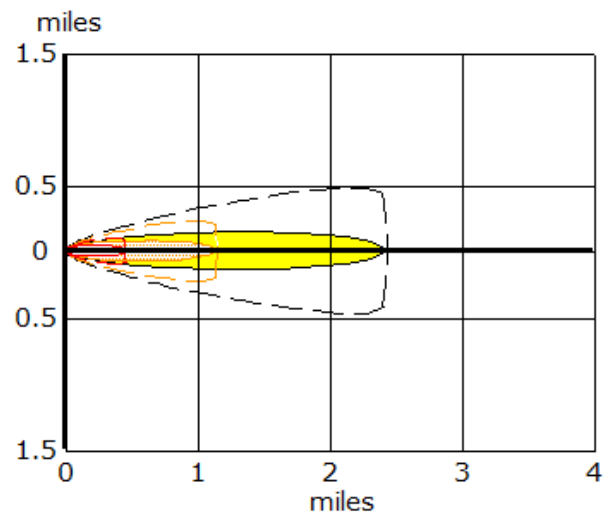
- greater than 15000 ppm (PAC-3)
- greater than 3300 ppm (PAC-2)
- greater than 1800 ppm (PAC-1)
- wind direction confidence lines

2. Methane (3405 lb.)



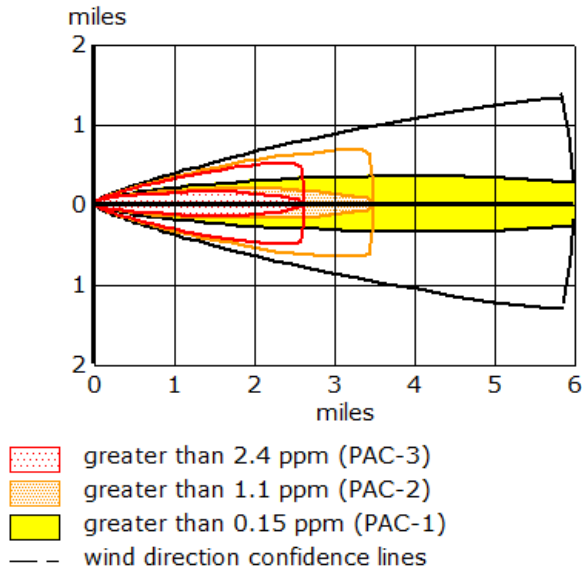
- greater than 400000 ppm (PAC-3)
- greater than 230000 ppm (PAC-2)
- greater than 65000 ppm (PAC-1)
- wind direction confidence lines

4. Acetic Acid (1564 lb.)

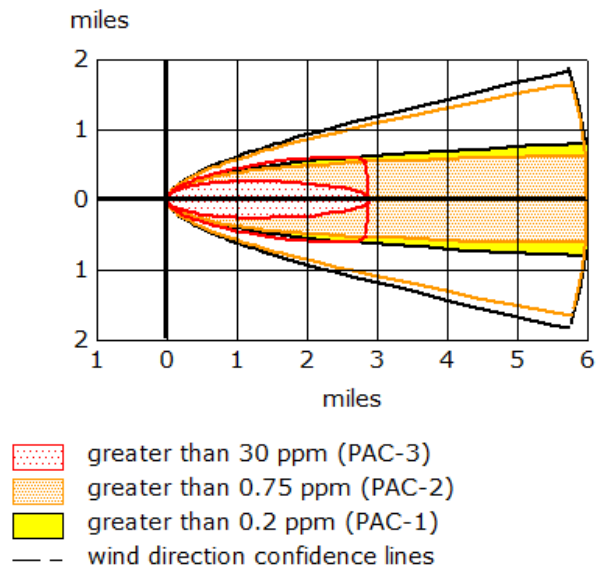


- greater than 250 ppm (PAC-3)
- greater than 35 ppm (PAC-2)
- greater than 5 ppm (PAC-1)
- wind direction confidence lines

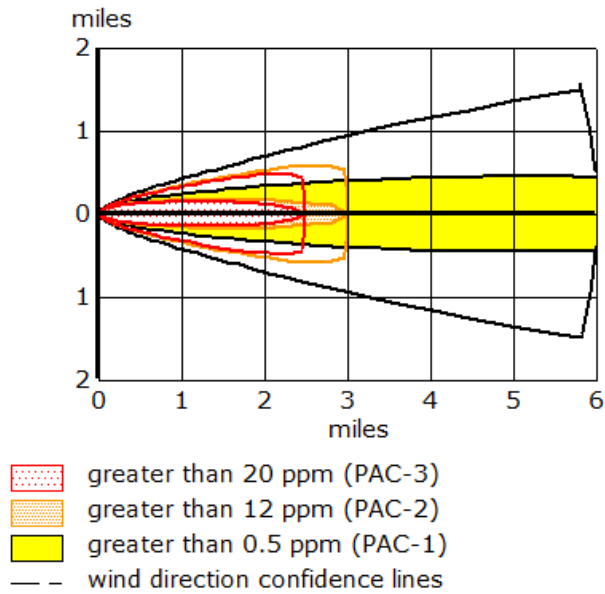
5. Chlorine Dioxide (23405 lb.)



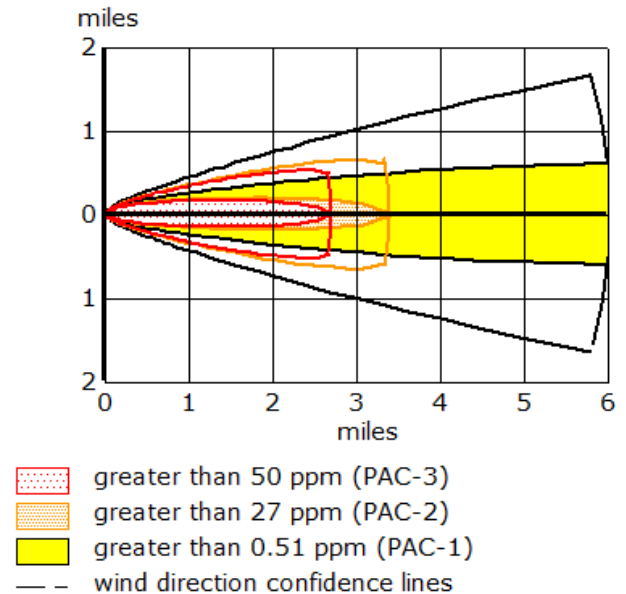
7. Sulfur Dioxide (22226 lb.)



6. Nitrogen Dioxide (4977 lb.)

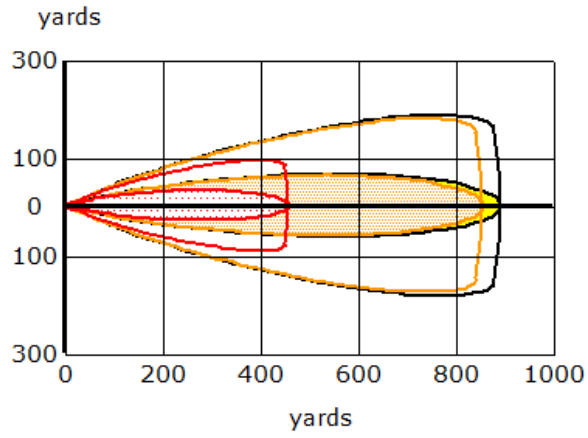





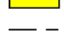
8. Hydrogen Sulfate (10984 lb.)



Warehouse 18

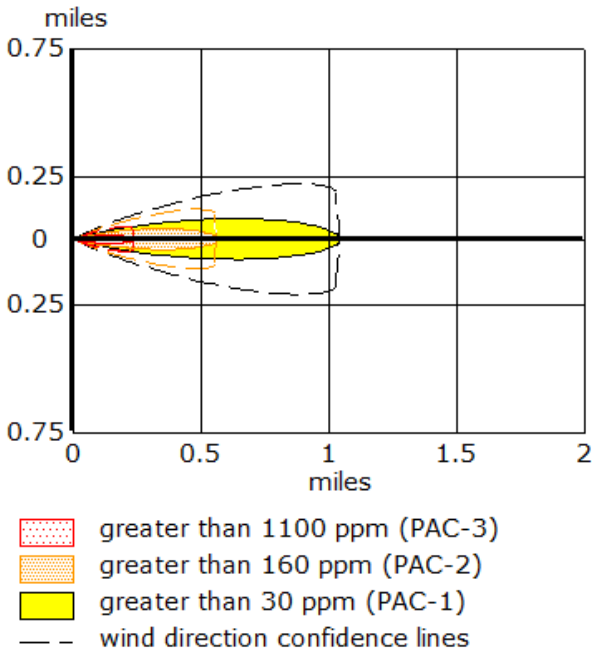
1. Carbon Monoxide (1041 lb.)



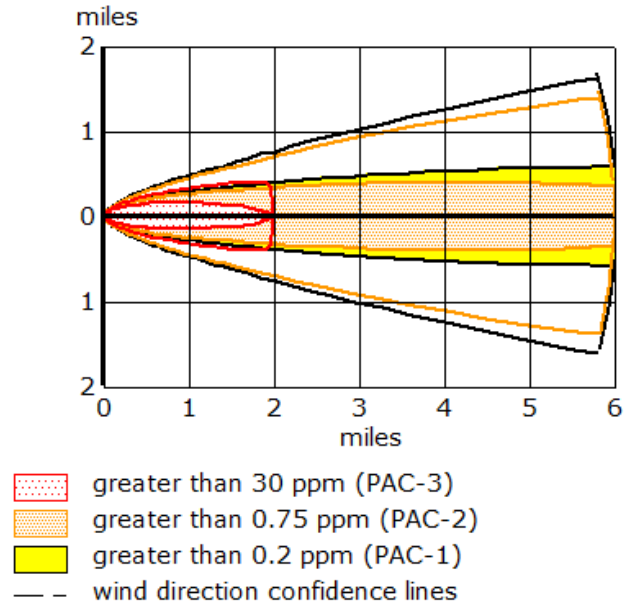
-  greater than 330 ppm (PAC-3)
-  greater than 83 ppm (PAC-2)
-  greater than 75 ppm (PAC-1)
-  wind direction confidence lines

Warehouse 23

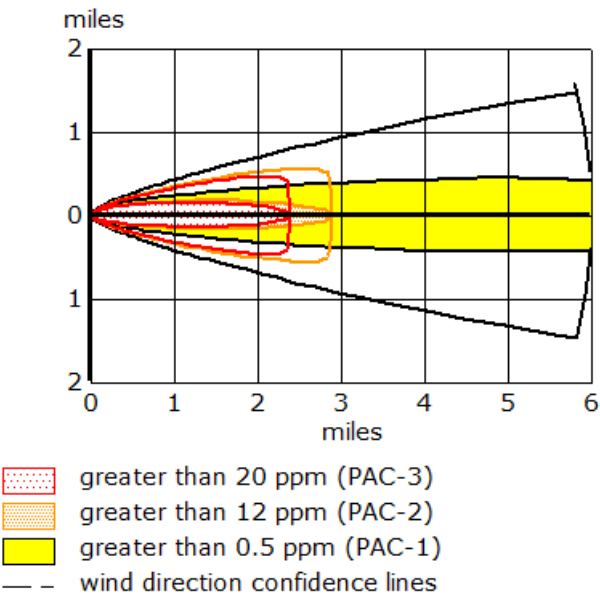
1. Ammonia (1764 lb.)



3. Sulfur Dioxide (6534 lb.)

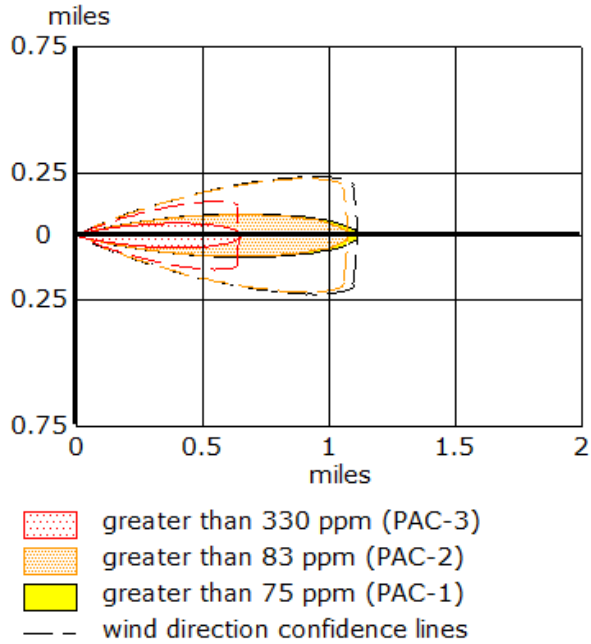


2. Nitrogen Dioxide (4485 lb.)

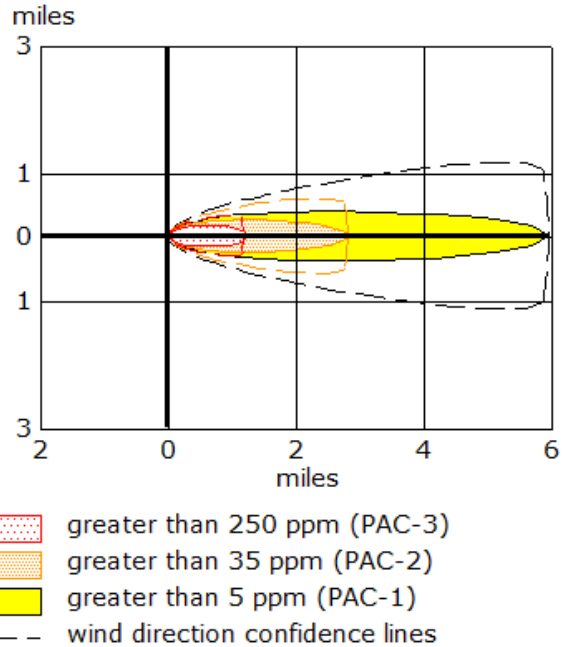


Warehouse 25

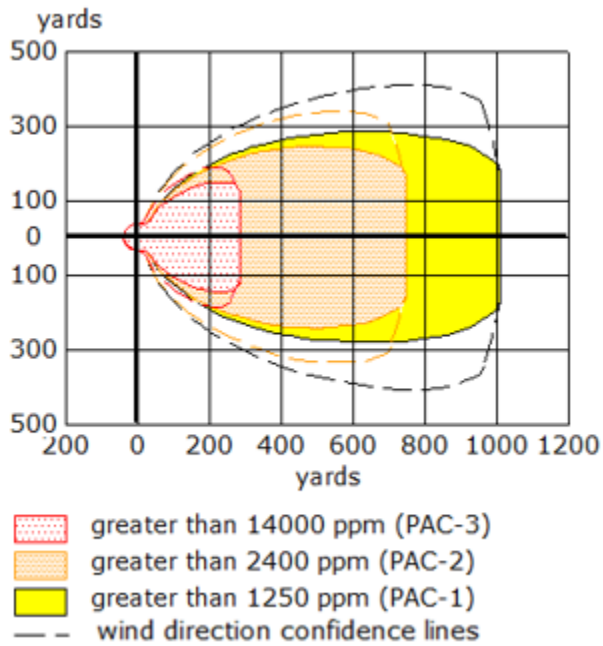
1. Carbon Monoxide (8781 lb.)



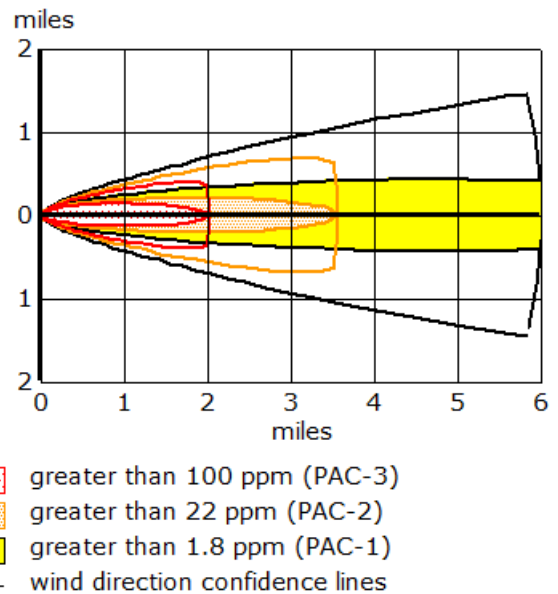
3. Acetic Acid (22226 lb.)



2. Chlorodifluoromethane (39128 lb.)

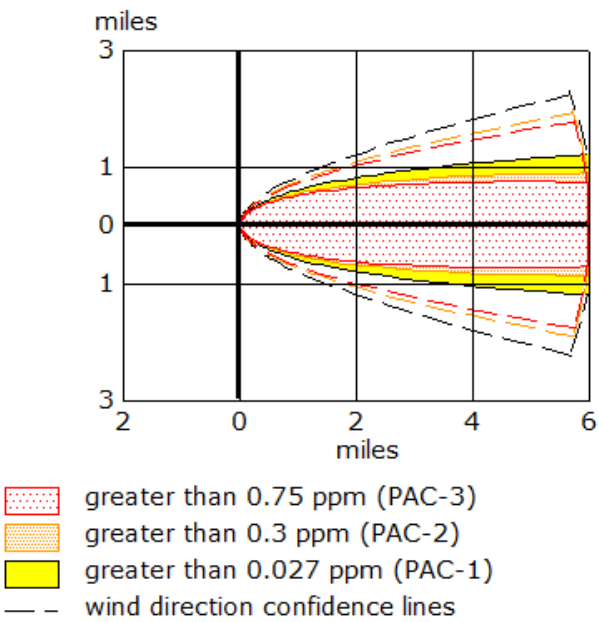


4. Hydrogen Chloride (11406 lb.)

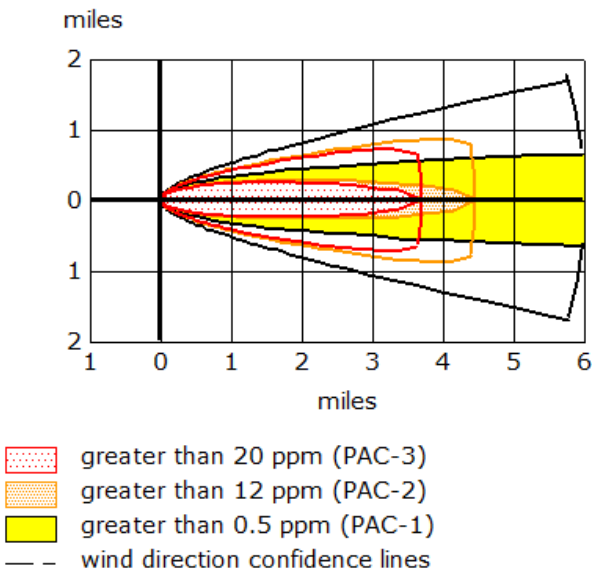




5. Phosgene (44738 lb.)

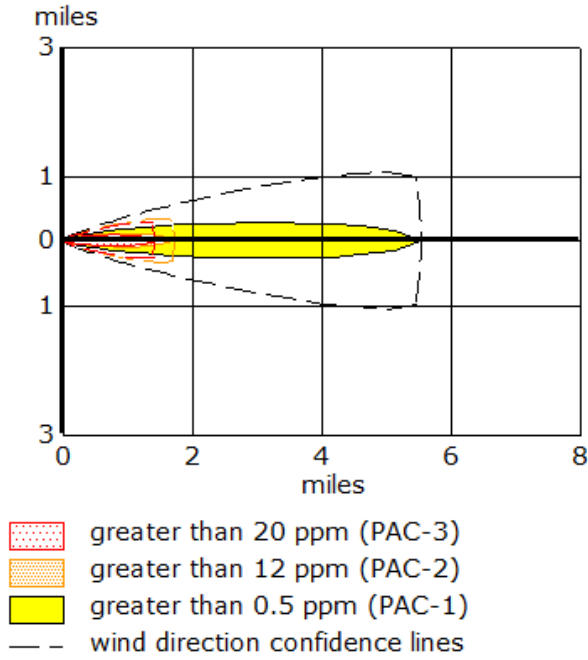


6. Nitrogen Dioxide (16272 lb.)

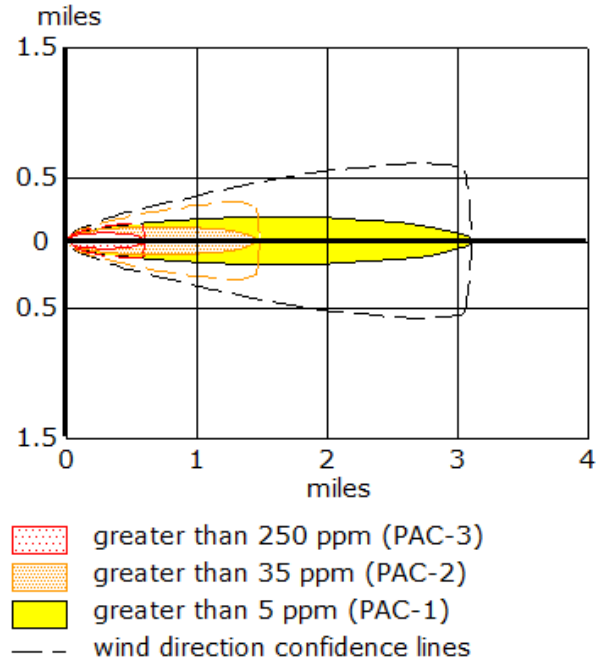


Warehouse 29

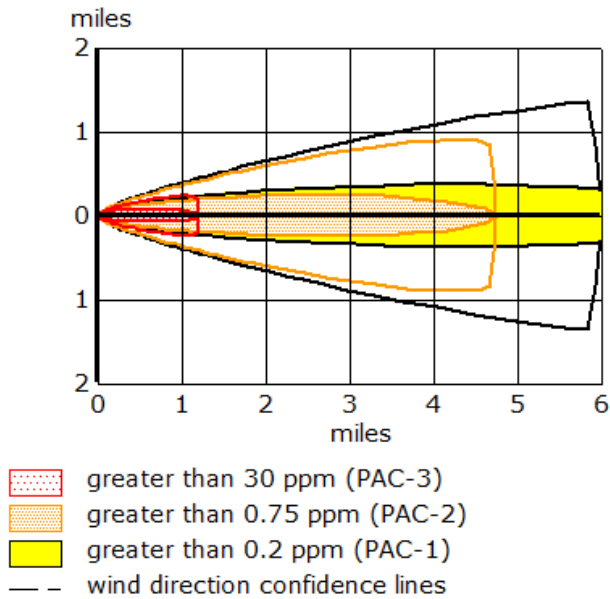
1. Nitrogen Dioxide (1062 lb.)



3. Acetic Acid (3063 lb.)

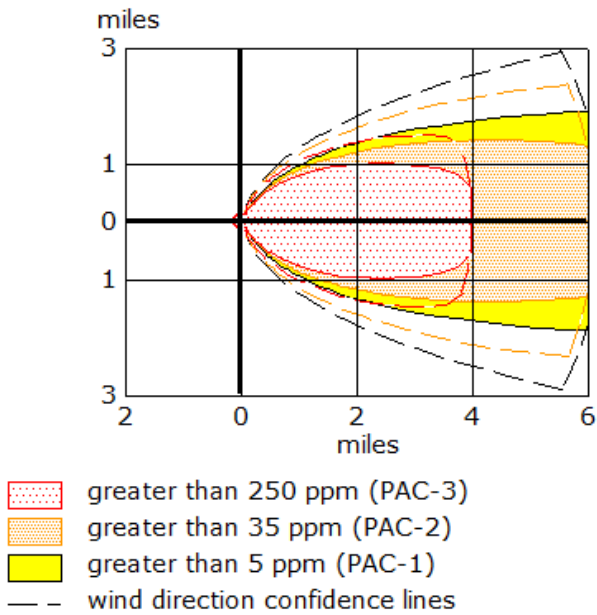


2. Sulfur Dioxide (1547 lb.)

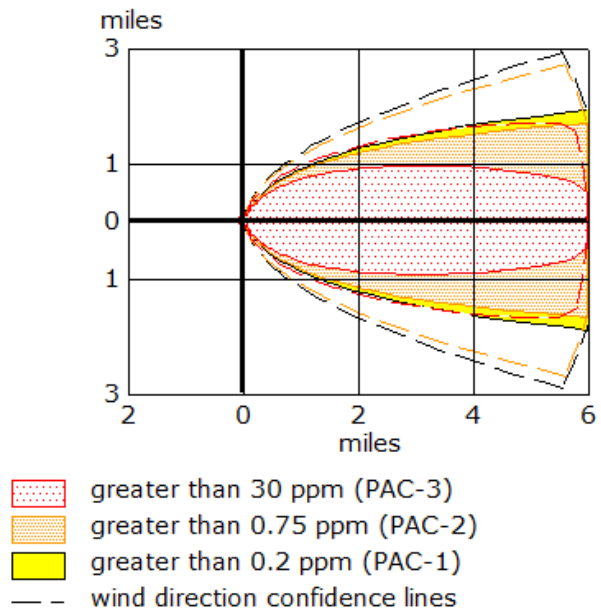


Warehouse 30

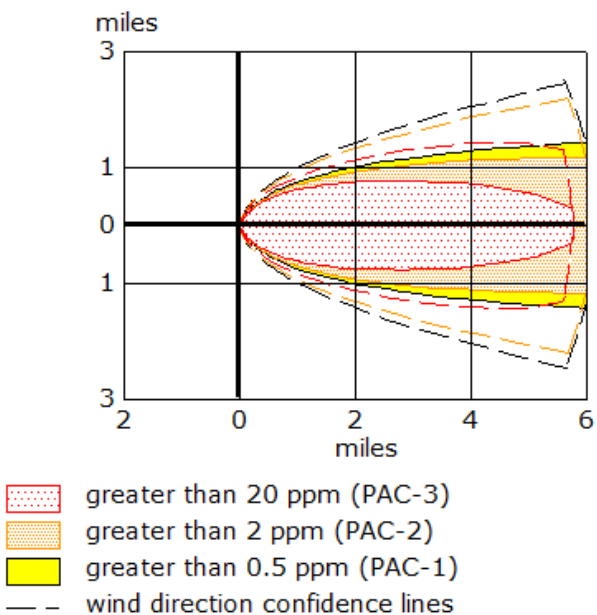
1. Acetic Acid (751250 lb.)



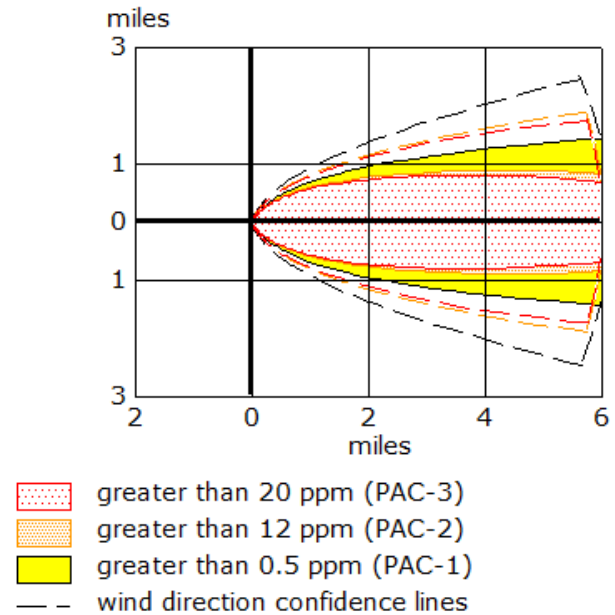
3. Sulfur Dioxide (326707 lb.)



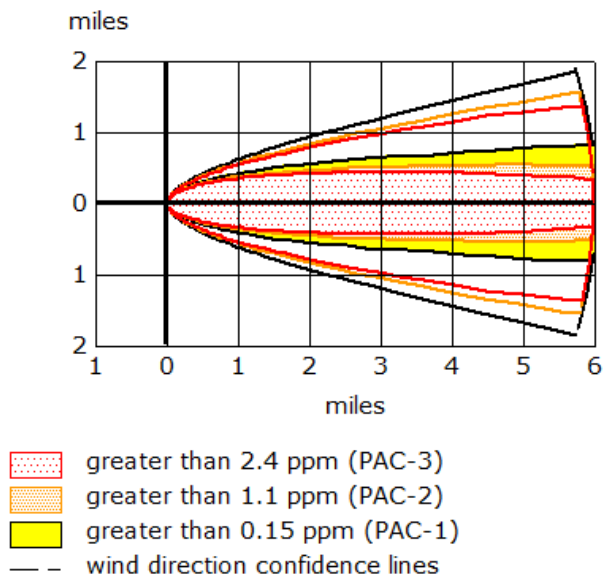
2. Chlorine (180938 lb.)



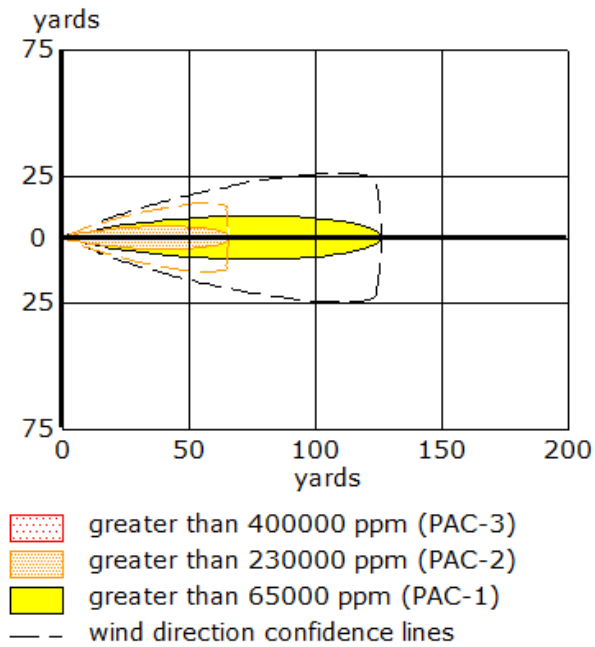
4. Nitrogen Dioxide (224261 lb.)



5. Chlorine Dioxide (21094 lb.)

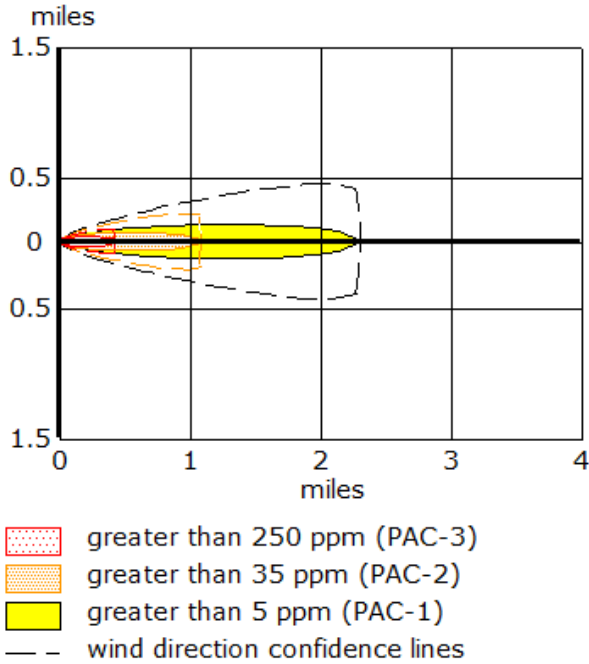


6. Methane (9406 lb.)

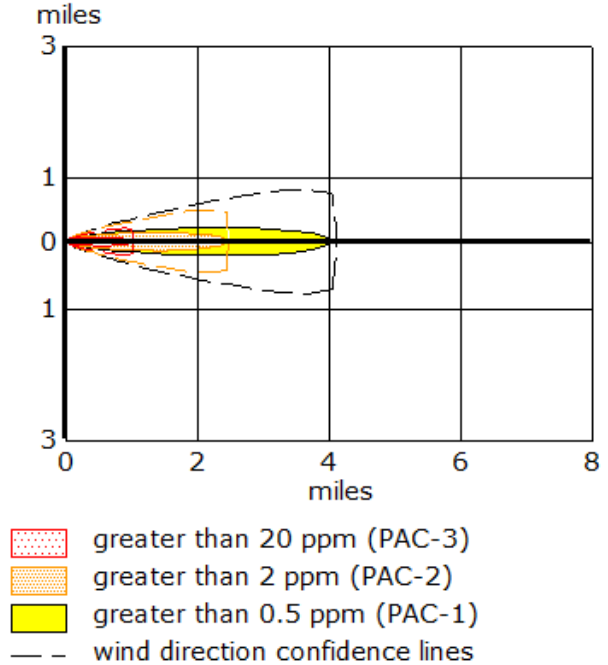


Warehouse 33

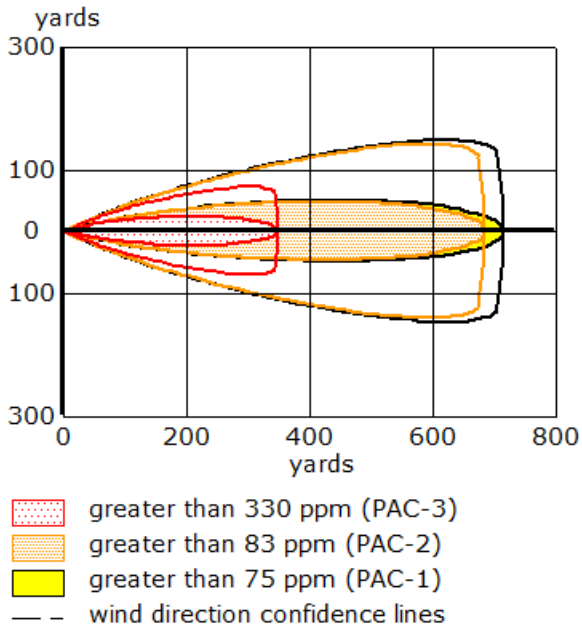
1. Acetic Acid (1317 lb.)



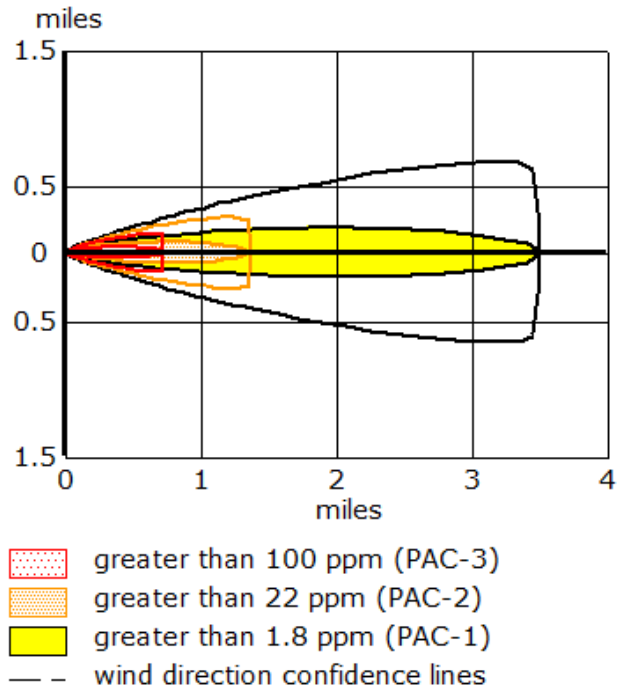
3. Chlorine (778 lb.)



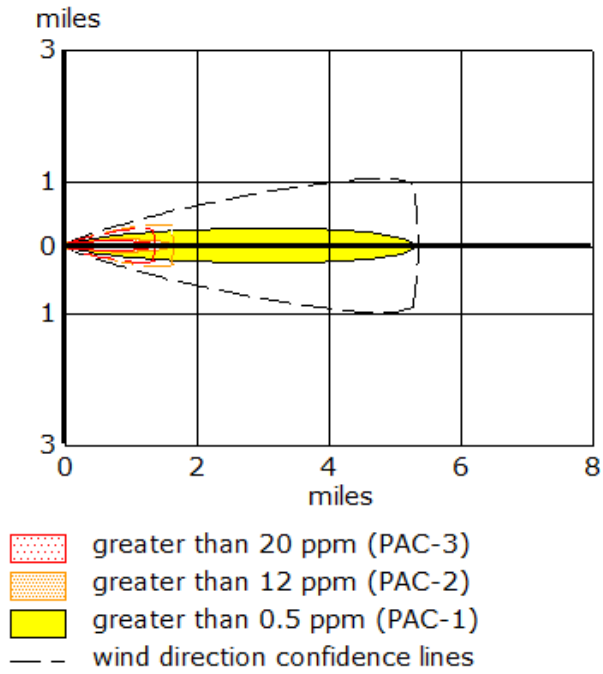
2. Carbon Monoxide (616 lb.)



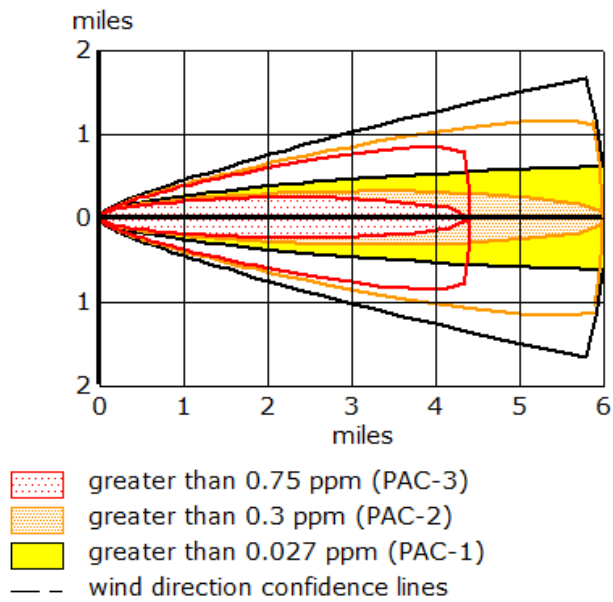
4. Hydrogen Chloride (800 lb.)



5. Nitrogen Dioxide (964 lb.)



6. Phosgene (2167 lb.)



## APPENDIX B

### 2-BUTANONE HEAT RELEASE AND FTIR DATA

Table B.1: Raw heat release data for Taguchi Orthogonal Array (OA) design for study of temperature, catalyst, and 2-butanol concentration impact on total heat generation

Run	Temperature (°C)	2-butanol concentration (mol/L)	Catalyst concentration (wt%)	Total heat generated (kJ)	Heat generated (kJ/kg reaction mass)
1	30	0.284	2.4	3.62	11.10
2	45	0.284	3.6	1.98	6.03
3	60	0.284	4.8	1.75	5.29
4	30	0.534	2.4	4.44	13.60
5	45	0.534	3.6	2.87	8.73
6	60	0.534	4.8	4.13	12.48
7	30	0.784	2.4	3.28	10.04
8	45	0.784	3.6	0.65	1.98
9	60	0.784	4.8	2.86	8.64

Temperature and heat release graphs for 9 experiments:

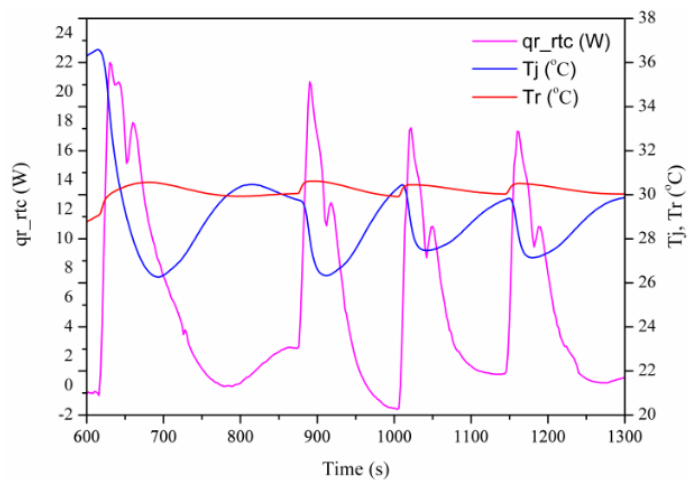


Fig. B.1: 30  $^{\circ}C$ , 2-Butanol Concentration: 0.28 mol/L, Catalyst Concentration: 2.4%

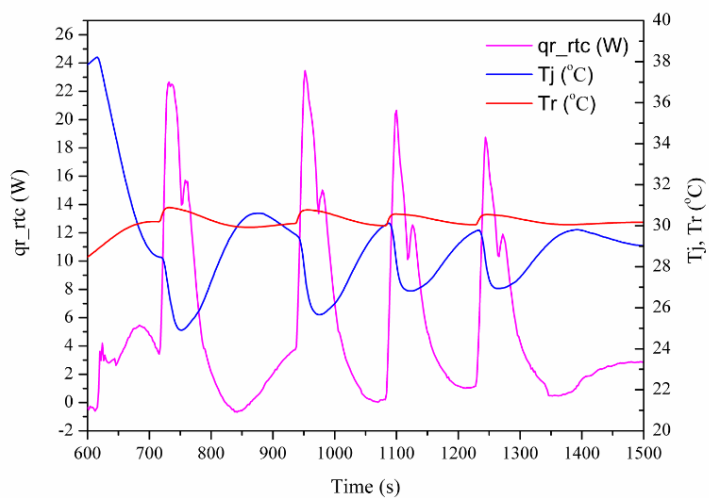


Fig. B.2: 30  $^{\circ}C$ , 2-Butanol Concentration: 0.53 mol/L, Catalyst Concentration: 2.4%



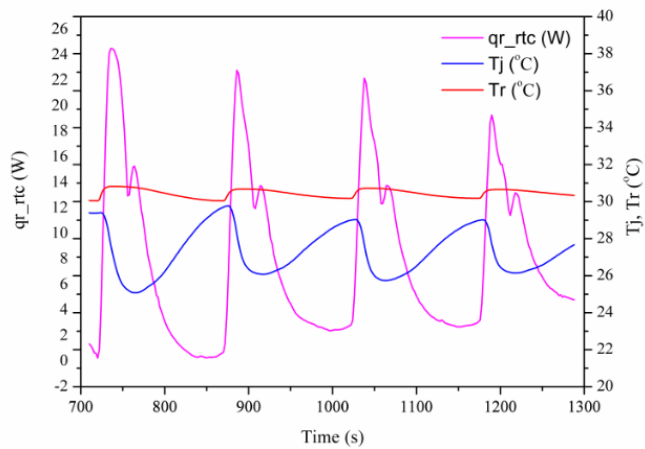


Fig. B.3: 30 °C, 2-Butanol Concentration: 0.78 mol/L, Catalyst Concentration: 2.4%

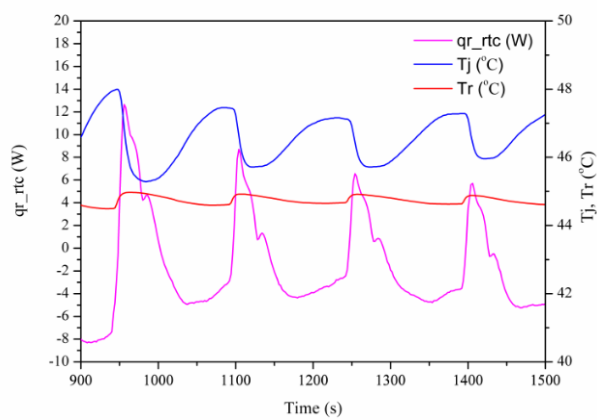


Fig. B.4: 45 °C, 2-Butanol Concentration: 0.28 mol/L, Catalyst Concentration: 3.6%

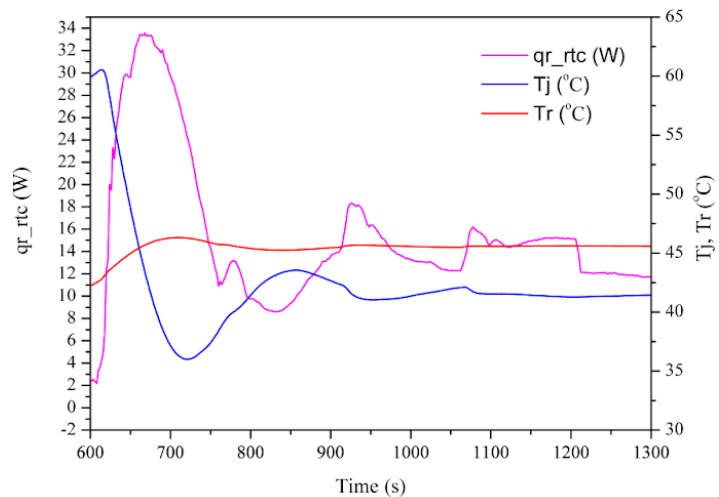


Fig. B.5: 45 °C, 2-Butanol Concentration: 0.53 mol/L, Catalyst Concentration: 3.6%

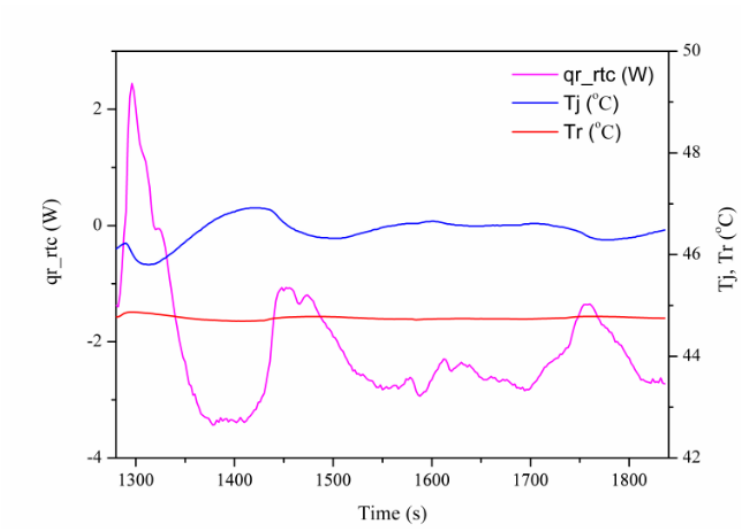


Fig. B.6: 45 °C, 2-Butanol Concentration: 0.78 mol/L, Catalyst Concentration: 3.6%

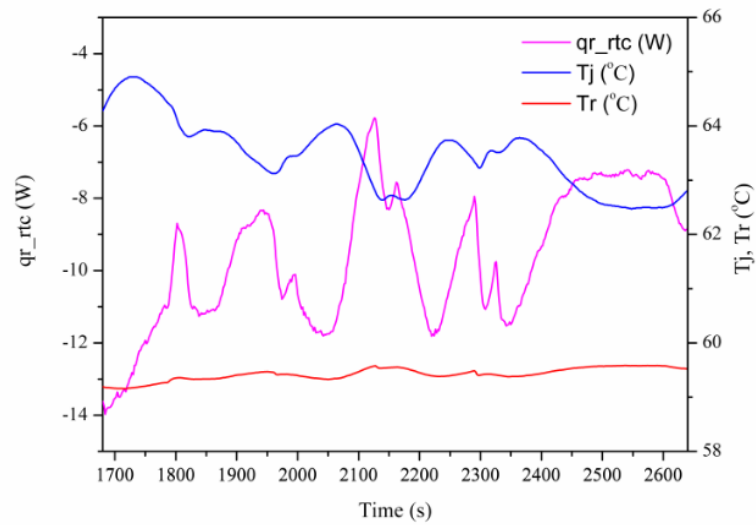


Fig. B.7: 60 °C, 2-Butanol Concentration: 0.28 mol/L, Catalyst Concentration: 4.8%

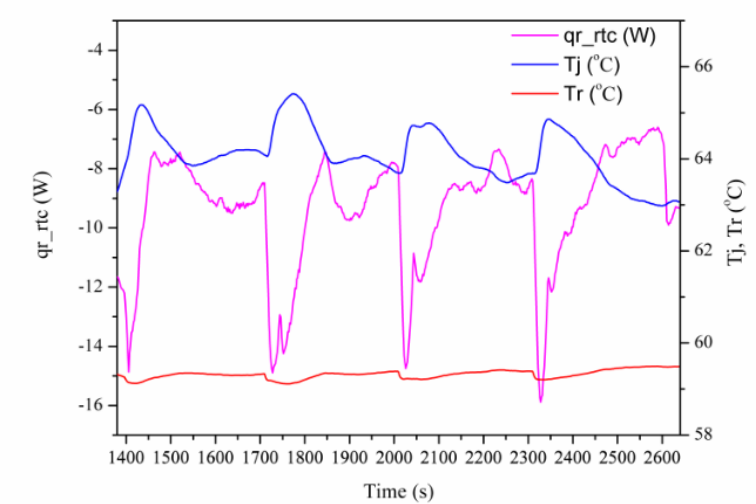


Fig. B.8: 60 °C, 2-Butanol Concentration: 0.53 mol/L, Catalyst Concentration: 4.8%

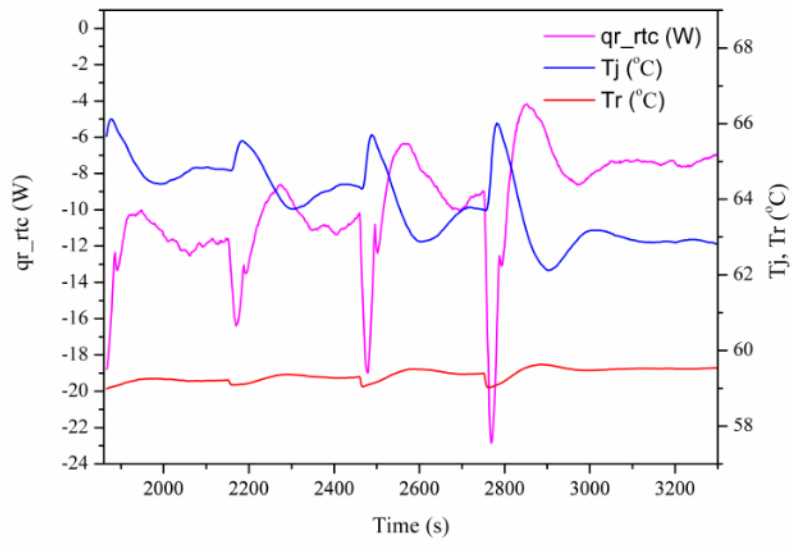
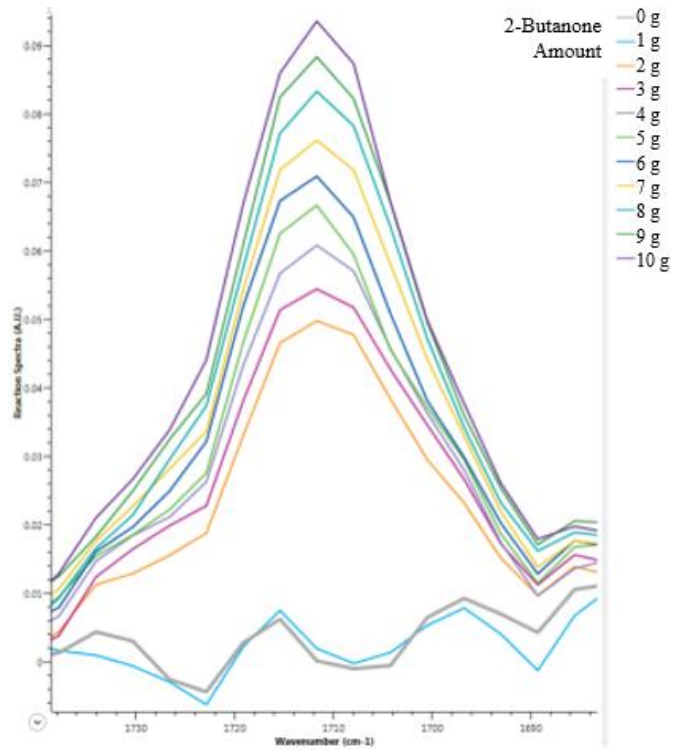
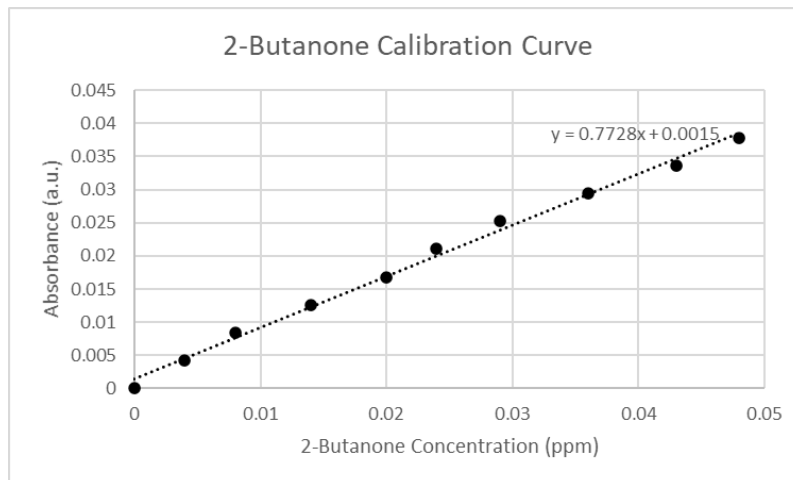


Fig. B.9: 60  $^{\circ}\text{C}$ , 2-Butanol Concentration: 0.78 mol/L, Catalyst Concentration: 4.8%

2-butanone FTIR calibration data and calibration curve:



2-butanone calibration data



2-butanone calibration curve

## APPENDIX C

### CYCLOHEXANONE HEAT RELEASE AND FTIR DATA

Table C.1: Raw heat release data for Taguchi Orthogonal Array (OA) design for study of temperature, P/R ratio, and number of peroxide injections impact on total heat generation and cyclohexanone yield

Run	Temperature (°C)	P/R Ratio	Number of Injections	Total heat generated (kJ)	Heat generated (kJ/kg reaction mass)	Cyclohexanone fractional yield (based on limiting reactant)
1	40	0.5	4	0.445	1.72	0.47
2	50	1	4	1.447	5.59	0.68
3	60	1.5	4	2.22	8.58	0.70
4	40	1	7	0.587	2.22	0.41
5	50	1.5	7	0.405	1.53	0.54
6	60	0.5	7	1.353	5.11	0.73
7	40	1.5	10	1.332	4.93	0.57
8	50	0.5	10	1.264	4.68	0.65
9	60	1	10	2.495	9.23	0.81

Temperature and heat release graphs for 9 experiments:

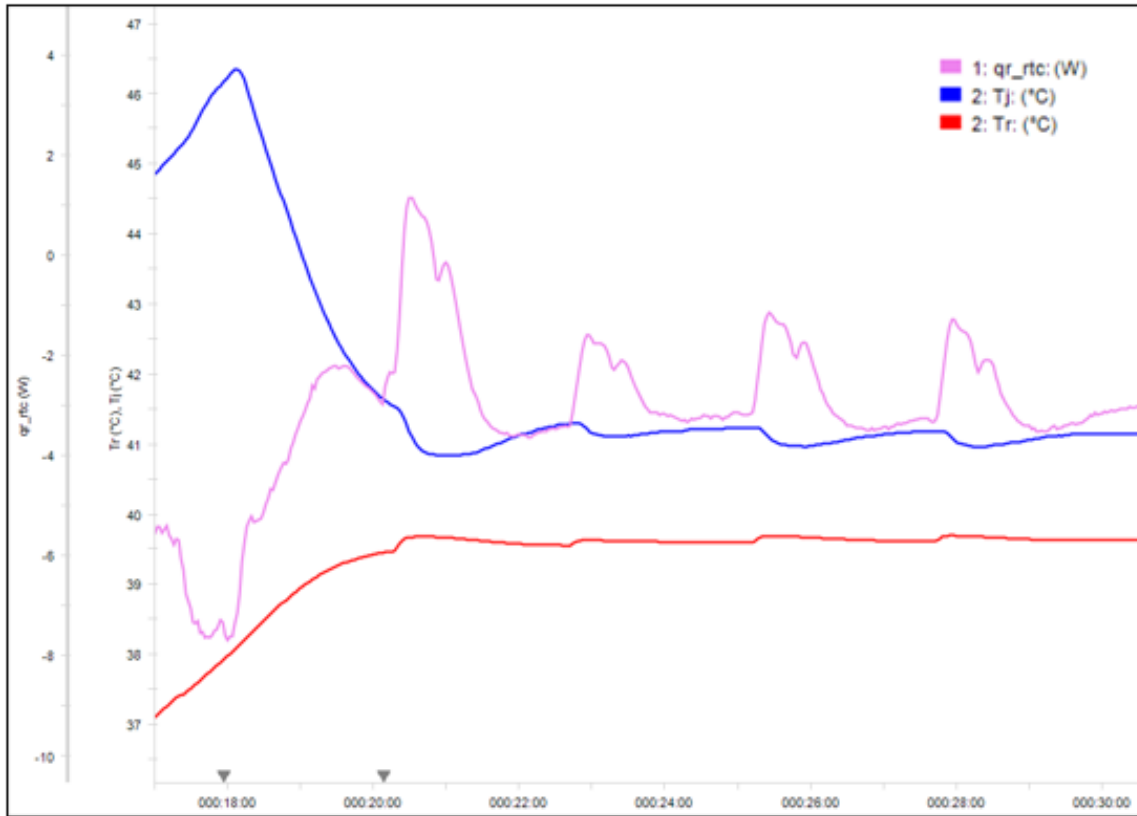


Fig. C.1: 40  $^{\circ}C$ , Peroxide/Reactant Ratio: 0.5, Number of Injections: 4

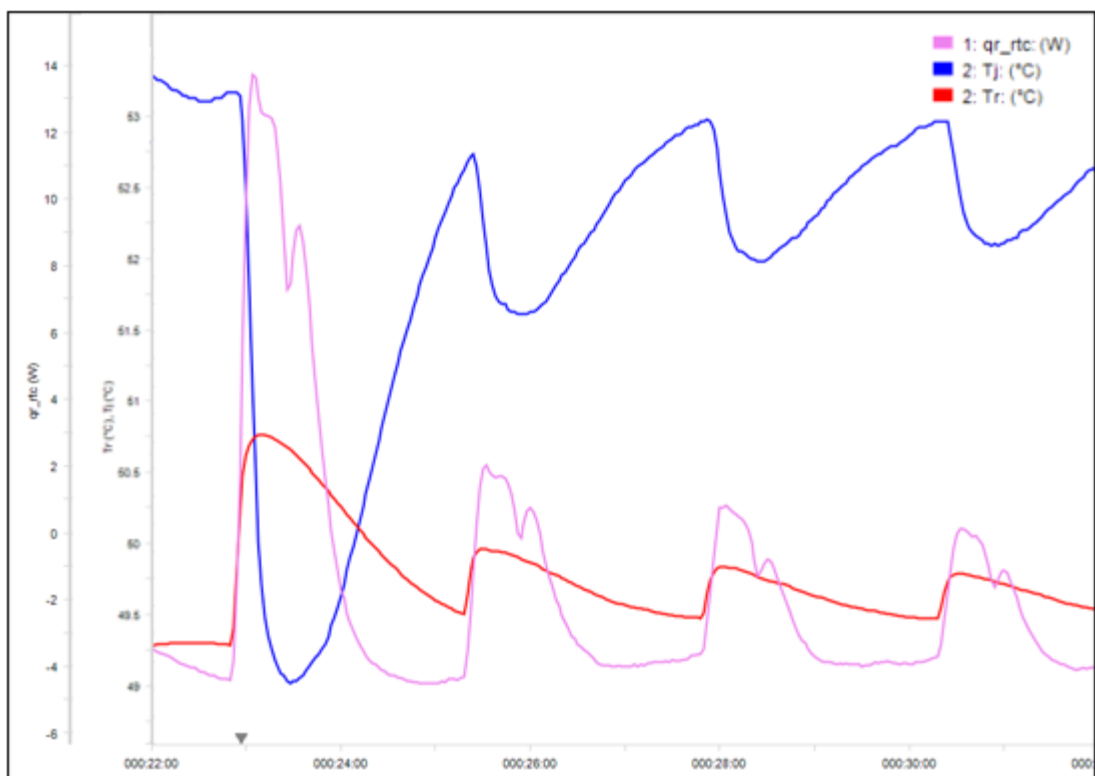


Fig. C.2: 50 °C, Peroxide/Reactant Ratio: 1.0, Number of Injections: 4



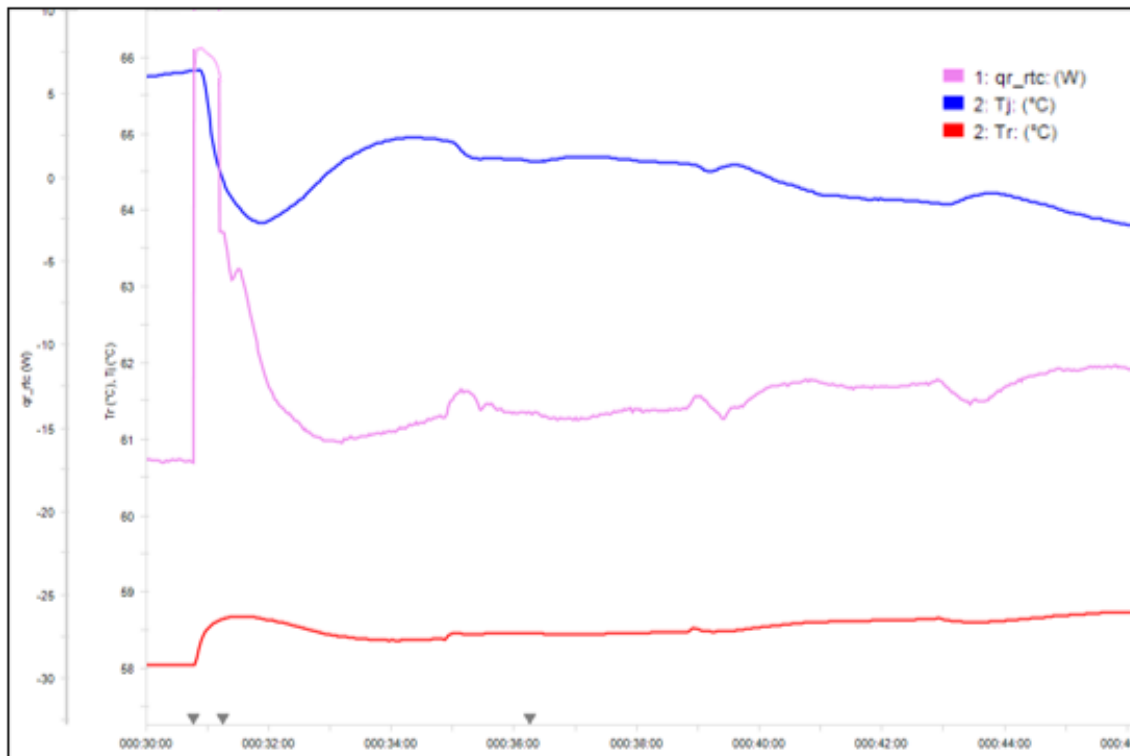


Fig. C.3: 60 °C, Peroxide/Reactant Ratio: 1.5, Number of Injections: 4

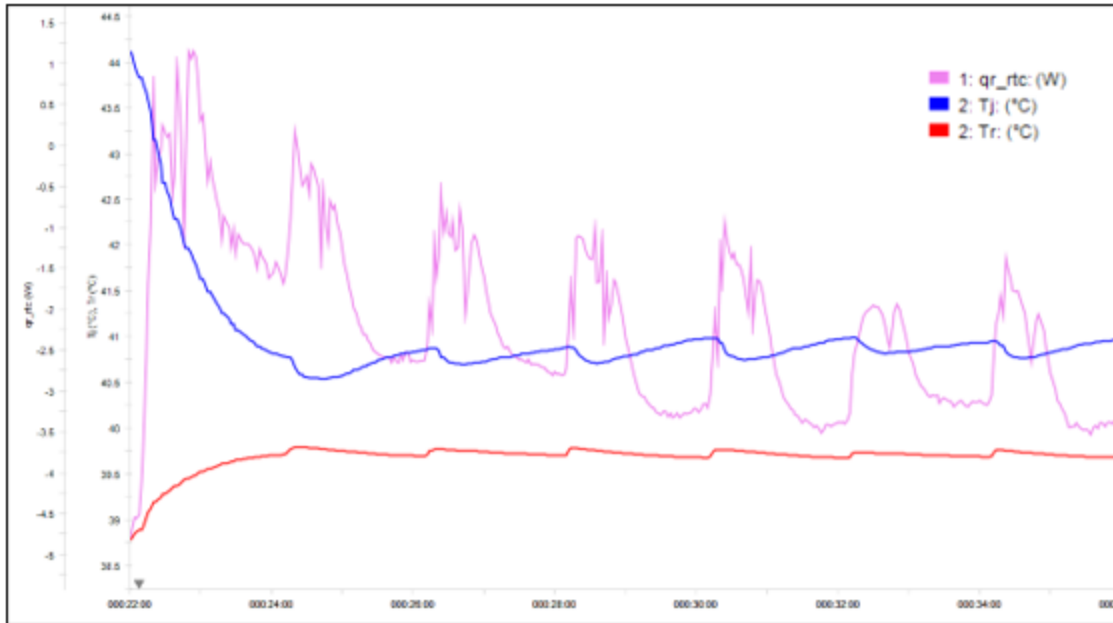


Fig. C.4: 40 °C, Peroxide/Reactant Ratio: 1.0, Number of Injections: 7

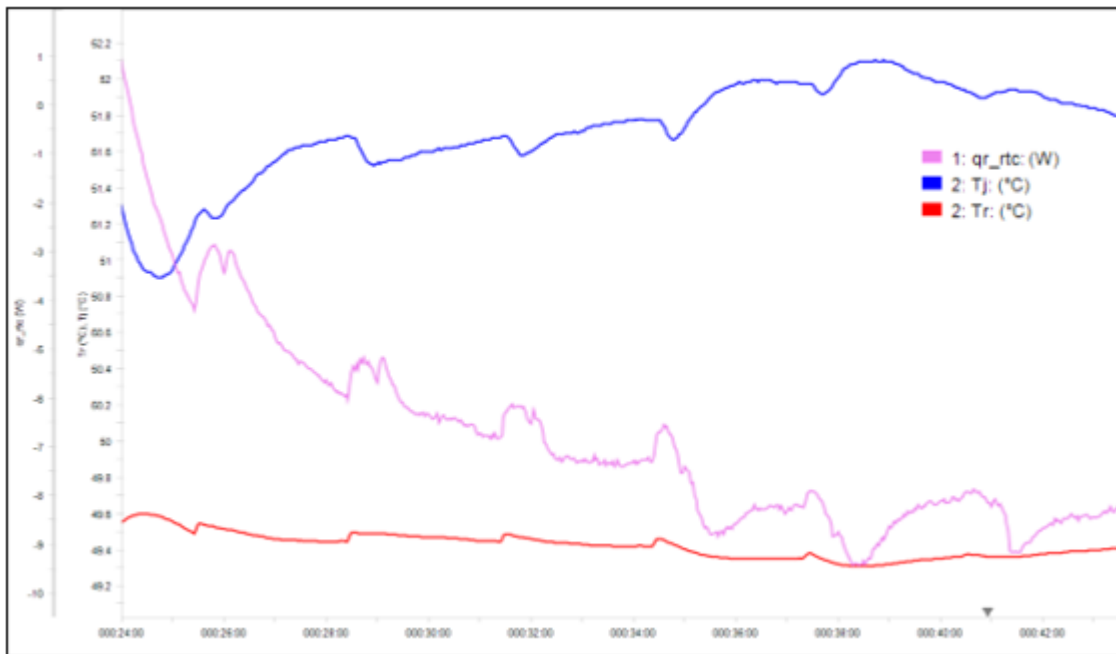


Fig. C.5: 50 °C, Peroxide/Reactant Ratio: 1.5, Number of Injections: 7

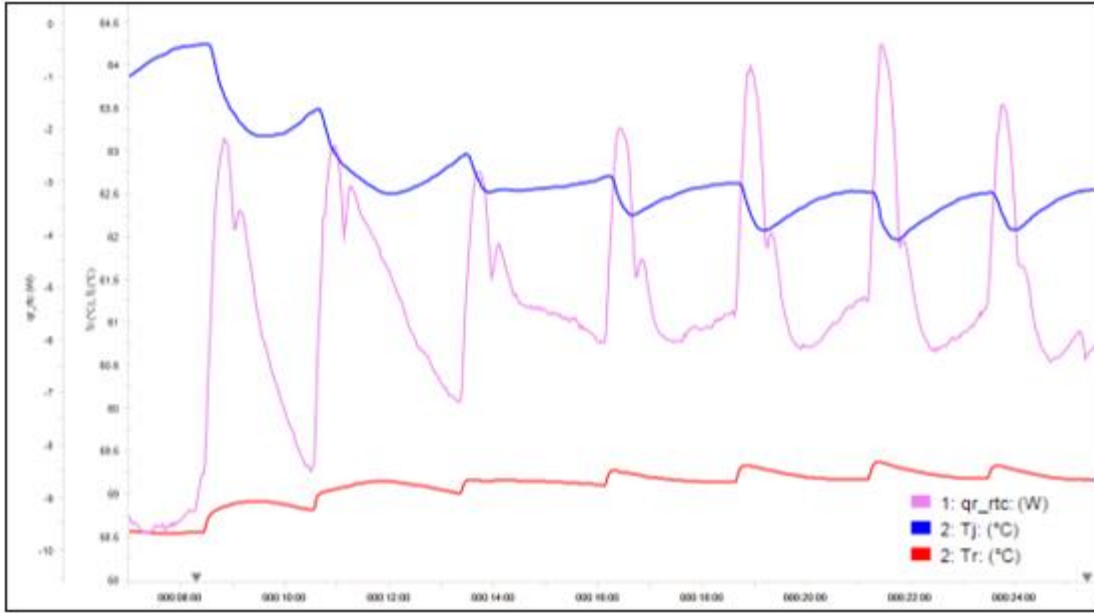


Fig. C.6: 60 °C, Peroxide/Reactant Ratio: 0.5, Number of Injections: 7

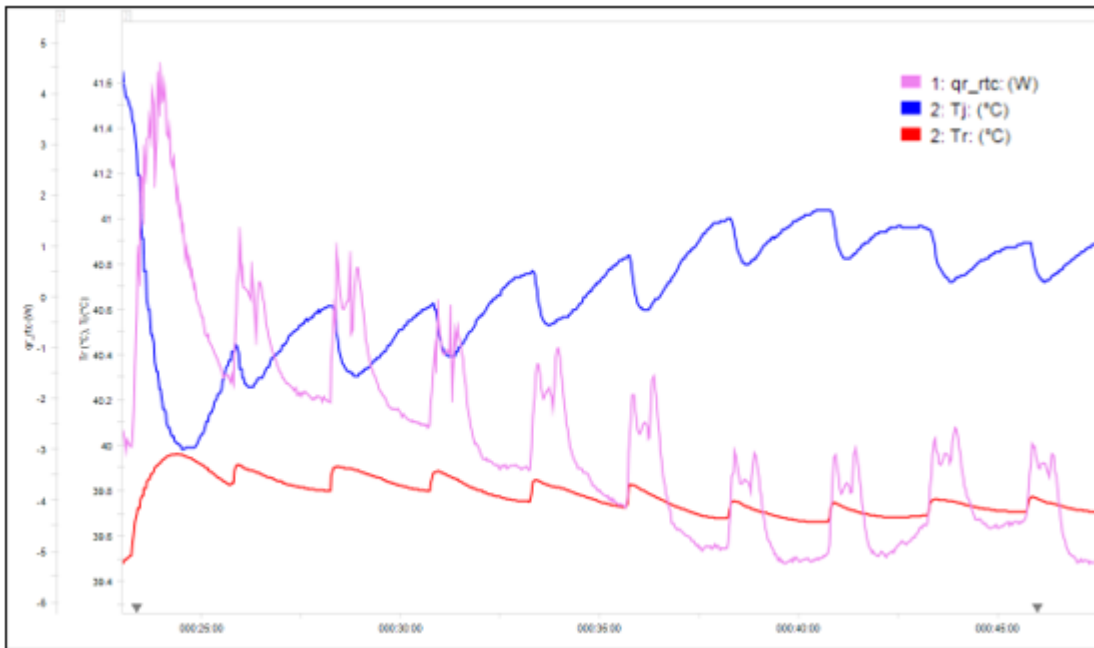


Fig. C.7: 40 °C, Peroxide/Reactant Ratio: 1.5, Number of Injections: 10

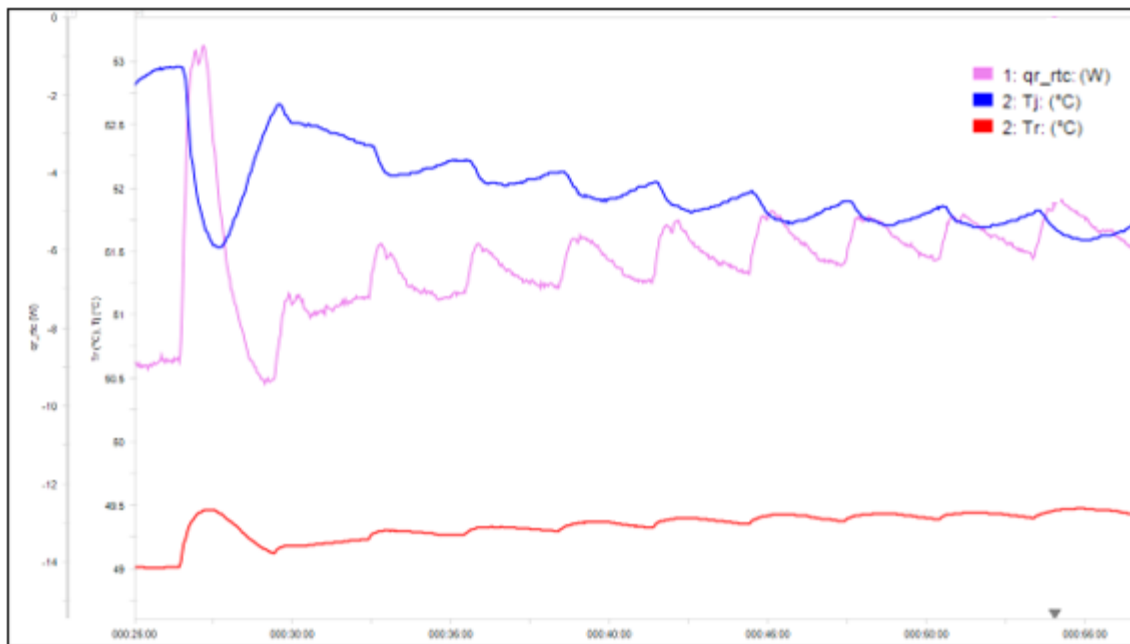


Fig. C.8: 50 °C, Peroxide/Reactant Ratio: 0.5, Number of Injections: 10

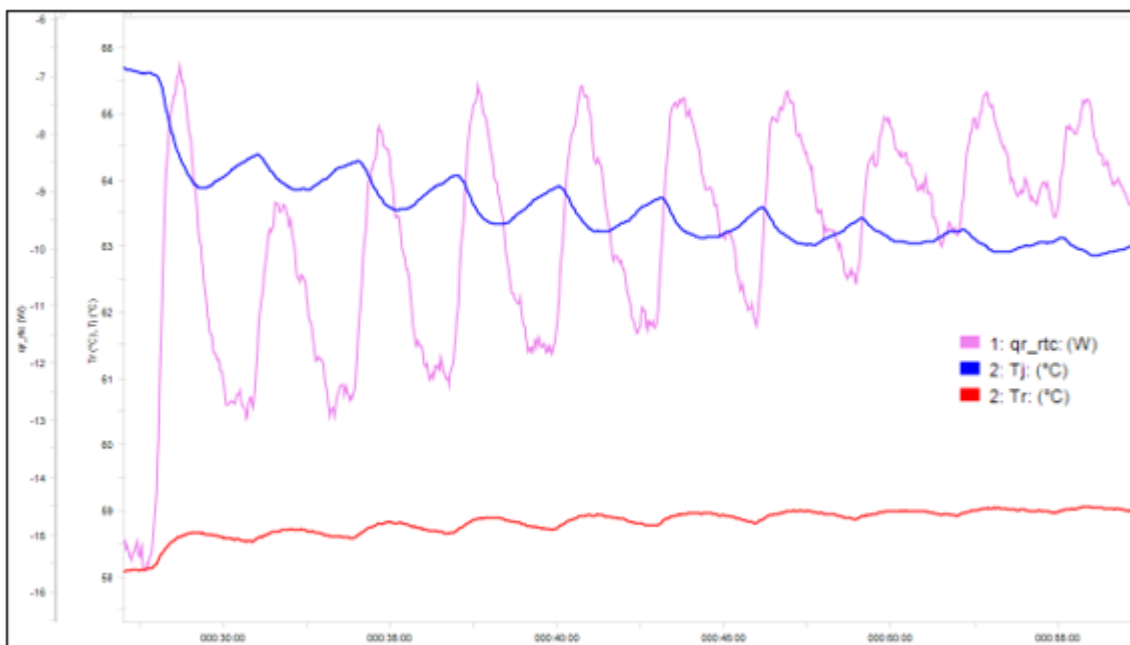
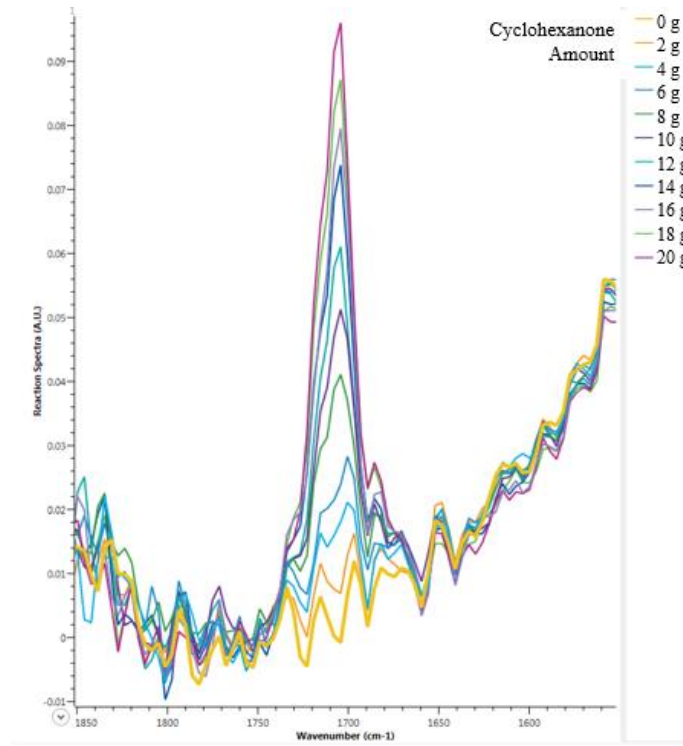
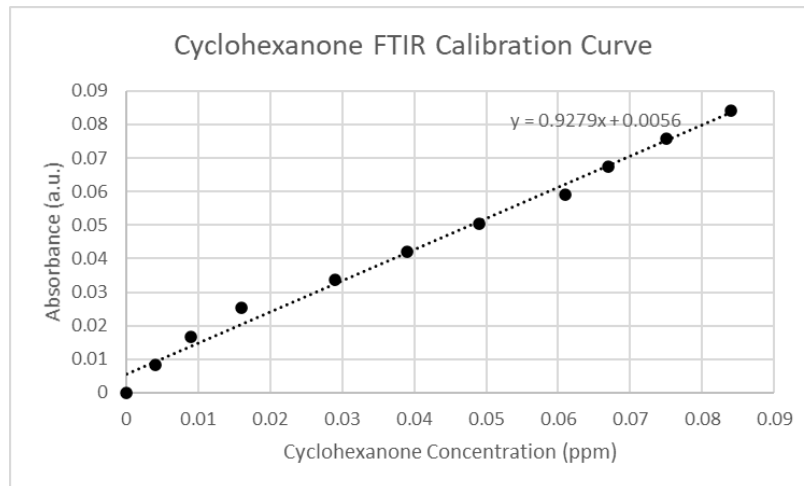


Fig. C.9: 60 °C, Peroxide/Reactant Ratio: 1.0, Number of Injections: 10

2-butanone FTIR calibration data and calibration curve:



Cyclohexanone calibration data



Cyclohexanone calibration curve